# Pathogenesis, immunity, and prevention of human norovirus infection in gnotobiotic pigs

Shaohua Lei

Dissertation submitted to the faculty of the Virginia Polytechnic Institute and State University in partial fulfillment of the requirements for the degree of

Doctor of Philosophy
In
Biomedical and Veterinary Sciences

Lijuan Yuan, Chair
Xiang-jin Meng
Xiaofeng Wang
Andrew B. Allison

March 20th, 2018
Blacksburg, VA

Keywords: gnotobiotic pigs, human norovirus, diarrhea, *Enterobacter cloacae*, RAG2/IL2RG, severe combined immunodeficiency, probiotics, rice bran

# Pathogenesis, immunity, and prevention of human norovirus infection in gnotobiotic pigs

Shaohua Lei

## ACADEMIC ABSTRACT

Human noroviruses (HuNoVs) are the leading cause of viral epidemic acute gastroenteritis and responsible for the deaths of over 200,000 children each year worldwide. HuNoV research has been hampered by the long absence of a readily reproducible cell culture system and a suitable small animal model, while gnotobiotic (Gn) pigs have been a unique animal model for understanding HuNoV pathogenesis and immunity, as well as evaluating vaccine and therapeutics. Recent reports of HuNoVs infection and replication in B cells supplemented with commensal bacteria *Enterobacter cloacae* and in Blab/c mice deficient in RAG/IL2RG have gained extensive attention, and my studies utilized the well-established Gn pig model to investigate the effects of these two interventions on HuNoV infection. Surprisingly, the colonization of *E. cloacae* inhibited HuNoV infectivity in Gn pigs, evidenced by the significantly reduced HuNoV shedding in feces and HuNoV titers in intestinal tissues and blood compared to control pigs. Moreover, HuNoV infection of enterocytes but not B cells was observed with or without *E. cloacae* colonization, indicating B cells were not a target cell type for HuNoV in Gn pigs. On the other hand, using RAG2/IL2RG deficient pigs generated by CRISPR/Cas9 system, with confirmed severe combined immunodeficiency, I evaluated the effects of host immune responses on HuNoV infection. Compared to wild-type Gn pigs, longer HuNoV shedding was observed in RAG2/IL2RG

deficient pigs (16 versus 27 days), and higher HuNoV titers were detected in intestinal tissues and contents and in blood, indicating increased and prolonged HuNoV infection in RAG2/IL2RG deficient pigs. In addition, I evaluated dietary interventions including probiotics and rice bran using Gn pig model of HuNoV infection and diarrhea. While the colonization of probiotic bacteria *Lactobacillus rhamnosus* GG (LGG) and *Escherichia coli* Nissle 1917 (EcN) in Gn pigs completely inhibited HuNoV fecal shedding, the two cocktail regimens, in which rice bran feeding started either 7 days prior to or 1 day after viral inoculation in the LGG+EcN colonized Gn pigs, exhibited dramatic anti-HuNoV effects, including reduced incidence and shorter duration of diarrhea, as well as shorter duration of virus fecal shedding. The anti-HuNoV effects of the cocktail regimens were associated with the enhanced IFN-$\gamma^+$ T cell responses, increased production of intestinal IgA and IgG, and longer villus length. Taken together, my dissertation work improves our understanding of HuNoV infection and immunity, and further supports for Gn pigs as a valuable model for future studies of human enteric virus infection, host immunity, and interventions.

# Pathogenesis, immunity, and prevention of human norovirus infection in gnotobiotic pigs

Shaohua Lei

## GENERAL AUDIENCE ABSTRACT

Human noroviruses (HuNoVs) are the leading cause of viral epidemic acute gastroenteritis. Using the gnotobiotic pig model of HuNoV infection and diarrhea, we found that (1) the colonization of a commensal bacterium *E. cloacae* inhibited HuNoV infectivity, and B cells were not a target cell type for HuNoV in gnotobiotic pigs. (2) Increased and prolonged HuNoV infection in RAG2/IL2RG deficient pigs, which had severe combined immunodeficiency. (3) The dietary supplementation of rice bran and colonization of two probiotic bacteria significantly reduced HuNoV infectivity and diarrhea, and the beneficial effects were associated with enhanced intestinal immunity and health. Taken together, the dissertation work improves our understanding of HuNoV infection and immunity, and further supports for gnotobiotic pigs as a valuable model for future studies of human enteric virus infection, host immunity, and interventions.

*Dedicated to my parents and sister for all their unwavering support and love.*

# ACKNOWLEDGEMENTS

First, I owe unending gratefulness and honor to my advisor, Dr. Lijuan Yuan. Back to 2013 when I finished my lab rotations in the Interdepartmental Microbiology Training Program, no one I asked was able to accept me as a graduate student, Dr. Yuan took a leap of faith and welcomed me into the lab during our first meeting. In addition to her outstanding graduate mentorship in guiding my doctoral education, Dr. Yuan is more like a mother helping manage my financial support, sharing with me her life experience, lending me assorted books, feeding me with wonderful dinners, introducing me to amazing friends, and allowing me to work in her garden. I truly admire her unceasing passion for research and various endeavors in life, and I will keep in mind the lessons I have learned from her.

I would like to thank all the members who served on my advisory committee, Drs. Lijuan Yuan, X.J. Meng, Xiaofeng Wang, Andrew B. Allison, Nanda Nanthakumar, and Husen Zhang. They motivated me to be prepared for the committee meeting each semester and urged me to hone my oral English and presentation skills. Their different expertise and merged guidance have fulfilled my doctoral education, so that I could not have asked for a better committee.

I would like to offer sincere appreciation to every individual I worked with in the Yuan Lab over the years. Graduate life with tons of lab work was busy, but because of you guys it was enriching and cheerful. Thank you all for the assistance, advice, and friendship. Special thanks to Jacob Kocher,Tammy Bui Castellucci, and Erna Giri-Rachman for leading me to HuNoV projects, Ke Wen and Ashwin Ramesh for performing flow cytometry, Erica Twitchell for evaluating pig histopathology, Mariah Weiss for managing pig work, and everyone including Guohua Li,

Xingdong Yang, Helen Samuel, Alissa Hendricks, Elizabeth Majette, Hong Tian, Christine Tin for contributing indispensably to my projects.

I would like to thank Drs. Sherrie Clark-Deener, Kevin Pelzer, and Nicole Lindstrom for veterinary services for gnotobiotic pigs, and TRACSS (The Teaching and Research Animal Care Support Services) members, specially Karen Hall, Kimberly Allen, Karen Young, Shannon Viers, and Jessica Park for their excellent animal care throughout the entire studies. In addition, I would like to thank Kristy DeCourcy for assisting on confocal microscope, Melissa Makris for operating flow cytometry, and Kathy Lowe for assisting on electron microscopy.

I am very fortunate to have many wonderful friends in such a terrific town like Blacksburg. Vivid memories come flooding back from when we hung out hiking, fishing, skiing, traveling, etc. I really cherish my friendship with each of them and appreciate their understanding, love, and company over these past years.

# TABLE OF CONTENTS

# LIST OF FIGURES

## Chapter 2



## Chapter 3



## Chapter 4

# LIST OF TABLES

## Chapter 1



## Chapter 2



## Chapter 3



## Chapter 4

# Chapter 1 Literature review

## Human norovirus pathogenesis and immunity;

## Probiotics and rice bran usage in gastroenteritis

Shaohua Lei

Department of Biomedical Sciences and Pathobiology,

Virginia-Maryland College of Veterinary Medicine,

Virginia Tech, Blacksburg, VA 24061, USA.

Partially published as a book chapter in *Mechanisms underlying host-microbiome interactions in pathophysiology of human diseases*. Edited by Sun J and Dudeja PK (2018). Used with permission. Partially to be published as a book chapter in *Dietary Interventions in Gastrointestinal Disease: Food, Nutrients and Dietary Supplements*. Edited by Watson RR and Preedy VR.

## 1.1 HuNoV pathogenesis and immunity in humans and in animal models

### 1.1.1 HuNoV gastroenteritis, pathogenesis and cell tropism in humans

Human noroviruses (HuNoVs) are positive-sense, single-stranded, non-enveloped RNA viruses that belong to the genus *Norovirus* in the family *Caliciviridae*[1]. Since the introduction of rotavirus vaccines (RotaTeq in 2006 and Rotarix in 2008), HuNoVs have become the predominant cause of viral epidemic acute gastroenteritis across the globe[2-4]. HuNoV is responsible for estimated 200,000 children lives each year globally, and approximately $284 million in healthcare charges, 20 million illness, and 800 deaths annually in the United States[5-7]. HuNoVs are highly contagious, infectious to people of all ages, with a higher infection incidence in children and underdeveloped areas[2]. Viral transmission occurs via the fecal-oral route by contaminated food or water and person-to-person spread[8]. HuNoV gastroenteritis is generally self-limiting with a duration of 2-3 days and consists of moderate to severe acute diarrhea episodes, sudden onset of vomiting, and mild or no fever[9], but the diseases can become more severe and prolonged in infants, elderly, and individuals with impaired immunity[10]. Despite the tremendous disease burden and financial cost, currently no virus-specific therapeutics or vaccines are available to treat or prevent HuNoV gastroenteritis[11], mainly because HuNoV research has been hampered by the long absence of a readily reproducible cell culture system and a suitable small animal model. HuNoV biology has been explored most frequently by viral challenge studies in human volunteers[10], chimpanzees[12], gnotobiotic (Gn) calves and pigs[13-15], and immunodeficient mice[16] (Table 1).

Challenging HuNoV in immunocompetent volunteers resulted in acute gastroenteritis, and biopsy specimens from the individuals who acquired clinical gastroenteritis displayed

histologic changes in the small intestine, including mucosal inflammation, villus blunting, microvillus shortening, and abnormal organelles such as endoplasmic reticulum and mitochondria[17-20]. Although intestinal epithelial cells (IECs) are the target for most enteric pathogens, the presence of HuNoV virions or antigen has not been reported in these biopsies from immunocompetent humans, and the cellular tropism of HuNoV has long been elusive[17-21]. Chronic HuNoV infection occurs in immunocompromised transplant patients. A recent study using intestinal biopsies from a patient cohort showed that HuNoV infection was observed in duodenal and jejunal enterocytes, and HuNoV-associated histopathological changes were present as the flattening of epithelial cells and the severe loss of villin in enterocytes[22]. In addition, stem cell-derived and non-transformed human intestinal enteroids have been recently established as a reproducible cultivation system for multiple HuNoV strains, confirming enterocytes as target cell types for HuNoV infection *in vitro* and *in vivo*[23]. B cells were suggested to be a permissive cell type for HuNoV replication *in vitro*, which is a novel HuNoV cultivation system in BJAB cell line supplemented with free histo-blood group antigen (HBGA) or HBGA-expressing inactivated enteric bacteria[24]. However, this cell culture system produced inconsistent results in other laboratories[25], and HuNoV infection was observed in B cell-deficient patients[26], along with the low virus yields in such an *in vitro* cell system compared with high-level virus shedding in patients[27], suggesting that B cells might not be the primary target cell of HuNoV.

### 1.1.2 HuNoV infection and pathophysiology in conventional animal models

Non-human primates (NHP), particularly chimpanzee (99%)[28], share the greatest genome similarities with humans, which makes them desirable models for studies on

several fastidious viral pathogens, such as human immunodeficiency virus and hepatitis viruses[29-31]. The chimpanzee was presented as a viable animal model for subclinical GI.1 HuNoV infection, characterized by intravenous inoculation, asymptomatic fecal virus shedding, and viral associated serum antibody responses[12]. Biopsies from the jejunum and duodenum showed no histological changes after HuNoV infection, although the viral genome was detectable up to 21 days post-inoculation. Interestingly, viral capsid antigen was only observed in cells of the duodenal and jejunal lamina propria, and further investigations indicated that viral antigen-positive cells were dendritic cells and B lymphocytes[12]. However, the chimpanzee is not available for biomedical research any longer owing to ethical concerns. Another animal model of subclinical HuNoV infection is the Balb/c mouse deficient in recombination activation gene (RAG) and common gamma chain (γc or IL2RG), which lacks T cells, B cells, and natural killer cells. In this mouse model, a HuNoV GII mix was inoculated intraperitoneally[16]. Although virus shedding and gastrointestinal diseases were not observed in those Balb/c RAG/γc$^{-/-}$ mice, viral genome was detected in the intestinal and systemic sites, with increased levels over the input virus 1-2 days post-inoculation. Viral structural and nonstructural proteins were observed in cells morphologically resembling macrophages in the liver and spleen, validating HuNoV propagation[16]. Moreover, Balb/c RAG/γc$^{-/-}$ mice can be used for the evaluation of anti-HuNoV drugs such as the nucleoside analog 2'-C-methylcytidine, which inhibited HuNoV replication *in vivo*[32].

**1.1.3 HuNoV infection and pathophysiology in gnotobiotic large animal models**

The neonatal Gn pig model is a well-established model of HuNoV infection and diarrhea, and it offers many benefits that other animal models lack. First, humans and pigs share high

homology in genome and proteome, omnivorous diet, analogous physiology of the gastrointestinal tract, and similar immune system[33-35]. Second, no maternal antibodies can be transferred via the porcine placenta, and Gn piglets are fed with no sow colostrum or milk, altogether excluding the effects of maternal antibodies on experimental studies. Third, it reflects HuNoV biology in terms of supporting the natural oral route of infection, resulting in diarrhea, transient viremia, and virus shedding in feces[14, 15, 36-38]. Viral structural and nonstructural proteins were detected in enterocytes in wild-type Gn pigs experimentally infected with HuNoV genotype GII.4[14, 15], indicating viral infection and replication in Gn pigs. HuNoV-induced diarrhea in Gn pigs was associated with mild villus atrophy and cytopathological changes in the small intestine, manifested as blunting and shortening of microvilli and necrosis and apoptosis of enterocytes[14, 15], which recapitulate the hallmark pathological features in humans.

Twenty-four units of the P domain of HuNoV capsid protein can form P particle, which efficiently induces innate, humoral, and cellular immune responses in mice[39]. Together with its easy and economical preparation in *E. coli*, P particle has gained recognition as a promising vaccine candidate against HuNoV infection[40]. In the study of P particle vaccination in Gn pigs, P particle exhibited 47% cross-variant protection against HuNoV diarrhea, and the protection correlated positively with T cell expansion in the ileum and spleen, while correlating inversely with T cell expansion in the duodenum[36].

Neonatal Gn calves serve as another large animal model that supports GII.4 HuNoV infection; viral capsid protein was detected in enterocytes of the jejunum and ileum, and in cells morphologically resembling macrophages in the lamina propria[13]. Similar to the findings in

Gn pigs, HuNoV challenge in Gn calves resulted in diarrhea along with intestinal lesions and mild villous atrophy, fecal virus shedding, transient viremia, and intestinal and systemic immune responses[13].

Notably, pigs are natural hosts of noroviruses GII (genotypes 11, 18, and 19); however, all porcine noroviruses were detected from conventional pigs without clinical signs[41]. Porcine norovirus has been detected in many countries and geographical distribution indicates the worldwide occurrence of porcine noroviruses among pigs on farms. The QW101/2003/US (GII.18) isolate from a healthy adult pig was genetically and antigenically related to HuNoVs and replicated in Gn pigs with fecal shedding coincident with mild diarrhea[42]. Seroprevalence of norovirus GII in pigs was reported to be 97% in the United States. Attempts have been made, but failed to infect conventional Göttingen miniature pigs (Marshall BioResources, North Rose, NY, USA) with HuNoV[43]. The miniature pigs neither shed virus nor seroconvert after oral and intravenous HuNoV inoculation. The difference in the susceptibility to norovirus infection and lack of disease in conventional pigs suggest that the gut microbiota or maternal antibodies might be protective. Effects of the gut microbiota on the resistance and immunity to norovirus infection are currently under investigation.

**1.1.4 Effects of microbiome on norovirus infection, immunity, and disease**

The notion that commensal bacteria can enhance enteric viral infection was demonstrated by two landmark studies published in 2011 using poliovirus, reovirus, and mouse mammary tumor virus[44, 45]. When intestinal bacteria were depleted by administering a cocktail of antibiotics to mice, poliovirus infection was dramatically attenuated in

comparison with normal mice with gut microbiota, as characterized by the reduced fecal virus shedding and mortality[44]. In addition, the reduced poliovirus infection was reversed by fecal transplantation to reconstitute intestinal microbes, and the status of the intestinal microbiota did not affect viral infectivity when poliovirus was inoculated intraperitoneally[44], indicating the role of intestinal bacteria in enhancing enteric viral infection. Poliovirus was shown to directly bind to the bacterial outer-membrane component lipopolysaccharide, resulting in virion thermo-stabilization and attachment to host cells[44, 46]. As a result, the interactions between host-microbiome and enteric viruses have been gaining intense attention. However, the understanding of effects of the intestinal microbiota on HuNoV has been impeded by the absence of a suitable cell culture system and animal model. Limited studies analyzing stool samples from human patients showed that HuNoV infection could alter microbial composition[47].

Murine norovirus (MNV) was first identified in 2002 from the brain of an immunocompromised mouse, RAG/STAT1$^{-/-}$ strain, because of its lethal infection[48]. Since then, MNV has been used widely as a surrogate to explore HuNoV biology regarding viral pathogenesis, host immunity, and interplays with gut microbiota. Antibiotic treatment reduced the acute MNV infection, and lower virus titers in the distal ileum, mesenteric lymph nodes, and colon were observed compared with control mice[24]. Antibiotics also prevented persistent MNV infection in mice, but persistent infection could be restored by microbial colonization[49], indicating the stimulatory role of microbiota in MNV infectivity. However, major disruptions of the microbiome were not observed following acute or persistent MNV infection in mice[50]. MNV infection is asymptomatic in wild-type

mice, but mucosal inflammation was observed in IL-10$^{-/-}$ mice maintained in a specific pathogen-free environment, and MNV-induced pathological changes such as reduced tight junction proteins and inflammatory lesions were lacking in germ-free IL-10$^{-/-}$ mice, suggesting that MNV-triggered intestinal diseases might be induced via bacterial microbiota[51].

## 1.2 Probiotics usage in gastroenteritis

Probiotics have been increasingly recognized as vaccine adjuvants and therapeutic agents to ameliorate acute gastroenteritis[52, 53]. The underlying mechanisms include competing with pathogens for nutrients and colonization sites, producing antimicrobial metabolites, modulating gut microbiota composition, enhancing intestinal barrier function, and promoting mucosal immunity[54]. Numerous probiotic strains have been investigated for reducing diarrhea in animal studies and human clinical trials. The efficiencies of probiotics vary in a strain-dependent and dose-dependent manner[55-58], and noteworthy examples include bacteria species of the genus *Lactobacillus* and *Bifidobacterium*, *Escherichia coli* Nissle 1917 (EcN), and yeast *Saccharomyces boulardii*. The usage of these four probiotic species/strains on gastroenteritis is discussed below with additional highlights on reducing diarrhea caused by human rotavirus (HRV), which is a leading cause of severe gastroenteritis in children under 5 years old[59, 60].

Gram-positive probiotic bacteria *Lactobacillus* spp. are most frequently investigated and used for alleviating clinical symptoms associated with gastrointestinal diseases[61]. As a prototypical and commercially available probiotic strain, *Lactobacillus rhamnosus* GG (LGG) has been extensively evaluated for its beneficial effects such as the prevention and relief of

multifarious type of diarrhea[62]. For instance, treatment with LGG reduced the risk of antibiotic-associated diarrhea in patients from 22.4% to 12.3% compared with mock or placebo controls[63], LGG is the most recommended probiotics for preventing nosocomial diarrhea in children based on currently available clinical data[64, 65], and LGG administration significantly lowered diarrhea incidence in post-weaning piglets induced by *Escherichia coli* K88[66]. Particularly, LGG has garnered overwhelming supportive evidence for lessening HRV infection and diarrhea[67]. Previous studies in our laboratory using Gn pig model have shown that LGG treatment could reduce HRV-induced intestinal tissue damage and diarrhea[68, 69], promote virus-specific immune responses[70], enhance the protective efficacy of HRV vaccine[58], and prevent the shift in microbiome composition caused by virulent HRV challenge in human gut microbiota transplanted Gn pigs[71].

Bifidobacteria are among the predominant bacterial inhabitants in the gastrointestinal tract of mammals, including humans[72], and they exhibit social behavior in shaping gut microbiota via metabolic interactions[73, 74]. In addition to the general benefits in maintaining homeostatic gut, some bifidobacterial strains have been used as probiotics for their positive effects on gastrointestinal functions and diseases, examples are *B. animalis lactis*, *B. bifidum*, *B. longum*, *and B. breve*[75]. Accumulating evidence has demonstrated that Bifidobacteria, administrated alone or in combination with other probiotics and/or prebiotics, exert promising efficacy in preventing and treating gastrointestinal disorders, including antibiotic-associated diarrhea, *Clostridium difficile*-associated diarrhea, *Helicobacter pylori* infection, colorectal cancer, necrotizing enterocolitis, inflammatory bowel disease, and irritable bowel syndrome[76]. Notably, *B. longum* subsp. *infantis* CECT 7210 could inhibit rotavirus replication in MA-104 and HT-29 cells and in a BALB/c mouse model[77], and its antiviral property was mediated by the secretion of an

11-amino acid peptide possessing protease activity[78]. When feeding *B. thermophilum* RBL67 in CD-1 suckling mice prior to simian rotavirus SA-11 infection, reduced viral replication, duration of diarrhea, and epithelial lesions were observed, along with accelerated recovery and enhanced virus-specific IgG and IgM response[79]. Moreover, co-colonization of *B. animalis lactis* Bb12 and LGG in Gn pigs lowered fecal virus shedding and diarrhea scores after attenuated HRV vaccination and virulent HRV challenge than those of non-colonized pigs, and the ameliorated clinical signs were associated with the enhanced intestinal HRV-specific IgA antibody responses[80].

Gram-negative EcN is also a well-characterized and commercially available probiotics used to treat inflammatory bowel disease[81], ulcerative colitis[82], and diarrhea in infants and young children[83, 84]. As a veterinary prophylactic and therapeutic option, EcN feeding in neonatal calves significantly reduced the incidence of diarrhea compared with placebo[85], and the pre-treatment of EcN in neonatal pigs provided complete protection from acute secretory diarrhea associated with porcine enterotoxigenic *E. coli* Abbotstown challenge[86]. The beneficial effects of EcN could be mediated by enhancing intestinal barrier function or ameliorating inflammatory responses[87-89], latter of which contributed to the protection in Gn piglets from lethal infection of *Salmonella* Typhimurium[88]. In addition, EcN was shown to possess HRV-binding and immunomodulatory properties, and the reduced HRV infection and diarrhea in Gn pigs were attributed to the enhanced B cell, plasmacytoid dendritic cell, and NK cell responses in the presence of EcN[90, 91]. However, such anti-HRV activities were not observed from the treatment of LGG, suggesting that the Gram-negative probiotic is more effective than various Gram-positive probiotics in promoting protective immunity against HRV infection[90-92].

Bacteria are not the only microorganisms used as probiotics. The yeast *Saccharomyces boulardii* is well-known for its wide use in the prevention and treatment of gastrointestinal dysfunction, including antibiotic-associated diarrhea[93], acute gastroenteritis in infants and children[94, 95], HIV-associated diarrhea[96, 97], irritable bowel syndrome and Crohn's disease[98], as well as the prevention of *C. difficile* infection and the elimination of *H. pylori* infection[99, 100]. In particular, when *S. boulardii* was administrated to children with acute rotavirus diarrhea in two double-blind randomized trials, the mean duration of diarrhea was significantly shorter than in controls, while no adverse events were observed[101, 102]. Rotavirus-associated diarrhea results from the viral destruction of absorptive enterocytes, villus ischemia, intestinal secretion induced by viral non-structural protein 4 (NSP4), and activation of the enteric nervous system[59, 60]. An *in vitro* study using Caco-2 cells and human intestinal organ culture model showed that rotavirus NSP4 induced chloride secretion through the generation of oxidative stress, and *S. boulardii* could inhibit chloride secretion, which was proposed as a mechanism for its anti-diarrhea property[103].

## 1.3 Rice bran usage in diarrhea

### 1.3.1 Overall health benefits of rice bran dietary supplement

Rice (*Oryza sativa* L.) is grown in over 100 countries and served as the staple food for around 3.5 billion people all over the world[104]. While the milled and polished rice grain widely counts for human consumption, the outer covering layer, rice bran, is usually considered as a type of livestock feed, mainly due to traditional perceptions and the rapid development of hydrolytic rancidity in the bran during stroage[105, 106]. Therefore, rice bran is known as an underutilized by-product of rice milling. To overcome the storage issue, heat stabilization is

applied to inactivate rancidity-inducing lipoxygenases and lipases in rice bran, the increased shelf life and retained bioactivity have expanded the usage of rice bran for human health and nutrition[107]. Rice bran is a natural mixture of a large variety of bioactive compounds. Rice bran metabolite profiling revealed a suite of 65 biochemical molecules with health properties including amino acids, vitamins & cofactors, and secondary metabolites[108]. The multifaceted health benefits of rice bran have been illuminated using whole rice bran as well as extracts such as rice bran oil, polysaccharides, proteins/peptides, and minerals[109]. As a result, there is an increasing interest in dietary rice bran supplementation in animals and humans for the medicinal and nutritional properties.

In mice, consumption of rice bran induced an increase in fecal and serum IgA, as well as increased antigen-presenting cells in mesenteric lymph nodes and lamina propria[110]. Another study showed that rice bran glycoprotein was able to help cyclophosphamide-treated mice recover from immunosuppression by promoting the proliferation of splenic lymphocytes[111]. These reports indicate the immunomodulatory effects of rice bran in enhancing mucosal and systemic immunity. In gnotobiotic (Gn) pigs, rice bran intake exhibited high protective efficacy against diarrhea induced by HRV infection[112]. In human clinical trials, dietary rice bran ameliorated type 2 diabetes by lowering lipid and glycemic levels[113, 114], and arabinoxylan rice bran has been evaluated with promising therapeutic effects on irritable bowel syndrome and chronic hepatitis C virus infection[115, 116]. In addition, emerging scientific evidence indicates that dietary rice bran represents chemopreventive potential against several types of cancer such as liver, lung, breast, and colon cancer[117]. Overall, rice bran is being recognized as an economical,

natural, novel, and safe dietary supplement with broad beneficial effects on animal and human health, including treating gastrointestinal diseases.

### 1.3.2 Dietary rice bran supplementation in reducing diarrhea

It is well known that rice bran has been a traditional home remedy for patients with acute or chronic gastrointestinal illnesses in Asian countries such as China and India, especially in the rurual areas due to its easy accessibility and low cost. Diarrhea is a manifestation of gastrointestinal malfunction, and the anti-diarrhea property of rice bran has been first tested in the cases of irritable bowel syndrome (IBS) and HRV infection.

IBS is a chronic functional bowel disorder in which recurrent abdominal pain is related to defecation or a change of stool frequency or pattern, including diarrhea, constipation, or mixed type[118]. As many patients recognize specific dietary contributors for their IBS symptoms, the traditional first recommended treatment is to increase the dietary fiber intake. In a randomized clinical trial, 20 patients in the placebo group and 19 patients in the modified arabinoxylan rice bran (also known as MGN-3 or Biobran) group all suffered from diarrhea, either IBS with diarrhea or mixed type IBS with both diarrhea and constipation. After 4 weeks of treatment with 2 grams of Bioran powder per day, the global assessment indicated that 30% of the placebo and 63.2% of the Biobran group had symptom relief in IBS, and significantly lower diarrhea scores over the baseline, but not constipation scores, were observed after Biobran treatment, indicating the therapeutic effects of dietary Biobran in reducing diarrhea in IBS[115].

The first report of rice bran's effects on reducing viral diarrhea was a study using the Gn pig model of HRV infection and disease. Heat-stabilized rice bran was added to the Gn pigs' daily milk diet to replace 10% of total calorie intake starting at 5 days of age, the virulent HRV challenge

was given at 33 days of age, and then all pigs were euthanized 7 days later. In the study, while the mock control Gn pigs experienced an average of 5.6 days of diarrhea, the rice bran treated Gn pigs had a significantly lower mean diarrhea duration of 0.2 days. A significantly lower incidence of diarrhea (20%) was observed when compared with the control pigs (100%). The protective effect outperformed two dosages of attenuated HRV vaccination[112]. Remarkably, Gn pigs were completely protected from HRV diarrhea when treated with rice bran feeding and attenuated HRV vaccinations[112]. In a follow-up study, co-colonization of LGG and EcN presented a significant protection against HRV diarrhea by lowering the mean duration to 0.7 days, and rice bran completely prevented HRV diarrhea in the LGG+EcN pre-colonized Gn pigs[119]. In all, the high protective efficacy of rice bran, used alone or together with vaccine or probiotics, validated it as a novel and effective measure to prevent and treat HRV-induced diarrhea.

### 1.3.3 Mechanisms for rice bran usage in reducing diarrhea

Rice bran comprises over 450 distinct phytochemicals[108], and the compositions and concentrations might differ across cultivars, cultivation regions, and extraction methods. Although numerous studies have demonstrated the beneficial effects of rice bran and extracts, the underlying mechanisms could vary case by case and depend on the experimental hosts and objectives. As to the diarrhea ameliorating property, we summarized the corresponding mechanisms in several aspects.

#### 1.3.3.1 Antimicrobial and antiviral activities

A traditional first-line treatment for diarrhea caused by pathogen is to interfere or eliminate the malicious microorganisms. At least 15 metabolites identified in rice bran might contribute to its antimicrobial and antiviral ability[108], which have been evaluated on a variety of

bacteria and viruses. For instance, rice bran extracts reduced the entry and replication of *Salmonella* in intestinal epithelial cells[120]. Sulfated rice bran glucans exhibited strong anti-cytomegalovirus activity on preventing viral entry of target hosts[121], indicating the blockade by rice bran at the stage of pathogen entry. Moreover, rice bran or extracts inhibited the colonization and/or replication of *Salmonella*[122, 123], *Vibrio cholerae*, *Shigella* spp, *Escherichia coli*[124], *Clostiridium*[125], hepatitis C virus[116], and human immunodeficiency virus[126].

**1.3.3.2 Prebiotic and microbiota-modulatory properties**

The prebiotic property of rice bran in enhancing the growth of probiotics was shown in many studies. Besides the *Salmonella* reducing effect, dietary rice bran promoted the colonization of native *Lactobacillus* spp in mice[110, 123]. Similarly, rice bran improved the health condition of weaning pigs by increasing intestinal *Bifidobacterium* spp[127]. The prebiotic activity of rice bran was also observed in Gn pigs by promoting the colonization of LGG and/or EcN, which was associated with their protective effects on HRV diarrhea[119].

Probiotic lactobacilli increase the production of colonic short-chain fatty acids (SCFA)[128, 129]. Rice bran also increases the production of SCFA by colonic bacterial fermentation[130]. SCFAs influence net intestinal $Na^+$, $Cl^-$ and water absorption by increasing $Na^+$ absorption via upregulation of NHE3 ($Na^+/H^+$ exchanger), $Cl^-$ absorption by upregulation of $Cl^-/HCO_3^-$ exchanger DRA (down-regulated in adenoma)[131], and inhibiting $Cl^-$ secretion[132-134]. Gn pigs fed rice bran and probiotics had drastically reduced incidence, shortened duration and reduced severity of HRV diarrhea, despite no reduction in virus shedding after challenge, suggesting modulation of ion transporter function by rice bran and/or probiotics as a possible mechanism[119].

In addition to regulating the growth of certain bacterial species, rice bran has a global impact on the entire gut microbial composition[135, 136]. Gut microbiome has gained unprecedented attention for its close association with human health and immunity, especially with gastrointestinal health[137], and emerging data in recent years indicates that microbiota modulates enteric viral infections[138, 139]. There is no doubt that the potential mechanisms of rice bran in alleviating diarrhea in terms of modulating diarrhea pathophysiology and intestinal microbiome warrants further investigation.

**1.3.3.3 Effects on intestinal immunity and overall health**

In general, the immunomodulatory role of rice bran largely accounts for its multifarious health benefits[109]. Enhanced activity of B cells, T cells, dendritic cells, and natural killer cells were observed from the treatment by rice bran or extracts *in vivo* or *in vitro*[110, 140-143], suggesting the potentially enhanced protective immunity against enteric infection. Specifically, in rice bran fed mice, reduced *Salmonella* colonization was positively correlated with the induction of cellular immune responses in the small intestine and certain metabolites, such as α-linolenic acid and γ-tocotrienol[122, 123]. In rice bran fed Gn pigs, the reduced HRV diarrhea could be attributed to the enhanced intestinal and systemic IFN-γ producing T cell responses and the elevated virus-specific intestinal IgA antibody levels[112]. Furthermore, the alterations of lipid and amino acid/peptide metabolism induced by rice bran consumption contributed to the complete protection against HRV diarrhea in Gn pigs[144].

Due to the macronutrient and micronutrient richness, rice bran improved the growth of human infants and Gn pigs[119], indicating enhanced nutrient intake via the gut and overall health. The beneficial effects on the gut might be exerted by the maintenance or improvement of healthy

intestinal morphology. For instance, rice bran fed Gn pigs had significantly lower ileal villus width and mitotic index under HRV infection[119], indicating that rice bran prevented viral induced damage on the intestine. Data from the pilot studies of rice bran intake in infants showed that rice bran-fed participants had markers of decreased intestinal permeability and inflammation, and increased growth, including lower fecal alpha-1-antitrypsin ($p$ = 0.02) and higher serum glucagon-like-peptide 2 ($p$ = 0.03) which is secreted from enteroendocrine L cells, associated with decreased inflammation, and promotes intestinal growth[145]. More importantly, the rice bran group had significantly increased length-for-age Z-score from 6 to 12 months compared to control ($p$ < 0.01). The diarrhea prevalence was 33% in the rice bran group compared to 79% in the control group. In the safety evaluation, there were no serious adverse events, no increases in serum heavy metal concentrations, and no decreases in iron absorption in the rice bran group (personal communication).

## 1.4 Concluding remarks

HuNoVs are the predominant cause of epidemic acute gastroenteritis worldwide. Given the enormous disease burden and financial cost, vaccines and antiviral drugs are in urgent demand to prevent and treat HuNoV infection and gastroenteritis. However, our understanding of HuNoV biology has been limited in the first place, by the long lack of a robust cell culture and small animal model. Hence, clinical stool samples from HuNoV-infected patients have been the only virus resource for HuNoV infection studies. Among the efforts in establishing *in vitro* models, HuNoV passage in 3D intestinal cells were not reproducible[146, 147]; reverse genetics enabled the production of virion or virus-like particle derived from HuNoV genomic or subgenomic RNA[148],

but the productivity remains to be improved. Later, B cells supplemented with free HBGA or HBGA-expressing *E. cloacae* was reported to have 10-100 times increase in HuNoV RNA copies after cultivation[24], which inspired us to expand our Gn pig model with *E. cloacae* colonization to achieve effective HuNoV propagation and to verify viral infection in B cells. However, our findings in Gn pigs do not support the conclusion from the *in vitro* studies.

HuNoV infection and replication were observed in Balb/c mice deficient in RAG/IL2RG, but the low level of replication and lack of virus shedding exclude its application for HuNoV propagation[16]. Recent advances in genome editing technology, especially the CRISPR/Cas9 system, allow us to generate genetically engineered pigs at higher efficiency[149]. Given the numerous advantages of Gn pigs in the study of HuNoV infection and disease, RAG2/IL2RG deficient Gn pigs are expected to support higher HuNoV infection than that of wild-type pigs and RAG2/IL2RG deficient mice. In addition, HuNoV infection can become persistent with prolonged virus shedding in immunocompromised patients, who may suffer from increasingly debilitating and life-threatening gastroenteritis[27, 150], and this patient cohort requires a specific animal model that supports HuNoV infection and mimics the immunodeficiency for the development of therapeutic strategies. By depleting all major lymphocytes, RAG2/IL2RG deficient Gn pigs present great promise to recapitulate the hallmarks of HuNoV infection in immunocompromised patients.

The combination of probiotics and rice bran is a promising approach to reduce HuNoV infection and diarrhea, with increasing specific evidences supporting the idea. Probiotic bacteria can bind HuNoV P particles on their surface *in vitro*, and the presence of *Lactobacillus casei* BL23 and EcN might inhibit P particle attachment to epithelial cells[151]. In another study, the presence of *Bifidobacterium adolescentis* inhibited the attachment of HuNoV GI.1 virus-like particle to

epithelial cells *in vitro*[152], indicating the inhibitory role of probiotics on the initial viral infection stage. However, instead of affecting the viral attachment, *B. adolescentis* decreased the replication of MNV in RAW 264.7 cells[152]. Vitamin A was shown to inhibit MNV replication in mice by upregulating lactobacilli in gut microbiota, and anti-MNV effects of lactobacilli were confirmed in RAW264.7 cells[153]. Evaluation of the effects of consuming *Lactobacillus casei* strain Shirota fermented milk on HuNoV gastroenteritis during an outbreak in Japan demonstrated that the elderly HuNoV-infected patients (about 84 years old) who continuously consumed the milk experienced a shorter duration of fever than the non-treated patients (1.5 versus 2.9 days), although the incidence of HuNoV gastroenteritis did not differ between the two groups[154]. Together with our previous success in reducing HRV diarrhea in Gn pigs using LGG+EcN and rice bran[112, 119], the intervention strategy of probiotics and rice bran on HuNoV infection and diarrhea warrants further studies in animal models to elucidate the mechanisms of action and in human clinical trials to evaluate the efficacy, safety and optimal dosage.

## Reference


1. Zheng, D.P. et al. Norovirus classification and proposed strain nomenclature. *Virology* **346**, 312-23 (2006).
2. Pringle, K. et al. Noroviruses: epidemiology, immunity and prospects for prevention. *Future Microbiol* **10**, 53-67 (2015).
3. Hemming, M. et al. Major reduction of rotavirus, but not norovirus, gastroenteritis in children seen in hospital after the introduction of RotaTeq vaccine into the National Immunization Programme in Finland. *Eur J Pediatr* **172**, 739-46 (2013).
4. Payne, D.C. et al. Norovirus and medically attended gastroenteritis in U.S. children. *N Engl J Med* **368**, 1121-30 (2013).
5. Patel, M.M. et al. Systematic literature review of role of noroviruses in sporadic gastroenteritis. *Emerg Infect Dis* **14**, 1224-31 (2008).
6. Gastanaduy, P.A., Hall, A.J., Curns, A.T., Parashar, U.D. & Lopman, B.A. Burden of norovirus gastroenteritis in the ambulatory setting--United States, 2001-2009. *J Infect Dis* **207**, 1058-65 (2013).
7. Hall, A.J. et al. Norovirus disease in the United States. *Emerg Infect Dis* **19**, 1198-205 (2013).
8. Patel, M.M., Hall, A.J., Vinje, J. & Parashar, U.D. Noroviruses: a comprehensive review. *J Clin Virol* **44**, 1-8 (2009).
9. O'Ryan, M.L. et al. Prospective characterization of norovirus compared with rotavirus acute diarrhea episodes in chilean children. *Pediatr Infect Dis J* **29**, 855-9 (2010).
10. Karst, S.M. Pathogenesis of noroviruses, emerging RNA viruses. *Viruses* **2**, 748-81 (2010).
11. Riddle, M.S. & Walker, R.I. Status of vaccine research and development for norovirus. *Vaccine* **34**, 2895-2899 (2016).
12. Bok, K. et al. Chimpanzees as an animal model for human norovirus infection and vaccine development. *Proc Natl Acad Sci U S A* **108**, 325-30 (2011).
13. Souza, M., Azevedo, M.S., Jung, K., Cheetham, S. & Saif, L.J. Pathogenesis and immune responses in gnotobiotic calves after infection with the genogroup II.4-HS66 strain of human norovirus. *J Virol* **82**, 1777-86 (2008).
14. Bui, T. et al. Median infectious dose of human norovirus GII.4 in gnotobiotic pigs is decreased by simvastatin treatment and increased by age. *J Gen Virol* **94**, 2005-16 (2013).
15. Cheetham, S. et al. Pathogenesis of a genogroup II human norovirus in gnotobiotic pigs. *J Virol* **80**, 10372-81 (2006).
16. Taube, S. et al. A mouse model for human norovirus. *MBio* **4**, e00450-13 (2013).
17. Agus, S.G., Dolin, R., Wyatt, R.G., Tousimis, A.J. & Northrup, R.S. Acute infectious nonbacterial gastroenteritis: intestinal histopathology. Histologic and enzymatic alterations during illness produced by the Norwalk agent in man. *Ann Intern Med* **79**, 18-25 (1973).
18. Schreiber, D.S., Blacklow, N.R. & Trier, J.S. The mucosal lesion of the proximal small intestine in acute infectious nonbacterial gastroenteritis. *N Engl J Med* **288**, 1318-23 (1973).
19. Schreiber, D.S., Blacklow, N.R. & Trier, J.S. The small intestinal lesion induced by Hawaii agent acute infectious nonbacterial gastroenteritis. *J Infect Dis* **129**, 705-8 (1974).
20. Dolin, R., Levy, A.G., Wyatt, R.G., Thornhill, T.S. & Gardner, J.D. Viral gastroenteritis induced by the Hawaii agent. Jejunal histopathology and serologic response. *Am J Med* **59**, 761-8 (1975).
21. Karst, S.M., Wobus, C.E., Goodfellow, I.G., Green, K.Y. & Virgin, H.W. Advances in norovirus biology. *Cell Host Microbe* **15**, 668-80 (2014).
22. Karandikar, U.C. et al. Detection of human norovirus in intestinal biopsies from immunocompromised transplant patients. *J Gen Virol* **97**, 2291-300 (2016).

23. Ettayebi, K. et al. Replication of human noroviruses in stem cell-derived human enteroids. *Science* **353**, 1387-1393 (2016).
24. Jones, M.K. et al. Enteric bacteria promote human and mouse norovirus infection of B cells. *Science* **346**, 755-9 (2014).
25. Jones, M.K. et al. Human norovirus culture in B cells. *Nat Protoc* **10**, 1939-47 (2015).
26. Brown, J.R., Gilmour, K. & Breuer, J. Norovirus Infections Occur in B-Cell-Deficient Patients. *Clin Infect Dis* **62**, 1136-8 (2016).
27. Bok, K. & Green, K.Y. Norovirus gastroenteritis in immunocompromised patients. *N Engl J Med* **367**, 2126-32 (2012).
28. Kehrer-Sawatzki, H. & Cooper, D.N. Understanding the recent evolution of the human genome: insights from human-chimpanzee genome comparisons. *Hum Mutat* **28**, 99-130 (2007).
29. O'Neil, S.P. et al. Progressive infection in a subset of HIV-1-positive chimpanzees. *J Infect Dis* **182**, 1051-62 (2000).
30. Pfaender, S., Brown, R.J., Pietschmann, T. & Steinmann, E. Natural reservoirs for homologs of hepatitis C virus. *Emerg Microbes Infect* **3**, e21 (2014).
31. Purcell, R.H. & Emerson, S.U. Animal models of hepatitis A and E. *ILAR J* **42**, 161-77 (2001).
32. Kolawole, A.O., Rocha-Pereira, J., Elftman, M.D., Neyts, J. & Wobus, C.E. Inhibition of human norovirus by a viral polymerase inhibitor in the B cell culture system and in the mouse model. *Antiviral Res* **132**, 46-9 (2016).
33. Wang, M. & Donovan, S.M. Human microbiota-associated swine: current progress and future opportunities. *ILAR J* **56**, 63-73 (2015).
34. Saif, L.J., Ward, L.A., Yuan, L., Rosen, B.I. & To, T.L. The gnotobiotic piglet as a model for studies of disease pathogenesis and immunity to human rotaviruses. *Arch Virol Suppl* **12**, 153-61 (1996).
35. Ball, R.O., House, J.D., Wykes, L.J. & Pencharz, P.B. in Advances in Swine in Biomedical Research (eds. Tumbleson, M.E. & Schook, L.B.) 713-731 (Plenum Press, New York, 1996).
36. Kocher, J. et al. Intranasal P particle vaccine provided partial cross-variant protection against human GII.4 norovirus diarrhea in gnotobiotic pigs. *J Virol* **88**, 9728-43 (2014).
37. Souza, M., Cheetham, S.M., Azevedo, M.S., Costantini, V. & Saif, L.J. Cytokine and antibody responses in gnotobiotic pigs after infection with human norovirus genogroup II.4 (HS66 strain). *J Virol* **81**, 9183-92 (2007).
38. Souza, M., Costantini, V., Azevedo, M.S. & Saif, L.J. A human norovirus-like particle vaccine adjuvanted with ISCOM or mLT induces cytokine and antibody responses and protection to the homologous GII.4 human norovirus in a gnotobiotic pig disease model. *Vaccine* **25**, 8448-59 (2007).
39. Fang, H., Tan, M., Xia, M., Wang, L. & Jiang, X. Norovirus P particle efficiently elicits innate, humoral and cellular immunity. *PLoS One* **8**, e63269 (2013).
40. Kocher, J. & Yuan, L. Norovirus vaccines and potential antinorovirus drugs: recent advances and future perspectives. *Future Virol* **10**, 899-913 (2015).
41. Knowles, N.J. & Reuter, G. in Diseases of Swine (eds. Zimmerman, J.J., Karriker, L.A., Ramirez, A., Schwartz, K.J. & Stevenson, G.W.) 493-500 (John Wiley & Sons, 2012).
42. Wang, Q.H. et al. Porcine noroviruses related to human noroviruses. *Emerg Infect Dis* **11**, 1874-81 (2005).
43. Tin, C.M. et al. A Luciferase Immunoprecipitation System (LIPS) assay for profiling human norovirus antibodies. *J Virol Methods* **248**, 116-129 (2017).
44. Kuss, S.K. et al. Intestinal microbiota promote enteric virus replication and systemic pathogenesis. *Science* **334**, 249-52 (2011).
45. Kane, M. et al. Successful transmission of a retrovirus depends on the commensal microbiota. *Science* **334**, 245-9 (2011).

46. Wilks, J. et al. Mammalian Lipopolysaccharide Receptors Incorporated into the Retroviral Envelope Augment Virus Transmission. *Cell Host Microbe* **18**, 456-62 (2015).
47. Nelson, A.M. et al. Disruption of the human gut microbiota following Norovirus infection. *PLoS One* **7**, e48224 (2012).
48. Karst, S.M., Wobus, C.E., Lay, M., Davidson, J. & Virgin, H.W.t. STAT1-dependent innate immunity to a Norwalk-like virus. *Science* **299**, 1575-8 (2003).
49. Baldridge, M.T. et al. Commensal microbes and interferon-lambda determine persistence of enteric murine norovirus infection. *Science* **347**, 266-9 (2015).
50. Nelson, A.M. et al. Murine norovirus infection does not cause major disruptions in the murine intestinal microbiota. *Microbiome* **1**, 7 (2013).
51. Basic, M. et al. Norovirus triggered microbiota-driven mucosal inflammation in interleukin 10-deficient mice. *Inflamm Bowel Dis* **20**, 431-43 (2014).
52. Schnadower, D., Finkelstein, Y. & Freedman, S.B. Ondansetron and probiotics in the management of pediatric acute gastroenteritis in developed countries. *Curr Opin Gastroenterol* **31**, 1-6 (2015).
53. Licciardi, P.V. & Tang, M.L. Vaccine adjuvant properties of probiotic bacteria. *Discov Med* **12**, 525-33 (2011).
54. Ng, S.C., Hart, A.L., Kamm, M.A., Stagg, A.J. & Knight, S.C. Mechanisms of action of probiotics: recent advances. *Inflamm Bowel Dis* **15**, 300-10 (2009).
55. Fang, S.B. et al. Dose-dependent effect of Lactobacillus rhamnosus on quantitative reduction of faecal rotavirus shedding in children. *J Trop Pediatr* **55**, 297-301 (2009).
56. Guarino, A., Guandalini, S. & Lo Vecchio, A. Probiotics for Prevention and Treatment of Diarrhea. *J Clin Gastroenterol* **49 Suppl 1**, S37-45 (2015).
57. Ouwehand, A.C. A review of dose-responses of probiotics in human studies. *Benef Microbes* **8**, 143-151 (2017).
58. Wen, K. et al. Lactobacillus rhamnosus GG Dosage Affects the Adjuvanticity and Protection Against Rotavirus Diarrhea in Gnotobiotic Pigs. *J Pediatr Gastroenterol Nutr* **60**, 834-43 (2015).
59. Crawford, S.E. et al. Rotavirus infection. *Nat Rev Dis Primers* **3**, 17083 (2017).
60. Desselberger, U. Rotaviruses. *Virus Research* **190**, 75-96 (2014).
61. Sarowska, J., Choroszy-Krol, I., Regulska-Ilow, B., Frej-Madrzak, M. & Jama-Kmiecik, A. The therapeutic effect of probiotic bacteria on gastrointestinal diseases. *Adv Clin Exp Med* **22**, 759-66 (2013).
62. Pace, F., Pace, M. & Quartarone, G. Probiotics in digestive diseases: focus on Lactobacillus GG. *Minerva Gastroenterol Dietol* **61**, 273-92 (2015).
63. Szajewska, H. & Kolodziej, M. Systematic review with meta-analysis: Lactobacillus rhamnosus GG in the prevention of antibiotic-associated diarrhoea in children and adults. *Aliment Pharmacol Ther* **42**, 1149-57 (2015).
64. Hojsak, I. et al. Probiotics for the Prevention of Nosocomial Diarrhea in Children. *J Pediatr Gastroenterol Nutr* **66**, 3-9 (2018).
65. Szajewska, H., Wanke, M. & Patro, B. Meta-analysis: the effects of Lactobacillus rhamnosus GG supplementation for the prevention of healthcare-associated diarrhoea in children. *Aliment Pharmacol Ther* **34**, 1079-87 (2011).
66. Zhang, L. et al. Evaluation of Lactobacillus rhamnosus GG using an Escherichia coli K88 model of piglet diarrhoea: Effects on diarrhoea incidence, faecal microflora and immune responses. *Vet Microbiol* **141**, 142-8 (2010).
67. Ahmadi, E., Alizadeh-Navaei, R. & Rezai, M.S. Efficacy of probiotic use in acute rotavirus diarrhea in children: A systematic review and meta-analysis. *Caspian Journal of Internal Medicine* **6**, 187-195 (2015).

68. Liu, F. et al. Lactobacillus rhamnosus GG on rotavirus-induced injury of ileal epithelium in gnotobiotic pigs. *J Pediatr Gastroenterol Nutr* **57**, 750-8 (2013).
69. Wu, S. et al. Probiotic Lactobacillus rhamnosus GG mono-association suppresses human rotavirus-induced autophagy in the gnotobiotic piglet intestine. *Gut Pathog* **5**, 22 (2013).
70. Wen, K. et al. Probiotic Lactobacillus rhamnosus GG enhanced Th1 cellular immunity but did not affect antibody responses in a human gut microbiota transplanted neonatal gnotobiotic pig model. *PLoS One* **9**, e94504 (2014).
71. Zhang, H. et al. Probiotics and virulent human rotavirus modulate the transplanted human gut microbiota in gnotobiotic pigs. *Gut Pathog* **6**, 39 (2014).
72. Turroni, F. et al. Exploring the diversity of the bifidobacterial population in the human intestinal tract. *Appl Environ Microbiol* **75**, 1534-45 (2009).
73. Turroni, F. et al. Deciphering bifidobacterial-mediated metabolic interactions and their impact on gut microbiota by a multi-omics approach. *Isme j* **10**, 1656-68 (2016).
74. Milani, C. et al. Bifidobacteria exhibit social behavior through carbohydrate resource sharing in the gut. *Sci Rep* **5**, 15782 (2015).
75. Tojo, R. et al. Intestinal microbiota in health and disease: role of bifidobacteria in gut homeostasis. *World J Gastroenterol* **20**, 15163-76 (2014).
76. Hidalgo-Cantabrana, C., Ruiz, S.D.L., Ruas-Madiedo, P., Sanchez, B. & Margolles, A. Bifidobacteria and Their Health-Promoting Effects. *Microbiology Spectrum* **5** (2017).
77. Munoz, J.A. et al. Novel probiotic Bifidobacterium longum subsp. infantis CECT 7210 strain active against rotavirus infections. *Appl Environ Microbiol* **77**, 8775-83 (2011).
78. Chenoll, E. et al. Identification of a Peptide Produced by Bifidobacterium longum CECT 7210 with Antirotaviral Activity. *Front Microbiol* **7**, 655 (2016).
79. Gagnon, M., Vimont, A., Darveau, A., Fliss, I. & Jean, J. Study of the Ability of Bifidobacteria of Human Origin to Prevent and Treat Rotavirus Infection Using Colonic Cell and Mouse Models. *PLoS One* **11**, e0164512 (2016).
80. Kandasamy, S., Chattha, K.S., Vlasova, A.N., Rajashekara, G. & Saif, L.J. Lactobacilli and Bifidobacteria enhance mucosal B cell responses and differentially modulate systemic antibody responses to an oral human rotavirus vaccine in a neonatal gnotobiotic pig disease model. *Gut Microbes* **5**, 639-51 (2014).
81. Schultz, M. Clinical use of E. coli Nissle 1917 in inflammatory bowel disease. *Inflamm Bowel Dis* **14**, 1012-8 (2008).
82. Losurdo, G. et al. Escherichia coli Nissle 1917 in Ulcerative Colitis Treatment: Systematic Review and Meta-analysis. *J Gastrointestin Liver Dis* **24**, 499-505 (2015).
83. Henker, J. et al. The probiotic Escherichia coli strain Nissle 1917 (EcN) stops acute diarrhoea in infants and toddlers. *Eur J Pediatr* **166**, 311-8 (2007).
84. Henker, J. et al. Probiotic Escherichia coli Nissle 1917 versus placebo for treating diarrhea of greater than 4 days duration in infants and toddlers. *Pediatr Infect Dis J* **27**, 494-9 (2008).
85. von Buenau, R. et al. Escherichia coli strain Nissle 1917: significant reduction of neonatal calf diarrhea. *J Dairy Sci* **88**, 317-23 (2005).
86. Schroeder, B. et al. Preventive effects of the probiotic Escherichia coli strain Nissle 1917 on acute secretory diarrhea in a pig model of intestinal infection. *Dig Dis Sci* **51**, 724-31 (2006).
87. Hering, N.A. et al. TcpC protein from E. coli Nissle improves epithelial barrier function involving PKCzeta and ERK1/2 signaling in HT-29/B6 cells. *Mucosal Immunol* **7**, 369-78 (2014).
88. Splichalova, A. et al. Interference of Bifidobacterium choerinum or Escherichia coli Nissle 1917 with Salmonella Typhimurium in gnotobiotic piglets correlates with cytokine patterns in blood and intestine. *Clin Exp Immunol* **163**, 242-9 (2011).

89. Helmy, Y.A., Kassem, II, Kumar, A. & Rajashekara, G. In Vitro Evaluation of the Impact of the Probiotic E. coli Nissle 1917 on Campylobacter jejuni's Invasion and Intracellular Survival in Human Colonic Cells. *Front Microbiol* **8**, 1588 (2017).
90. Kandasamy, S. et al. Differential Effects of Escherichia coli Nissle and Lactobacillus rhamnosus Strain GG on Human Rotavirus Binding, Infection, and B Cell Immunity. *J Immunol* **196**, 1780-9 (2016).
91. Vlasova, A.N. et al. Escherichia coli Nissle 1917 protects gnotobiotic pigs against human rotavirus by modulating pDC and NK-cell responses. *Eur J Immunol* **46**, 2426-2437 (2016).
92. Kandasamy, S. et al. Unraveling the Differences between Gram-Positive and Gram-Negative Probiotics in Modulating Protective Immunity to Enteric Infections. *Front Immunol* **8**, 334 (2017).
93. Szajewska, H. & Kolodziej, M. Systematic review with meta-analysis: Saccharomyces boulardii in the prevention of antibiotic-associated diarrhoea. *Aliment Pharmacol Ther* **42**, 793-801 (2015).
94. Correa, N.B., Penna, F.J., Lima, F.M., Nicoli, J.R. & Filho, L.A. Treatment of acute diarrhea with Saccharomyces boulardii in infants. *J Pediatr Gastroenterol Nutr* **53**, 497-501 (2011).
95. Szajewska, H. et al. Use of Probiotics for Management of Acute Gastroenteritis: A Position Paper by the ESPGHAN Working Group for Probiotics and Prebiotics. *Journal of Pediatric Gastroenterology and Nutrition* **58**, 531-539 (2014).
96. Born, P., Lersch, C., Zimmerhackl, B. & Classen, M. [The Saccharomyces boulardii therapy of HIV-associated diarrhea]. *Dtsch Med Wochenschr* **118**, 765 (1993).
97. James, J.S. Diarrhea, and the experimental treatment Saccharomyces boulardii. *AIDS Treat News*, 1-4 (1995).
98. McFarland, L.V. Systematic review and meta-analysis of Saccharomyces boulardii in adult patients. *World J Gastroenterol* **16**, 2202-22 (2010).
99. Tung, J.M., Dolovich, L.R. & Lee, C.H. Prevention of Clostridium difficile infection with Saccharomyces boulardii: a systematic review. *Can J Gastroenterol* **23**, 817-21 (2009).
100. Szajewska, H., Horvath, A. & Kolodziej, M. Systematic review with meta-analysis: Saccharomyces boulardii supplementation and eradication of Helicobacter pylori infection. *Aliment Pharmacol Ther* **41**, 1237-45 (2015).
101. Das, S., Gupta, P.K. & Das, R.R. Efficacy and Safety of Saccharomyces boulardii in Acute Rotavirus Diarrhea: Double Blind Randomized Controlled Trial from a Developing Country. *J Trop Pediatr* **62**, 464-470 (2016).
102. Grandy, G., Medina, M., Soria, R., Teran, C.G. & Araya, M. Probiotics in the treatment of acute rotavirus diarrhoea. A randomized, double-blind, controlled trial using two different probiotic preparations in Bolivian children. *BMC Infect Dis* **10**, 253 (2010).
103. Buccigrossi, V. et al. Chloride secretion induced by rotavirus is oxidative stress-dependent and inhibited by Saccharomyces boulardii in human enterocytes. *PLoS One* **9**, e99830 (2014).
104. Muthayya, S., Sugimoto, J.D., Montgomery, S. & Maberly, G.F. An overview of global rice production, supply, trade, and consumption. *Ann N Y Acad Sci* **1324**, 7-14 (2014).
105. da Silva, M.A., Sanches, C. & Amante, E.R. Prevention of hydrolytic rancidity in rice bran. *Journal of Food Engineering* **75**, 487-491 (2006).
106. Ramezanzadeh, F.M. et al. Prevention of hydrolytic rancidity in rice bran during storage. *J Agric Food Chem* **47**, 3050-2 (1999).
107. Prasad, M.N., Sanjay, K., Khatokar, M.S., Vismaya, M. & Swamy, S.N. Health Benefits of Rice Bran - A Review. *Journal of Nutrition & Food Sciences* **01** (2011).
108. Zarei, I., Brown, D.G., Nealon, N.J. & Ryan, E.P. Rice Bran Metabolome Contains Amino Acids, Vitamins & Cofactors, and Phytochemicals with Medicinal and Nutritional Properties. *Rice (N Y)* **10**, 24 (2017).

109. Park, H.Y., Lee, K.W. & Choi, H.D. Rice bran constituents: immunomodulatory and therapeutic activities. *Food Funct* **8**, 935-943 (2017).
110. Henderson, A.J., Kumar, A., Barnett, B., Dow, S.W. & Ryan, E.P. Consumption of rice bran increases mucosal immunoglobulin A concentrations and numbers of intestinal Lactobacillus spp. *J Med Food* **15**, 469-75 (2012).
111. Park, H.Y. et al. Immunomodulatory Effects of Nontoxic Glycoprotein Fraction Isolated from Rice Bran. *Planta Med* (2016).
112. Yang, X. et al. Dietary rice bran protects against rotavirus diarrhea and promotes Th1-type immune responses to human rotavirus vaccine in gnotobiotic pigs. *Clin Vaccine Immunol* **21**, 1396-403 (2014).
113. Cheng, H.H. et al. Ameliorative effects of stabilized rice bran on type 2 diabetes patients. *Ann Nutr Metab* **56**, 45-51 (2010).
114. de Munter, J.S., Hu, F.B., Spiegelman, D., Franz, M. & van Dam, R.M. Whole grain, bran, and germ intake and risk of type 2 diabetes: a prospective cohort study and systematic review. *PLoS Med* **4**, e261 (2007).
115. Kamiya, T. et al. Therapeutic effects of biobran, modified arabinoxylan rice bran, in improving symptoms of diarrhea predominant or mixed type irritable bowel syndrome: a pilot, randomized controlled study. *Evid Based Complement Alternat Med* **2014**, 828137 (2014).
116. Salama, H. et al. Arabinoxylan rice bran (Biobran) suppresses the viremia level in patients with chronic HCV infection: A randomized trial. *Int J Immunopathol Pharmacol* **29**, 647-653 (2016).
117. Henderson, A.J. et al. Chemopreventive properties of dietary rice bran: current status and future prospects. *Adv Nutr* **3**, 643-53 (2012).
118. Holtmann, G.J., Ford, A.C. & Talley, N.J. Pathophysiology of irritable bowel syndrome. *Lancet Gastroenterol Hepatol* **1**, 133-146 (2016).
119. Yang, X. et al. High protective efficacy of rice bran against human rotavirus diarrhea via enhancing probiotic growth, gut barrier function, and innate immunity. *Sci Rep* **5**, 15004 (2015).
120. Ghazi, I.A. et al. Rice Bran Extracts Inhibit Invasion and Intracellular Replication ofSalmonella typhimurium in Mouse and Porcine Intestinal Epithelial Cells. *Med Aromat Plants (Los Angel)* **5**, 271 (2016).
121. Ray, B. et al. Chemically Engineered Sulfated Glucans from Rice Bran Exert Strong Antiviral Activity at the Stage of Viral Entry. *Journal of Natural Products* **76**, 2180-2188 (2013).
122. Goodyear, A. et al. Dietary rice bran supplementation prevents Salmonella colonization differentially across varieties and by priming intestinal immunity. *Journal of Functional Foods* **18**, 653-664 (2015).
123. Kumar, A. et al. Dietary rice bran promotes resistance to Salmonella enterica serovar Typhimurium colonization in mice. *BMC Microbiol* **12**, 71 (2012).
124. Kondo, S., Teongtip, R., Srichana, D. & Itharat, A. Antimicrobial activity of rice bran extracts for diarrheal disease. *J Med Assoc Thai* **94 Suppl 7**, S117-21 (2011).
125. Komiyama, Y. et al. New prebiotics from rice bran ameliorate inflammation in murine colitis models through the modulation of intestinal homeostasis and the mucosal immune system. *Scand J Gastroenterol* **46**, 40-52 (2011).
126. Ghoneum, M. Anti-HIV activity in vitro of MGN-3, an activated arabinoxylane from rice bran. *Biochem Biophys Res Commun* **243**, 25-9 (1998).
127. Herfel, T. et al. Stabilized rice bran improves weaning pig performance via a prebiotic mechanism. *J Anim Sci* **91**, 907-13 (2013).
128. Tsukahara, T., Hashizume, K., Koyama, H. & Ushida, K. Stimulation of butyrate production through the metabolic interaction among lactic acid bacteria, Lactobacillus acidophilus, and lactic acid-

utilizing bacteria, Megasphaera elsdenii, in porcine cecal digesta. *Animal Science Journal* **77**, 454-461 (2006).
129. Wullt, M., Johansson Hagslatt, M.L., Odenholt, I. & Berggren, A. Lactobacillus plantarum 299v enhances the concentrations of fecal short-chain fatty acids in patients with recurrent clostridium difficile-associated diarrhea. *Dig Dis Sci* **52**, 2082-6 (2007).
130. Fukushima, M., Fujii, S., Yoshimura, Y., Endo, T. & Nakano, M. Effect of rice bran on intraintestinal fermentation and cholesterol metabolism in cecectomized rats. *Nutrition Research* **19**, 235-245 (1999).
131. Malakooti, J., Saksena, S., Gill, R.K. & Dudeja, P.K. Transcriptional regulation of the intestinal luminal Na(+) and Cl(-) transporters. *Biochem J* **435**, 313-25 (2011).
132. Binder, H.J. Role of colonic short-chain fatty acid transport in diarrhea. *Annu Rev Physiol* **72**, 297-313 (2010).
133. den Besten, G. et al. The role of short-chain fatty acids in the interplay between diet, gut microbiota, and host energy metabolism. *J Lipid Res* **54**, 2325-40 (2013).
134. Musch, M.W., Bookstein, C., Xie, Y., Sellin, J.H. & Chang, E.B. SCFA increase intestinal Na absorption by induction of NHE3 in rat colon and human intestinal C2/bbe cells. *Am J Physiol Gastrointest Liver Physiol* **280**, G687-93 (2001).
135. Sheflin, A.M. et al. Dietary supplementation with rice bran or navy bean alters gut bacterial metabolism in colorectal cancer survivors. *Mol Nutr Food Res* **61** (2017).
136. Sheflin, A.M. et al. Pilot dietary intervention with heat-stabilized rice bran modulates stool microbiota and metabolites in healthy adults. *Nutrients* **7**, 1282-300 (2015).
137. Thaiss, C.A., Zmora, N., Levy, M. & Elinav, E. The microbiome and innate immunity. *Nature* **535**, 65-74 (2016).
138. Pfeiffer, J.K. & Virgin, H.W. Viral immunity. Transkingdom control of viral infection and immunity in the mammalian intestine. *Science* **351** (2016).
139. Uchiyama, R., Chassaing, B., Zhang, B. & Gewirtz, A.T. Antibiotic treatment suppresses rotavirus infection and enhances specific humoral immunity. *J Infect Dis* **210**, 171-82 (2014).
140. Ghoneum, M. & Gollapudi, S. Modified arabinoxylan rice bran (MGN-3/Biobran) sensitizes human T cell leukemia cells to death receptor (CD95)-induced apoptosis. *Cancer Lett* **201**, 41-9 (2003).
141. Ghoneum, M. & Abedi, S. Enhancement of natural killer cell activity of aged mice by modified arabinoxylan rice bran (MGN-3/Biobran). *J Pharm Pharmacol* **56**, 1581-8 (2004).
142. Ghoneum, M. & Agrawal, S. Activation of human monocyte-derived dendritic cells in vitro by the biological response modifier arabinoxylan rice bran (MGN-3/Biobran). *Int J Immunopathol Pharmacol* **24**, 941-8 (2011).
143. Cholujova, D., Jakubikova, J. & Sedlak, J. BioBran-augmented maturation of human monocyte-derived dendritic cells. *Neoplasma* **56**, 89-95 (2009).
144. Nealon, N.J., Yuan, L., Yang, X. & Ryan, E.P. Rice Bran and Probiotics Alter the Porcine Large Intestine and Serum Metabolomes for Protection against Human Rotavirus Diarrhea. *Front Microbiol* **8**, 653 (2017).
145. Burrin, D.G., Petersen, Y., Stoll, B. & Sangild, P. Glucagon-like peptide 2: a nutrient-responsive gut growth factor. *J Nutr* **131**, 709-12 (2001).
146. Papafragkou, E., Hewitt, J., Park, G.W., Greening, G. & Vinje, J. Challenges of culturing human norovirus in three-dimensional organoid intestinal cell culture models. *PLoS One* **8**, e63485 (2014).
147. Herbst-Kralovetz, M.M. et al. Lack of norovirus replication and histo-blood group antigen expression in 3-dimensional intestinal epithelial cells. *Emerg Infect Dis* **19**, 431-8 (2013).
148. Katayama, K. et al. Plasmid-based human norovirus reverse genetics system produces reporter-tagged progeny virus containing infectious genomic RNA. *Proc Natl Acad Sci U S A* **111**, E4043-52 (2014).

149. Gaj, T., Gersbach, C.A. & Barbas, C.F., 3rd. ZFN, TALEN, and CRISPR/Cas-based methods for genome engineering. *Trends Biotechnol* **31**, 397-405 (2013).
150. Green, K.Y. Norovirus infection in immunocompromised hosts. *Clin Microbiol Infect* **20**, 717-23 (2014).
151. Rubio-del-Campo, A. et al. Noroviral p-particles as an in vitro model to assess the interactions of noroviruses with probiotics. *PLoS One* **9**, e89586 (2014).
152. Li, D., Breiman, A., le Pendu, J. & Uyttendaele, M. Anti-viral Effect of Bifidobacterium adolescentis against Noroviruses. *Front Microbiol* **7**, 864 (2016).
153. Lee, H. & Ko, G. Antiviral effect of vitamin A on norovirus infection via modulation of the gut microbiome. *Sci Rep* **6**, 25835 (2016).
154. Nagata, S. et al. Effect of the continuous intake of probiotic-fermented milk containing Lactobacillus casei strain Shirota on fever in a mass outbreak of norovirus gastroenteritis and the faecal microflora in a health service facility for the aged. *Br J Nutr* **106**, 549-56 (2011).
155. Wyatt, R.G. et al. Experimental infection of chimpanzees with the Norwalk agent of epidemic viral gastroenteritis. *J Med Virol* **2**, 89-96 (1978).

**Table 1 Features of animal models for HuNoV infection**

| Host | Gem-free condition | Viral strain | Route of infection | Viral antigen location | Fecal virus shedding | Viremia | Diseases | Pathological changes |
|---|---|---|---|---|---|---|---|---|
| Immunocompetent humans | - | Multiple | oral | N/A | + | +/- | Vomiting and severe diarrhea | + [17-21] |
| Immunocompromised humans | - | Multiple | oral | IECs | + | N/A | Vomiting and severe diarrhea | + [22, 27, 150] |
| Chimpanzees | - | GI.1 | oral [155]; intravenous [12] | intestinal DC and B cells | + | - | asymptomatic | - [12] |
| Balb/c RAG/$\gamma c^{-/-}$ mice | - | GII mix | intraperitoneally | Mϕ-like cells in liver and spleen | - | N/A | asymptomatic | - [16] |
| Gnotobiotic pigs | + | GII.4 | oral | IECs | + | + | mild diarrhea | + [14, 15] |
| Gnotobiotic calves | + | GII.4 | oral | IECs and intestinal Mϕ-like cells | + | + | mild diarrhea | + [13] |

IECs: intestinal epithelial cells. Mϕ: macrophage. N/A, not available.

# Chapter 2

## *Enterobacter cloacae* inhibits human norovirus infectivity in gnotobiotic pigs

Shaohua Lei[1], Helen Samuel[1], Erica Twitchell[1], Tammy Bui[1], Ashwin Ramesh[1], Ke Wen[1], Mariah Weiss[1], Guohua Li[1], Xingdong Yang[1], Xi Jiang[2], Lijuan Yuan[1,*]

[1]Department of Biomedical Sciences and Pathobiology, Virginia-Maryland College of Veterinary Medicine, Virginia Tech, Blacksburg, VA 24061, USA.

[2]Division of Infectious Diseases, Cincinnati Children's Hospital Medical Center, Cincinnati, OH 45229, USA.

*Correspondence and requests for materials should be addressed to L.Y. (email: lyuan@vt.edu)

Published in *Scientific Reports*. 2016 Apr 26; 6:25017. Used with permission.

## Abstract

Human noroviruses (HuNoVs) are the leading cause of epidemic gastroenteritis worldwide. Study of HuNoV biology has been hampered by the lack of an efficient cell culture system. Recently, enteric commensal bacteria *Enterobacter cloacae* has been recognized as a helper in HuNoV infection of B cells *in vitro*. To test the influences of *E. cloacae* on HuNoV infectivity and to determine whether HuNoV infects B cells *in vivo*, we colonized gnotobiotic pigs with *E. cloacae* and inoculated pigs with $2.74 \times 10^4$ genome copies of HuNoV. Compared to control pigs, reduced HuNoV shedding was observed in *E. cloacae* colonized pigs, characterized by significantly shorter duration of shedding in post-inoculation day 10 subgroup and lower cumulative shedding and peak shedding in individual pigs. Colonization of *E. cloacae* also reduced HuNoV titers in intestinal tissues and in blood. In both control and *E. cloacae* colonized pigs, HuNoV infection of enterocytes was confirmed, however infection of B cells was not observed in ileum, and the entire lamina propria in sections of duodenum, jejunum, and ileum were HuNoV-negative. In summary, *E. cloacae* inhibited HuNoV infectivity, and B cells were not a target cell type for HuNoV in gnotobiotic pigs, with or without *E. cloacae* colonization.

## Introduction

Human noroviruses (HuNoVs), non-enveloped positive-strand RNA viruses, are the leading cause of viral epidemic acute gastroenteritis worldwide[1]. HuNoVs infect people of all ages, the gastroenteritis is characteristically self-limiting with a duration of 1 to 3 days, but it can be severe and prolonged in infants, young children, elderly, and immunocompromised individuals[2]. As members of the *Norovirus* genus in the *Caliciviridae* family, noroviruses are divided into six genogroups (GI - GVI) based on viral capsid gene sequences, but only GI, GII, and GIV are found in humans and thus known as HuNoVs[3]. Although at least 32 different HuNoV genotypes have been further classified[4], genogroup II genotype 4 (GII.4) has been the predominant genotype causing global acute gastroenteritis outbreaks[5]. In the past two decades, six major epidemics have occurred due to novel GII.4 variants that evolved by recombination and mutation, including the most recent strain, GII.4 Sydney_2012[6]. During the season of 2014-2015, newly emerging GII.17 variants caused outbreaks in Asia, and the urgent need to control the global spread of GII.17 has gained recent attention[7-9]. Unfortunately, no vaccines or virus-specific therapies are currently available to prevent or treat HuNoV infection[10].

HuNoV research has long been impeded by the lack of a robust cultivation system and a suitable animal model. Limited knowledge of HuNoV biology are mainly from viral infection studies in chimpanzees[11], gnotobiotic (Gn) calves and pigs[12-15], immunodeficient mice[16], and human volunteers[2]. *Enterobacter cloacae* was screened from commensal enteric bacteria with surface histo-blood group antigen (HBGA) expression and the ability to bind to HuNoV specifically[17]. *E. cloacae* was subsequently found to promote HuNoV infection of human B cells (BJAB cell line) *in vitro*[18], which is a novel HuNoV infection system that redefined the range of

HuNoV cell tropism and viral infection factors. In this cell culture model, B cells supplemented with free HBGA or HBGA-expressing enteric bacteria, such as *E. cloacae*, were susceptible to HuNoV infection[19]. However, there is a total lack of *in vivo* studies to support the role of *E. cloacae* or other HBGA-expressing enteric bacteria in enhancing HuNoV infection of B cells. In addition, the low-level viral replication in such cultured B cells was inconsistent with high-level virus shedding in human patients, suggesting that B cells might not be the major target cell type of HuNoV[20]. Therefore, *in vivo* evidence is essential to test the stimulatory role of *E. cloacae* and to confirm that B cells are a natural target for robust HuNoV infection and replication.

The neonatal Gn pigs recapitulate the hallmark features of the gastrointestinal tract in young children and have been widely used for enteric virus infection[21, 22]. HuNoV pathogenesis studies and vaccine evaluations in Gn pigs have high translational relevance to those of humans[13, 14, 23]. Compared to chimpanzees (no longer available for biomedical research) and immunodeficient mice, Gn pigs are currently preferable for HuNoV infection study in many ways, such as the ability to become infected via oral route and resulting in diarrhea and fecal virus shedding[24]. In addition, the germ-free environment in the Gn system has enabled the studies of interaction between virus and specific bacterial strains[25-27], as well as human microbiota[28, 29]. In this study, via *E. cloacae* colonization in the well-established neonatal Gn pig model of HuNoV infection and diarrhea, we aimed to (i) elucidate the effects of *E. cloacae* on HuNoV infectivity *in vivo*, (ii) determine whether HuNoV infects B cells *in vivo*, and (iii) explore the mechanism of altered HuNoV infectivity in the presence of *E. cloacae*.

## Results

### *E. cloacae* reduced HuNoV shedding but not diarrhea

To evaluate the effects of *E. cloacae* on HuNoV infection and diseases *in vivo*, a group of Gn pigs were inoculated with three doses of *E. cloacae* on 3, 4, and 5 days of age. Together with another group of control pigs, all were inoculated with $2.74 \times 10^4$ genome copies of HuNoV GII.4/2006b at 6 days of age, which was post inoculation day 0 (PID0), then euthanized on PID3, PID7, or PID10. To confirm the colonization of *E. cloacae* in these Gn pigs, fecal *E. cloacae* shedding was determined daily from PID0 to euthanasia day. *E. cloacae* was detected in all treated pigs (Fig. 1), whereas the control pigs remained sterile throughout this study (data not shown).

Fecal HuNoV shedding was monitored daily in both control and *E. cloacae* colonized Gn pigs after viral inoculation (Fig. 2a). In *E. cloacae* colonized pigs, virus shedding was clearly lower than that of control, as the shedding titers for all pigs on each day were below 5000 genome copies per gram of feces. The incidence of virus shedding showed that compared to control pigs, *E. cloacae* colonized pigs had a significantly shorter mean duration in PID10 subgroup (6.7 versus 5.5 days) (Table 1). To further characterize the shedding titers, cumulative and peak shedding for individual pigs were calculated. The cumulative virus shedding in *E. cloacae* colonized pigs was significantly lower on PID7 and PID10 (Fig. 1b), and there was also a trend for lower peak shedding titers in *E. cloacae* colonized pigs (Fig. 1c). No significant difference in the incidence of diarrhea was observed among groups at any time points (Table 1), indicating *E. cloacae* colonization did not affect the incidence of diarrhea in Gn pigs after HuNoV infection. These data demonstrated that *E. cloacae* colonization inhibited HuNoV shedding in Gn pigs.

### *E. cloacae* reduced HuNoV titers in intestinal tissues and blood

Previous studies showed that HuNoV (GII.4) antigen was observed in duodenum and jejunum of Gn pigs[13-15]. In this study, analysis of the tissue samples confirmed the existence of HuNoV genomes in duodenum and jejunum, and viral genomes were also detectable in ileum for both control and *E. cloacae* colonized pigs (Fig. 3a, b). Compared to control pigs, on PID3, virus titers were significantly lower in duodenum and ileum of *E. cloacae* colonized pigs (Fig. 3a). On PID10, virus titer was significantly lower in ileum of *E. cloacae* colonized pigs (Fig. 3b).

Previously, HuNoV was detected in blood in humans with gastroenteritis[30, 31], as well as in Gn calves and pigs after HuNoV challenge[12, 13]. In this study, viral genomes were present in plasma in 4 of 6 control pigs (66.7%) and 5 of 8 (62.5%) *E. cloacae* colonized pigs, and virus titer on PID3 was significantly lower in *E. cloacae* colonized pigs (Fig. 3c). In addition, viral genomes were also detectable in whole blood cells in 2 of 6 control pigs (33.3%) and in 1 of 8 *E. cloacae* colonized pigs (12.5%) (Fig. 3d). Taken together, the reduced HuNoV titers in intestinal tissues and in blood indicated the inhibitive role of *E. cloacae* for HuNoV infection in Gn pigs.

### HuNoV antigen was observed in enterocytes but not in B cells

To confirm HuNoV infection of enterocytes in Gn pigs and to identify virus-infected cells in *E. cloacae* colonized pigs, immunohistochemistry (IHC) was performed to detect the viral capsid protein VP1 on sections of small intestine from both groups. As expected, HuNoV antigen was observed in enterocytes of duodenum and jejunum from control pigs. In *E. cloacae* colonized pigs, both duodenal and jejunal enterocytes were also the only positive cells, whereas cells of the lamina propria were negative for both groups (Fig. 4).

To determine whether HuNoV infects B cells in the presence of *E. cloacae* in Gn pigs, we isolated total mononuclear cells (MNC) from ileum and spleen, then performed qRT-PCR to detect viral genomes. 1 of 6 control pigs had detectable viral genomes in ileal MNC (Fig. 5a), and 3 of 6 control pigs had detectable viral genomes in splenic MNC (Fig. 5b), although the titers were as low as 20 genomic copies in $10^7$ MNC. However, no viral genomes were detected in ileal or splenic MNC in *E. cloacae* colonized pigs, presumably resulting from the lower HuNoV infection in these pigs. Furthermore, IHC for both viral antigen and B cells was performed in ileum, because ileum is populated with B cells in conventional and Gn pigs[32], and viral genomes were detected in ileum (Fig. 3a). B cells were observed in the lamina propria, as probed by primary antibody targeting cellular marker CD79, while HuNoV antigen was observed only in enterocytes. Thus, there was no signal co-localization in sections from control and *E. cloacae* colonized pigs, even though B cells could be located in close proximity to HuNoV positive cells (Fig. 5c). In all, these data suggest that B cells are not a HuNoV target in Gn pigs, with or without *E. cloacae* colonization.

### *E. cloacae* promoted gut immunity

Probiotic lactobacilli colonization enhanced gut immunity in Gn pigs by promoting intestinal T cell and B cell responses, as well as the secretion of intestinal immunoglobulins[25, 26]. Lactobacilli protected against rotavirus diarrhea and also functioned as adjuvants for rotavirus vaccine by promoting protective immune responses[27, 33, 34]. We hypothesized that *E. cloacae* colonization might promote gut immunity in Gn pigs as well, which in return would inhibit HuNoV infectivity. To determine the role of *E. cloacae* in intestinal immune system development, we compared the sizes of ileal Peyer's patches (IPP) for both groups. In *E. cloacae* colonized pigs, IPP

were significantly larger and more developed than those of control pigs on 6 days and 13 days post inoculation of *E. cloacae* (Fig. 6a). The IPP in *E. cloacae* colonized pigs were characterized by significantly greater width from muscularis mucosae to muscularis associated with gut associated lymphoid tissue (GALT), width of GALT, height and width of follicles (Fig. 6b).

## Discussion

The lack of a robust cell culture and animal model for HuNoVs propagation has long eluded study of HuNoV biology and development of antiviral therapies. Among the *in vitro* models, HuNoVs reverse genetics systems containing subgenomic or genomic RNA have been established[35, 36], but the virus-like particle or virion production was inefficient. Reports of HuNoVs infection and replication observed in 3D intestinal epithelial cells were not reproducible[37, 38]. Although HuNoV infection has been observed in chimpanzees[11], the species is no longer available for the entire biomedical research due to ethical concerns. The BALB/c Rag/$\gamma c^{-/-}$ mouse was recognized as a HuNoV infection model via intraperitoneal inoculation[16], but it is not suitable for HuNoV propagation due to the low robustness of replication and the lack of virus shedding. Given the limitations of current models, clinical fecal samples containing HuNoV from patients have been the only resource for HuNoV infection studies. Recently, HuNoV cultivation was described in human B cells (BJAB cell line) with free HBGA or HBGA-expressing *E..cloacae* supplementation[18, 19]. Hence, we expanded our Gn pig model with *E. cloacae* colonization, which should enhance HuNoV infection and replication. Our original objective was to develop a pig model for effective HuNoV propagation. Surprisingly, *E. cloacae* inhibited HuNoV infectivity in Gn pigs instead.

First, fecal virus shedding has been used as direct evidence to characterize the status of HuNoV infection *in vivo*. Our data showed that the incidence of shedding and the shedding amount in *E. cloacae* colonized pigs were less than those of control pigs, including lower cumulative shedding and peak shedding in individual pigs (Table 1 and Fig. 2). Second, the small intestine has been shown to be the primary HuNoV infection site in Gn pigs[13-15]. We also confirmed the existence of viral genomes in all sections of small intestine in both groups, and the titers were significantly lower in *E. cloacae* colonized pigs. In addition, lower viremia was observed in *E. cloacae* colonized pigs (Fig. 3). As HuNoV genomes were present in whole blood cells, it is likely that those were virions captured by phagocytes and translocated through blood circulation, since ileal and splenic MNC had detectable viral genomes as well. Third, *E. cloacae* was expected to facilitate HuNoV infection of B cells based on the *in vitro* model, but no HuNoV-positive B cells were observed in ileum sections even though the adjacent enterocytes were HuNoV positive. In addition, the entire lamina propria in sections of duodenum, jejunum, and ileum were HuNoV-negative, in both control and *E. cloacae* colonized pigs.

Enteric bacteria can bind to HuNoV via surface HBGA[17]. It is likely that HBGA-expressing *E. cloacae* serves as a blockade between HuNoV and target cells *in vivo* instead of facilitating virion attachment, and thus leads to lower rates of infection. Both inhibition and enhancement of HuNoV P particles attachment via such binding have been observed *in vitro* for other probiotic bacteria, such as *Lactobacillus casei* BL23 and *Escherichia coli* Nissle 1917[39]. Our data suggested that inhibition of attachment by *E. cloacae* was the scenario in pigs *in vivo*, resulting in decreased HuNoV infectivity. Another reason for the lower HuNoV infectivity might be due to the enhanced development of gut immunity by *E. cloacae* colonization. We observed that colonization of *E.*

*cloacae* in Gn pigs stimulated the development of IPP. Further and longer term studies will be required to determine the magnitude of immune responses to HuNoV infection between the two groups.

The binding between *E. cloacae* and HuNoV may also play a role in virus retention *in vivo*. We observed that virus titer in duodenum decreased from PID3 to PID10 in control pigs, but it appeared to be unchanged or even increased in *E. cloacae* colonized pigs (Fig. 3a, b). *E. cloacae* is naturally resistant to broad-spectrum antibiotics[40], thus it could be dominant in gut microbiota in immunocompromised patients, who also require antibiotic therapy to manage microbial infections in many cases[41]. Increased *E. cloacae* might in return contribute to persistence of HuNoV infection in immunocompromised hosts by virus retention.

In summary, colonization of *E. cloacae* in neonatal Gn pigs inhibited HuNoV infectivity, including reduced virus shedding, lower viral genome titers in intestinal tissues and in blood. HuNoV infection of B cells was not observed in duodenum, jejunum, or ileum in either control or *E. cloacae* colonized pigs. To our knowledge, this is the first *in vivo* study to evaluate the effects of *E. cloacae* on HuNoV infectivity, and our study paves the way for future studies of the interaction between HuNoV and enteric bacteria *in vivo*.

## Materials and Methods

**Virus and bacterium**. A pool of stool containing GII.4/2006b variant 092895 (GenBank accession no. KC990829) was collected in 2008 by Dr. Xi Jiang's laboratory at Cincinnati Children's Hospital Medical Center from a child with HuNoV gastroenteritis. Stool sample collection was conducted in accordance with protocols approved by the institutional review boards of the Cincinnati

Children's Hospital Medical Center (IRB number: 2008-1131), and informed consent was obtained from parents or child. The stool was processed as inoculum and stored in our laboratory for studies of HuNoV infection in Gn pigs[14]. *Enterobacter cloacae* was purchased from ATCC (ATCC 13047) and grown in nutrient broth overnight at 30℃ with shaking at 250 rpm. Overnight cultures containing 15% glycerol were stored in -80℃ freezer for colonization of Gn pigs. The final concentration of *E. cloacae* was measured in serial dilutions by enumeration of colony forming unit grown on nutrient broth agar plates.

***E. cloacae* colonization and HuNoV inoculation of Gn pigs.** Near-term Yorkshire cross breed pigs were derived by hysterectomy and maintained in Gn pig isolators as described previously[42]. A subset of pigs was orally inoculated with $10^4$ CFU of *E. cloacae* daily on 3, 4, and 5 days of age to initiate colonization, which was monitored via testing fecal shedding. Control pigs received a diluent only. All pigs were orally inoculated with $2.74 \times 10^4$ viral RNA copies of HuNoV at 6 days of age. Four ml of 200 mM sodium bicarbonate was given 15 min prior to HuNoV inoculation to reduce gastric acidity. Pigs were euthanized on PID3, PID7, or PID10 for collection of blood, intestinal contents, and tissues. Forty cm of distal ileum and whole spleen organ were collected for the isolation of MNC[22]. Pigs used in this study were HBGA-typed to be $A^+$ and/or $H^+$, and sterility was confirmed one day before *E. cloacae* inoculation for all pigs, as well as on euthanasia day for control pigs, as previously described[14]. All animal experimental procedures were conducted in accordance with protocols approved by the Institutional Animal Care and Use Committee at Virginia Tech (IACUC protocol: 14-108-CVM).

**Assessment of diarrhea and HuNoV shedding.** Pig feces were collected daily by rectal swabs following HuNoV inoculation to assess diarrhea and fecal virus shedding. Fecal consistency was scored as follows: 0, solid; 1, semisolid; 2, pasty; 3, semiliquid; and 4, liquid. Pigs with daily fecal scores of 2 or greater were considered diarrheic. Virus shedding was determined as described previously[14]. Briefly, pig feces on rectal swabs were released by swirling in 1 ml PBS and processed as solution, 250 µl of which was prepared for total RNA isolation using TRIzol LS (Thermo Fisher Scientific). The RNA pellet was resuspended in 40 µl RNase-free water, and 5 µl RNA was used in a TaqMan qRT-PCR reaction to detect HuNoV genomes following the manufacturer's instructions in the SensiFAST Probe No-ROX One-Step Kit (Bioline).

**Detection of HuNoV genome in tissues and blood.** Small intestinal tissues were collected during necropsies, directly frozen in liquid nitrogen, and then stored in -80℃ freezer. 40 to 60 mg of frozen tissues were thawed at room temperature, washed in 1 ml PBS once, then homogenized in 0.2 ml TRIzol LS using Bullet Blender with 100 mg of 1.0 mm Zirconium Oxide beads (Next Advance). Total RNA from the homogenized tissues was isolated by adding 0.55 ml TRIzol LS. Blood was collected immediately after euthanasia, and 30% of ACD was added to prevent coagulation. Plasma and whole blood cells were separated by centrifugation at 2000*g* for 5 min. Plasma from 250 µl blood and whole blood cells from 50 µl blood for each pig were used for RNA isolation. $1 \times 10^7$ MNC from ileum and spleen were used for RNA isolation. For these samples, RNA was isolated using 750 µl TRIzol LS following the manufacturer's instructions, and the HuNoV genome copies were determined by TaqMan qRT-PCR as described above.

**Immunohistochemistry.** Small intestinal tissues were collected upon euthanasia, fixed in 4% paraformaldehyde overnight, embedded in paraffin, sectioned at 5 μm, and placed on positively charged glass slides. Tissue slides were deparaffinized and rehydrated by washing in a graded ethanol series. For enzymatic antigen retrieval, slides were digested in 80 μg/ml proteinase K solution (Sigma Aldrich) for 30 min at 37 ℃, followed by washing with tris-buffered saline (TBS). For blocking, slides were incubated in TBS containing 10% normal pig serum and 1% BSA for 2 h at room temperature. For IHC of duodenum and jejunum, slides were incubated with a goat anti-HuNoV GII.4 VLP polyclonal antibody diluted in TBS containing 1% BSA overnight at 4 ℃, then washed with TBS containing 0.025% Triton X-100, and incubated with Alexa Fluor 488-labeled donkey anti-goat secondary antibody (A-11055; Thermo Fisher Scientific; 1:500) diluted in TBS containing 1% BSA for 1 h at room temperature. For IHC of ileum, mouse anti-CD79 (VP-C366; Vector Laboratories; 1:1000) and Alexa Fluor 546-labeled donkey anti-mouse secondary antibody (A10036; Thermo Fisher Scientific; 1:500) were also included in the two incubation steps above. Finally, slides were washed in TBS and mounted in Vectashield containing 4,6-diamidino-2-phenylindole (DAPI) for counterstaining cell nuclei (Vector Laboratories). Images were acquired on a Zeiss LSM 880 confocal laser scanning microscope in Fralin Imaging Center at Virginia Tech.

**Ileum Peyer's patches histopathology.** Sections of ileum were prepared as described above, and H&E staining was performed routinely. A pathologist was blinded to identification of the samples and evaluated the IPP histopathology using a light microscope with an ocular micrometer. To characterize the IPP sizes, muscularis mucosae to muscularis (mm to m) associated with gut

associated lymphoid tissue (GALT), width of GALT, height and width of follicles were measured. For each parameter, 12 random locations including all pigs in each group were measured.

**Statistics.** Pigs (male and female) were randomly divided to control group and *E. cloacae* group, pigs infected with HuNoV in each group were randomly assigned to be euthanized on PID3, PID7, or PID10. To assess clinical signs and virus shedding, pigs euthanized on PID10 contributed data to PID3 and PID7 subgroups, as did PID7 contributed data to PID3 subgroup. Statistical significance was determined with analyses specified in figure legends and table notes using GraphPad Prism 6.0 (GraphPad Software). *P* value < 0.05 was indicated as statistically significant.

## Acknowledgements

We gratefully thank X.J. Meng, X. Wang, and N. Nanthakumar for critical discussion. We thank K. Pelzer for veterinary services for Gn pigs, K. Young, K. Allen, K. Hall, S. Viers, and J. Park for animal care throughout the study. This work was supported by NIH grant R01AI089634 (to L.Y.).

## Author contributions

S.L. and L.Y. designed the project. S.L. performed most of the experiments and analyzed data. H.S., E.T., T.B., K.W., M.W., G.L, and X.Y. performed experiments. X.J. contributed materials. S.L. and L.Y. wrote the manuscript. All authors reviewed the manuscript.

## Additional Information

**Competing financial interests:** The authors declare no competing financial interests.

## References


1. Ahmed, S.M. et al. Global prevalence of norovirus in cases of gastroenteritis: a systematic review and meta-analysis. *Lancet Infect Dis* **14**, 725-30 (2014).
2. Karst, S.M. Pathogenesis of noroviruses, emerging RNA viruses. *Viruses* **2**, 748-81 (2010).
3. Zheng, D.P. et al. Norovirus classification and proposed strain nomenclature. *Virology* **346**, 312-23 (2006).
4. Kroneman, A. et al. Proposal for a unified norovirus nomenclature and genotyping. *Arch Virol* **158**, 2059-68 (2013).
5. Bull, R.A., Eden, J.S., Rawlinson, W.D. & White, P.A. Rapid evolution of pandemic noroviruses of the GII.4 lineage. *PLoS Pathog* **6**, e1000831 (2010).
6. White, P.A. Evolution of norovirus. *Clin Microbiol Infect* **20**, 741-5 (2014).
7. Chan, M.C. et al. Rapid emergence and predominance of a broadly recognizing and fast-evolving norovirus GII.17 variant in late 2014. *Nat Commun* **6**, 10061 (2015).
8. Wang, H.B. et al. Complete nucleotide sequence analysis of the norovirus GII.17: A newly emerging and dominant variant in China, 2015. *Infect Genet Evol* **38**, 47-53 (2015).
9. Lee, C.C. et al. Emerging Norovirus GII.17 in Taiwan. *Clin Infect Dis* **61**, 1762-4 (2015).
10. Kocher, J. & Yuan, L. Norovirus vaccines and potential antinorovirus drugs: recent advances and future perspectives. *Future Virol* **10**, 899-913 (2015).
11. Bok, K. et al. Chimpanzees as an animal model for human norovirus infection and vaccine development. *Proc Natl Acad Sci U S A* **108**, 325-30 (2011).
12. Souza, M., Azevedo, M.S., Jung, K., Cheetham, S. & Saif, L.J. Pathogenesis and immune responses in gnotobiotic calves after infection with the genogroup II.4-HS66 strain of human norovirus. *J Virol* **82**, 1777-86 (2008).
13. Cheetham, S. et al. Pathogenesis of a genogroup II human norovirus in gnotobiotic pigs. *J Virol* **80**, 10372-81 (2006).
14. Bui, T. et al. Median infectious dose of human norovirus GII.4 in gnotobiotic pigs is decreased by simvastatin treatment and increased by age. *J Gen Virol* **94**, 2005-16 (2013).
15. Jung, K. et al. The effects of simvastatin or interferon-alpha on infectivity of human norovirus using a gnotobiotic pig model for the study of antivirals. *PLoS One* **7**, e41619 (2012).
16. Taube, S. et al. A mouse model for human norovirus. *MBio* **4**, e00450-13 (2013).
17. Miura, T. et al. Histo-blood group antigen-like substances of human enteric bacteria as specific adsorbents for human noroviruses. *J Virol* **87**, 9441-51 (2013).
18. Jones, M.K. et al. Enteric bacteria promote human and mouse norovirus infection of B cells. *Science* **346**, 755-9 (2014).
19. Jones, M.K. et al. Human norovirus culture in B cells. *Nat Protoc* **10**, 1939-47 (2015).
20. Karst, S.M. & Wobus, C.E. A working model of how noroviruses infect the intestine. *PLoS Pathog* **11**, e1004626 (2015).
21. Saif, L.J., Ward, L.A., Yuan, L., Rosen, B.I. & To, T.L. The gnotobiotic piglet as a model for studies of disease pathogenesis and immunity to human rotaviruses. *Arch Virol Suppl* **12**, 153-61 (1996).
22. Yuan, L., Ward, L.A., Rosen, B.I., To, T.L. & Saif, L.J. Systematic and intestinal antibody-secreting cell responses and correlates of protective immunity to human rotavirus in a gnotobiotic pig model of disease. *J Virol* **70**, 3075-83 (1996).
23. Kocher, J. et al. Intranasal P particle vaccine provided partial cross-variant protection against human GII.4 norovirus diarrhea in gnotobiotic pigs. *J Virol* **88**, 9728-43 (2014).
24. Karst, S.M., Wobus, C.E., Goodfellow, I.G., Green, K.Y. & Virgin, H.W. Advances in norovirus biology. *Cell Host Microbe* **15**, 668-80 (2014).

25. Zhang, W. et al. Influence of probiotic Lactobacilli colonization on neonatal B cell responses in a gnotobiotic pig model of human rotavirus infection and disease. *Vet Immunol Immunopathol* **122**, 175-81 (2008).
26. Wen, K. et al. Development of gammadelta T cell subset responses in gnotobiotic pigs infected with human rotaviruses and colonized with probiotic lactobacilli. *Vet Immunol Immunopathol* **141**, 267-75 (2011).
27. Wen, K. et al. Lactobacillus rhamnosus GG Dosage Affects the Adjuvanticity and Protection Against Rotavirus Diarrhea in Gnotobiotic Pigs. *J Pediatr Gastroenterol Nutr* **60**, 834-43 (2015).
28. Zhang, H. et al. Probiotics and virulent human rotavirus modulate the transplanted human gut microbiota in gnotobiotic pigs. *Gut Pathog* **6**, 39 (2014).
29. Wen, K. et al. Probiotic Lactobacillus rhamnosus GG enhanced Th1 cellular immunity but did not affect antibody responses in a human gut microbiota transplanted neonatal gnotobiotic pig model. *PLoS One* **9**, e94504 (2014).
30. Takanashi, S. et al. Detection, genetic characterization, and quantification of norovirus RNA from sera of children with gastroenteritis. *J Clin Virol* **44**, 161-3 (2009).
31. Fumian, T.M. et al. Quantitative and molecular analysis of noroviruses RNA in blood from children hospitalized for acute gastroenteritis in Belem, Brazil. *J Clin Virol* **58**, 31-5 (2013).
32. Potockova, H., Sinkorova, J., Karova, K. & Sinkora, M. The distribution of lymphoid cells in the small intestine of germ-free and conventional piglets. *Dev Comp Immunol* **51**, 99-107 (2015).
33. Wen, K. et al. High dose and low dose Lactobacillus acidophilus exerted differential immune modulating effects on T cell immune responses induced by an oral human rotavirus vaccine in gnotobiotic pigs. *Vaccine* **30**, 1198-207 (2012).
34. Liu, F. et al. Dual functions of Lactobacillus acidophilus NCFM as protection against rotavirus diarrhea. *J Pediatr Gastroenterol Nutr* **58**, 169-76 (2014).
35. Asanaka, M. et al. Replication and packaging of Norwalk virus RNA in cultured mammalian cells. *Proc Natl Acad Sci U S A* **102**, 10327-32 (2005).
36. Katayama, K. et al. Plasmid-based human norovirus reverse genetics system produces reporter-tagged progeny virus containing infectious genomic RNA. *Proc Natl Acad Sci U S A* **111**, E4043-52 (2014).
37. Papafragkou, E., Hewitt, J., Park, G.W., Greening, G. & Vinje, J. Challenges of culturing human norovirus in three-dimensional organoid intestinal cell culture models. *PLoS One* **8**, e63485 (2014).
38. Herbst-Kralovetz, M.M. et al. Lack of norovirus replication and histo-blood group antigen expression in 3-dimensional intestinal epithelial cells. *Emerg Infect Dis* **19**, 431-8 (2013).
39. Rubio-del-Campo, A. et al. Noroviral p-particles as an in vitro model to assess the interactions of noroviruses with probiotics. *PLoS One* **9**, e89586 (2014).
40. Davin-Regli, A. & Pages, J.M. Enterobacter aerogenes and Enterobacter cloacae; versatile bacterial pathogens confronting antibiotic treatment. *Front Microbiol* **6**, 392 (2015).
41. Bodey, G.P. Managing infections in the immunocompromised patient. *Clin Infect Dis* **40 Suppl 4**, S239 (2005).
42. Meyer, R.C., Bohl, E.H. & Kohler, E.M. Procurement and Maintenance of Germ-Free Seine for Microbiological Investigations. *Appl Microbiol* **12**, 295-300 (1964).

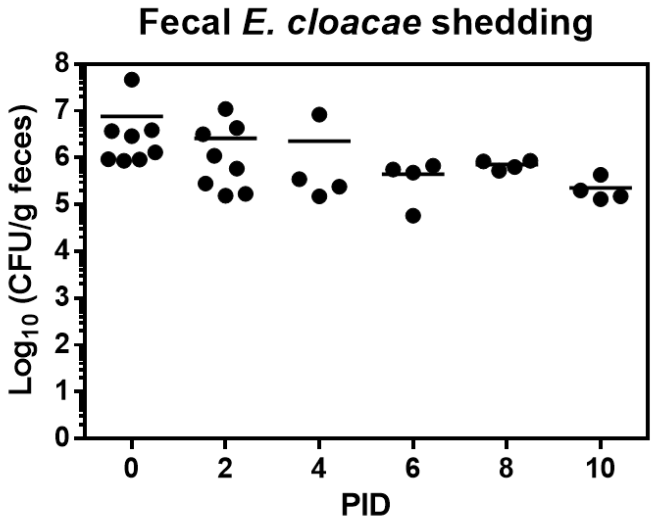


**Figure 1. Fecal *E. cloacae* shedding.** Colonization of *E. cloacae* in the Gn pigs throughout the HuNoV infection study was confirmed by monitoring fecal shedding. The colony forming unit (CFU) was measured in serial dilutions of fecal samples by enumeration of colonies grown on agar plates of culture media. Data shown are pooled from independent experiments performed on each day, with individual animal data points.

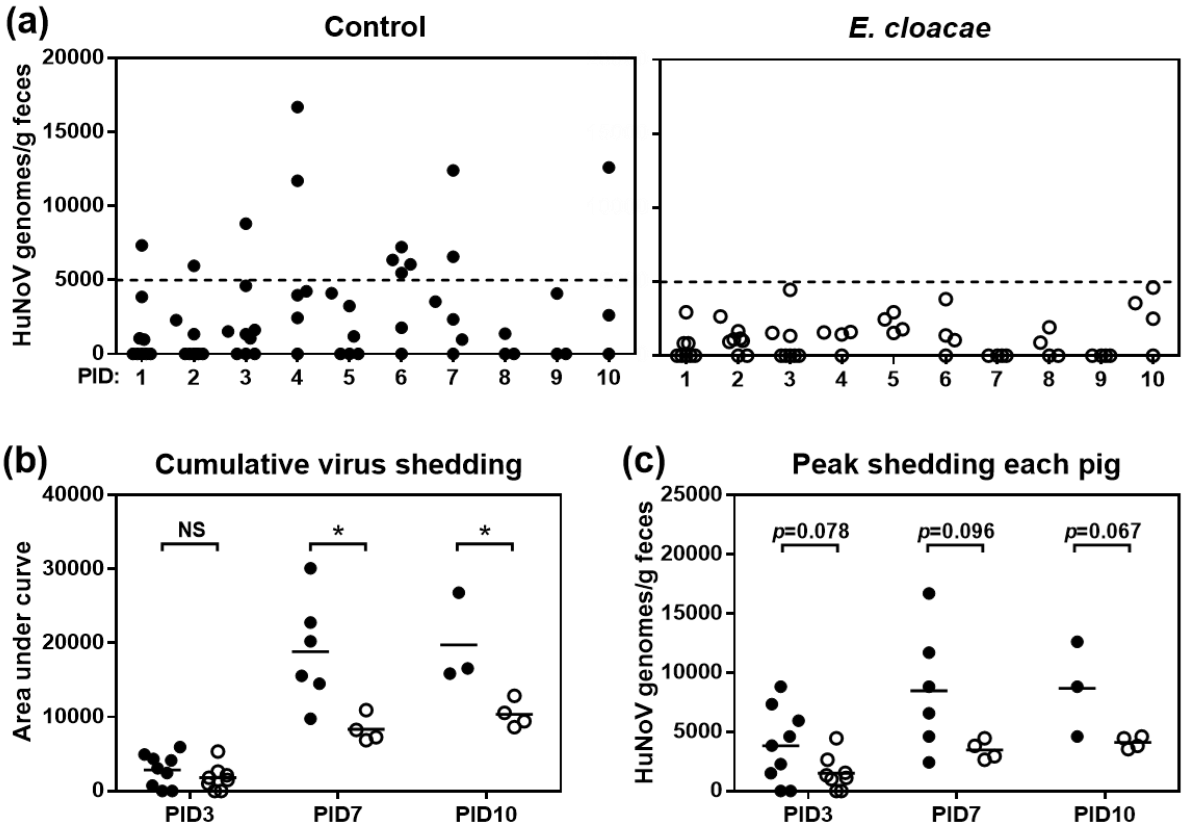


**Figure 2. Lower HuNoV shedding in *E. cloacae* colonized Gn pigs.** (**a**) Fecal HuNoV shedding was monitored daily from PID1 to PID10 by qRT-PCR to quantify viral genomes in feces. Dashed line indicates 5000 HuNoV genomes. (**b**) Cumulative virus shedding was shown as area under curve calculated for individual pigs based on (**a**). (**c**) Peak shedding titers from PID1 to PID3, PID7, or PID10 in each pig was presented. Sample sizes are shown in **Table 1**. Data are presented as mean with individual animal data points (**b**-**c**). Statistical significance was determined by Student's *t*-test. NS, not significant, **P*<0.05.

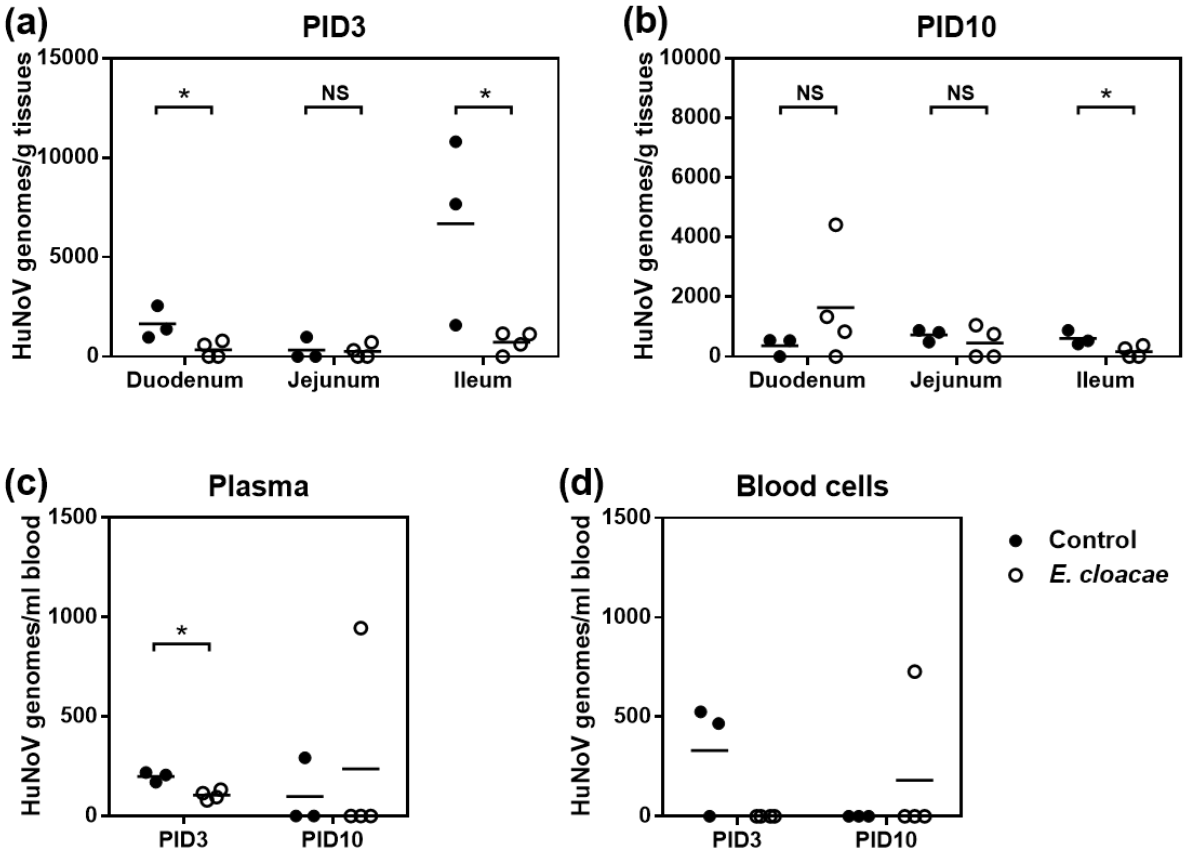


**Figure 3. Lower HuNoV titers in small intestine and blood in *E. cloacae* colonized Gn pigs**. HuNoV genomes in duodenum, jejunum, and ileum in pigs euthanized on PID3 (**a**) and PID10 (**b**) were measured by qRT-PCR. HuNoV genomes in plasma (**c**) and whole blood cells (**d**) were measured by qRT-PCR. Sample sizes in control groups, PID3 *n*=3, PID10 *n*=3; in *E. cloacae* groups, PID3 *n*=4, PID10 *n*=4. Data are presented as mean with individual animal data points. Statistical significance was determined by Student's *t*-test. NS, not significant, *$P$<0.05.

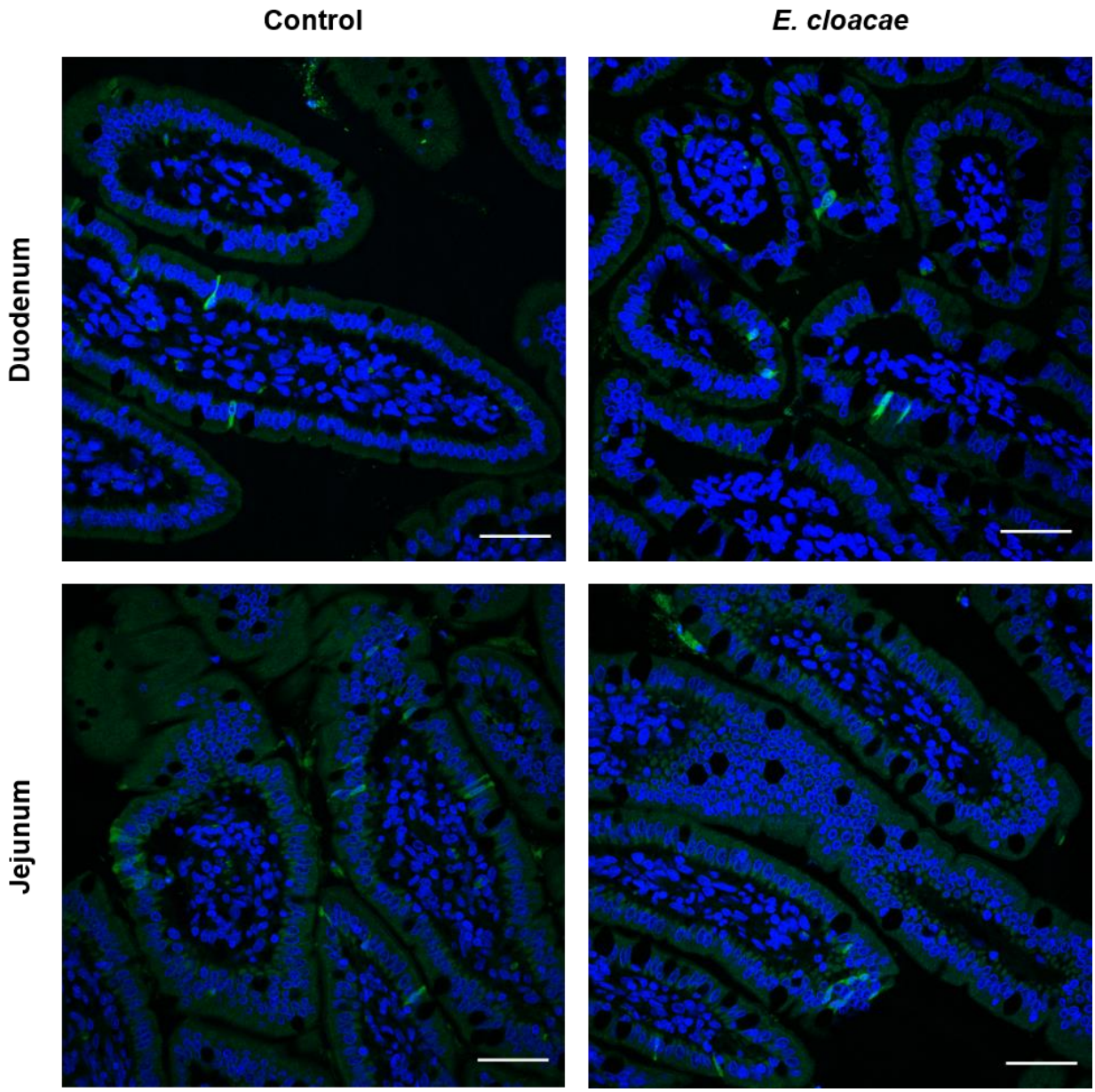


**Figure 4. HuNoV infection of enterocytes in Gn pigs.** HuNoV capsid in duodenum (top panel) and jejunum (bottom panel) of Gn pigs euthanized on PID3 was detected by immunohistochemistry. Cell nuclei (blue) were counterstained with HuNoV capsid (bright green). Representative images showing HuNoV was detected in enterocytes in control and *E. cloacae* colonized Gn pigs. Scale bar, 50 µm.

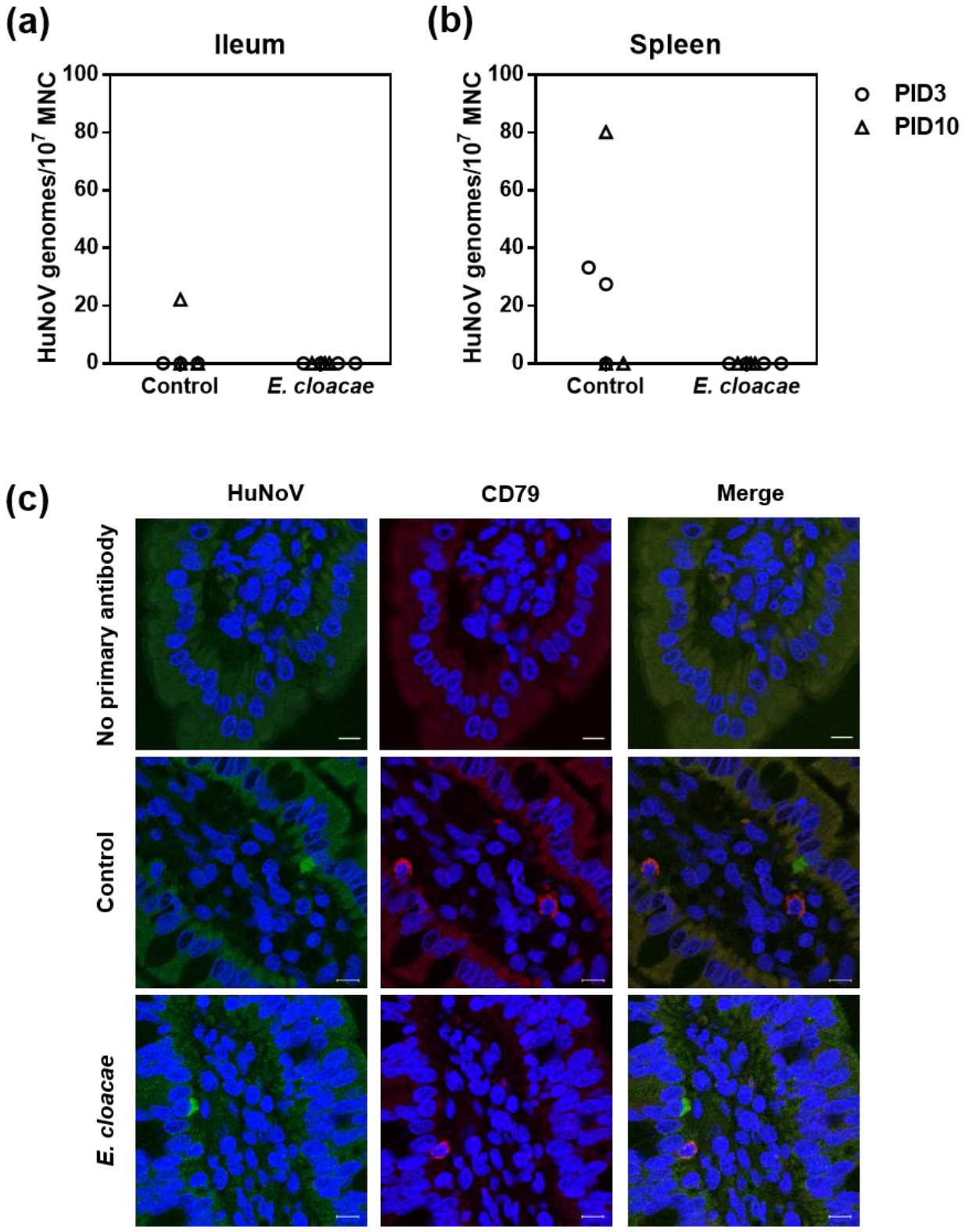
(a)
Ileum
HuNoV genomes/10^7 MNC
100
80
60
40
20
0
Control
E. cloacae
(b)
Spleen
HuNoV genomes/10^7 MNC
100
80
60
40
20
0
Control
E. cloacae
PID3
PID10
(c)
HuNoV
CD79
Merge
No primary antibody
Control
E. cloacae

**Figure 5. HuNoV infection of B cells was not observed in Gn pigs.** MNC from ileum (**a**) and spleen (**b**) were isolated and measured for HuNoV titers by qRT-PCR. Data are presented as individual animal data points. (**c**) Ileum tissue sections were stained to detect HuNoV capsid protein (bright green) and B cells ($CD79^+$, red) with counterstain of cell nuclei (DAPI, blue). Representative images showing that HuNoV were observed in enterocytes but not in B cells in control and *E. cloacae* colonized Gn pigs. Scale bar, 10 μm.

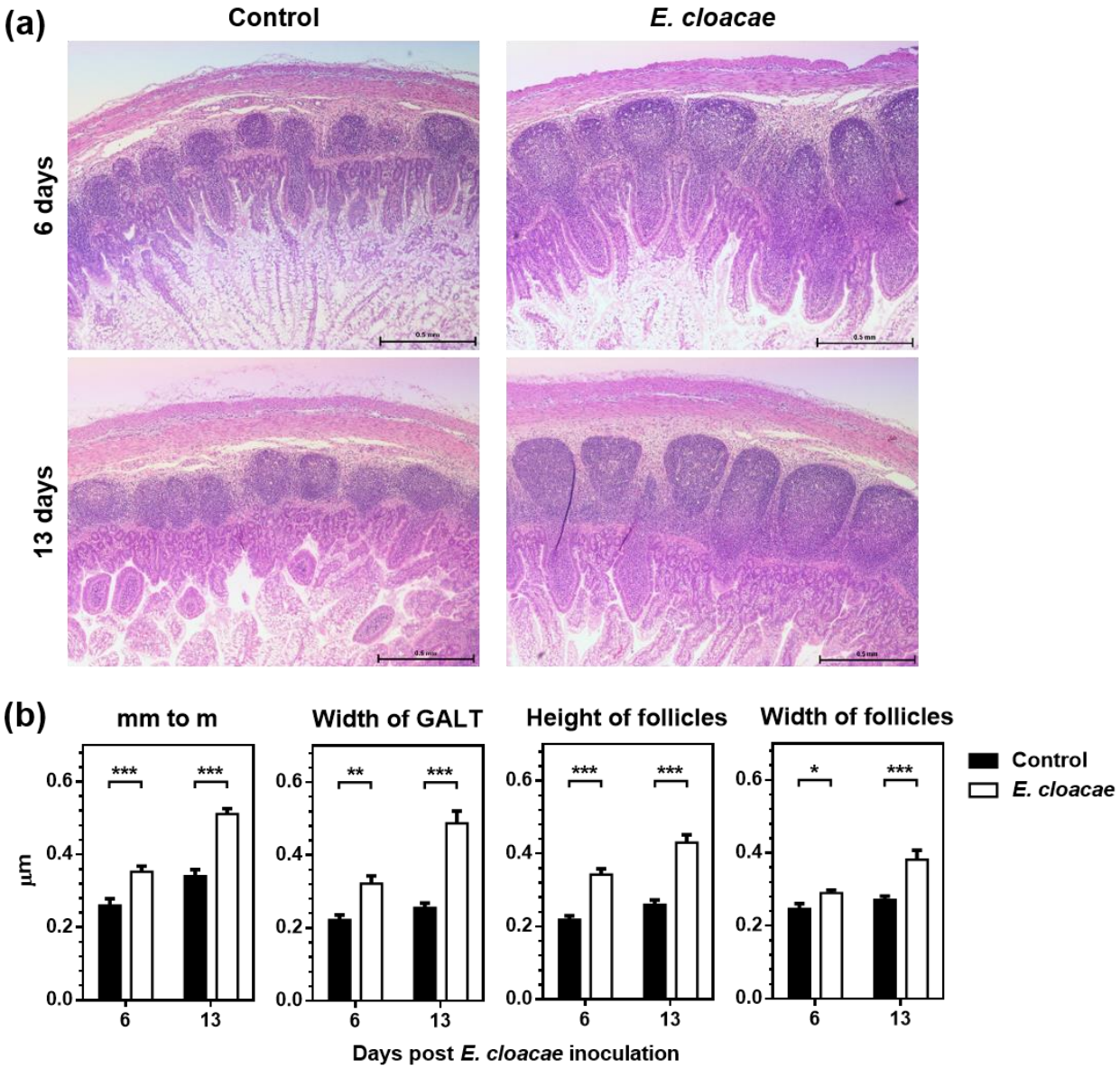


**Figure 6. Colonization of *E. cloacae* in Gn pigs stimulated the development of IPP.** (**a**) Representative H&E staining images of ileum showing more developed IPP in *E. cloacae* colonized Gn pigs compared to that of control pigs on both 6 days (top panel) and 13 days (bottom panel) post *E. cloacae* inoculation, Scale bar, 0.5 mm. (**b**) 12 random locations including all pigs in each group were measured to characterize the IPP size, including width from muscularis mucosae to muscularis (mm to m) associated with gut associated lymphoid tissue (GALT), width of GALT, height and width of follicles. Statistical significance was determined by Mann-Whitney test. **P*<0.05; ***P*<0.01; ****P*<0.001. Error bars denote SEM.

| Group | Time | *n* | Diarrhea[a, b] | | | Virus shedding[b] | | |
|---|---|---|---|---|---|---|---|---|
| | | | Pigs with diarrhea (%)* | Mean days to onset (SEM)** | Mean duration days (SEM)** | Pigs shedding virus (%)* | Mean days to onset (SEM)** | Mean duration days (SEM)** |
| Control | PID3 | 9 | 4 (44%) | 3.2 (0.3) | 0.4 (0.2) | 7 (78%) | 2.1 (0.4) | 1.4 (0.3) |
| *E. cloacae* | | 8 | 4 (50%) | 3.0 (0.4) | 0.7 (0.3) | 6 (75%) | 2.1 (0.4) | 1.5 (0.4) |
| Control | PID7 | 6 | 6 (100%) | 3.8 (0.7) | 3.0 (0.4) | 6 (100%) | 2.3 (0.6) | 4.3 (0.5) |
| *E. cloacae* | | 4 | 4 (100%) | 4.3 (1.5) | 2.0 (1.0) | 4 (100%) | 1.8 (0.3) | 4.3 (0.5) |
| Control | PID10 | 3 | 3 (100%) | 2.3 (0.3) | 3.7 (0.3) | 3 (100%) | 1.3 (0.3) | 6.7 (0.3)[A] |
| *E. cloacae* | | 4 | 4 (100%) | 4.3 (1.5) | 2.7 (0.9) | 4 (100%) | 1.8 (0.3) | 5.5 (0.3)[B] |

**Table 1. Incidence of clinical signs and fecal virus shedding in Gn pigs after HuNoV GII.4 2006b infection.** All pigs were inoculated with a HuNoV GII.4 2006b variant 092895 at 6 days of age. Daily rectal swabs were collected after inoculation to assess diarrhea and HuNoV shedding by Taqman qRT-PCR. [a]Pigs with daily fecal scores of ≥2 were considered diarrheic. Fecal consistency was scored as follows: 0, solid; 1, semisolid; 2, pasty; 3, semiliquid; and 4, liquid. [b]Fecal consistency score or virus shedding calculation included all the pigs in each group from PID1 to PID3, PID7, or PID10. If no diarrhea or virus shedding was observed, the days to onset were recorded as 1 day longer than each timepoint (4, 8, or 11) and the duration days were recorded as 0 for statistical analysis. *Fisher's exact test or **Student's *t*-test was used for statistical analysis. Groups with significant differences ($P<0.05$) were indicated with letters A and B.

# Chapter 3

## Increased and prolonged human norovirus infection in RAG2/IL2RG deficient gnotobiotic pigs with severe combined immunodeficiency

Shaohua Lei[1], Junghyun Ryu[2], Ke Wen[1], Erica Twitchell[1], Tammy Bui[1], Ashwin Ramesh[1], Mariah Weiss[1], Guohua Li[1], Helen Samuel[1], Sherrie Clark-Deener[3], Xi Jiang[4], Kiho Lee[2], Lijuan Yuan[1,*]

[1]Department of Biomedical Sciences and Pathobiology, Virginia-Maryland College of Veterinary Medicine, Virginia Tech, Blacksburg, VA 24061, USA.

[2]Department of Animal and Poultry Sciences, College of Agriculture and Life Sciences, Virginia Tech, Blacksburg, VA 24061, USA.

[3]Department of Large Animal Clinical Sciences, Virginia-Maryland College of Veterinary Medicine, Virginia Tech, Blacksburg, VA 24061, USA.

[4]Division of Infectious Diseases, Cincinnati Children's Hospital Medical Center, Cincinnati, OH 45229, USA.

*Correspondence and requests for materials should be addressed to L.Y. (email: lyuan@vt.edu)

Published in *Scientific Reports*. 2016 Apr 27; 6:25222. Used with permission.

## Abstract

Application of genetically engineered (GE) large animals carrying multi-allelic modifications has been hampered by low efficiency in production and extended gestation period compared to rodents. Here, we rapidly generated *RAG2/IL2RG* double knockout pigs using direct injection of CRISPR/Cas9 system into developing embryos. RAG2/IL2RG deficient pigs were immunodeficient, characterized by depletion of lymphocytes and either absence of or structurally abnormal immune organs. Pigs were maintained in gnotobiotic facility and evaluated for human norovirus (HuNoV) infection. HuNoV shedding lasted for 16 days in wild type pigs, compared to 27 days (until the end of trials) in RAG2/IL2RG deficient pigs. Additionally, higher HuNoV titers were detected in intestinal tissues and contents and in blood, indicating increased and prolonged HuNoV infection in RAG2/IL2RG deficient pigs and the importance of lymphocytes in HuNoV clearance. These results suggest that GE immunodeficient gnotobiotic pigs serve as a novel model for biomedical research and will facilitate HuNoV studies, especially mimicking the persistent HuNoV infection in immunocompromised patients.

## Introduction

Pigs are an excellent animal model in biomedicine because of their similarity in physiology and immunology to humans[1]. For instance, disruption of IL2RG in pigs recapitulates the phenotype of X-linked severe combined immunodeficiency (SCID) patients much closer than *Il2rg* knockout rodent models[2]. RAG2/IL2RG deficient pigs would lack B cells, T cells, and natural killer cells (B/T/NK cells). By removing all major lymphocytes, they are an ideal animal model to represent SCID patients and to study virus infection and pathogenesis in immunocompromised hosts. Recent advances in genome editing technology, especially the CRISPR/Cas9 system, allow us to generate GE pigs at higher efficiency[3].

Human noroviruses (HuNoVs), members of the *Norovirus* genus in the *Caliciviridae* family, are the major cause of nonbacterial epidemic acute gastroenteritis worldwide[4], especially since the introduction of rotavirus vaccines[5, 6]. HuNoV claims over 200,000 lives in children under 5 years old, mostly in developing countries annually[7]. In the United States, HuNoV accounts for approximately 800 deaths, 21 million illness, and $284 million in healthcare costs each year[8, 9]. HuNoV gastroenteritis is generally self-limiting, but the disease can be severe and prolonged in specific risk groups, i.e., infants, young children, elderly, and immunocompromised individuals[10]. Although vaccine candidates are under development[11, 12], currently no licensed vaccines or therapeutics against HuNoV gastroenteritis are available.

The lack of a robust cell culture system and a suitable animal model has been an impediment for understanding HuNoV biology and testing antiviral strategies; limited knowledge comes primarily from studies of infected human volunteers[10], chimpanzees[13], gnotobiotic (Gn) calves[14], and Gn pigs[15-17]. Novel animal models are urgently needed to further elucidate the

molecular mechanisms of HuNoV infection, replication, and host protective immunity. Both pigs and humans are omnivorous, the general anatomy and physiology of the gastrointestinal tracts of the neonatal pig and the human are very similar[18]. After rotavirus or HuNoV infection, neonatal Gn pigs develop similar pathological changes and immune responses in the small intestine as those in humans[15, 19, 20]. In addition, the Gn pig model is better suited than other animal models for studies of HuNoV-induced diseases in terms of oral route of infection, clinical presence of diarrhea, and viral shedding[21]. HuNoV infection can become persistent with prolonged virus shedding in immunocompromised patients, who may suffer from increasingly debilitating and life threatening gastroenteritis[22, 23]. Therefore, SCID Gn pigs present great promise for the study of HuNoV biology and the development of therapeutic strategies for this patient cohort.

Here, we disrupted *RAG2/IL2RG* via direct injection of CRISPR/Cas9 system into developing embryos. In this approach, we rapidly generated RAG2/IL2RG deficient pigs presenting SCID phenotype, including substantial depletion of B/T/NK cells in ileum and blood, either absence of or structurally abnormal thymuses, mesenteric lymph nodes (MLN), and ileal Peyer's patches (IPP), as well as impaired production of immunoglobulins. To evaluate the application of RAG2/IL2RG deficient pigs in biomedical research, we inoculated them with HuNoV in comparison with wild type (WT) pigs under Gn condition. HuNoV shedding in WT pigs only lasted for 16 days, whereas the shedding in RAG2/IL2RG deficient pigs was as long as 27 days, and the prolonged shedding was asymptomatic and sporadic. Higher HuNoV genomic titers were detected in intestinal tissues and contents and in blood compared to WT pigs, indicating increased and prolonged HuNoV infection in RAG2/IL2RG deficient Gn pigs.

## Results

### Generation of RAG2/IL2RG deficient pigs

RAG2/IL2RG deficient pigs were generated by injecting CRISPR/Cas9 RNA into early *in vitro* fertilization (IVF)-derived zygotes and performing embryo transfer. Embryos were transferred into five surrogate sows, piglets were subsequently derived by hysterectomy and maintained in Gn isolators under germ-free condition (Fig. 1). The generation of RAG2/IL2RG deficient pigs and subsequent genotyping were performed by Junghyun Ryu under the supervision of Dr. Kiho Lee, more information is available in our full-length publication[24].

### SCID phenotype in RAG2/IL2RG deficient pigs

Postmortem analysis of the RAG2/IL2RG deficient pigs showed clear gross or histological evidence of SCID phenotype. As summarized in Supplementary Table 1, eight pigs lacked thoracic thymus, and three lacked lymphocytes within observed thoracic thymuses; seven lacked cervical thymus, and six lacked lymphocytes within cervical thymuses; ten lacked MLN; and eleven lacked IPP (also see Figs. 2a, b and Supplementary Fig. 1). Although thymus, MLN, and/or IPP were observed in some RAG2/IL2RG deficient pigs, their morphology was abnormal compared to those of WT pigs, including the lack of corticomedullary distinction in thymuses, the absence of follicles in MLN, as well as poorly developed and unstructured small IPP (Supplementary Fig. 2).

To characterize the immune system of RAG2/IL2RG deficient pigs, especially the intestinal immune cells, ileum and circulating blood from each pig were collected for the isolation of mononuclear cells (MNC). Compared to WT pigs, flow cytometry analysis showed that their B/T/NK cells were substantially depleted in ileum and blood (Figs. 2c, d). The total number of

MNC was about 10-fold lower in the ileum (Fig. 2e). Together with the proportion of B/T/NK cells within MNC (Supplementary Fig. 3), the total number of B and T cells were significantly lower in ileum and blood (Fig. 2f). The significant difference of NK cells was observed in ileum, but not in blood (Fig. 2f), because two out of six measured pigs possessed hypomorphic IL2RG mutations, resulting in partial disruption of IL2RG and incomplete depletion of NK cells (Supplementary Table 4 and 5). To confirm the depletion of B cells in RAG2/IL2RG deficient pigs, total immunoglobulin titers in serum were measured. IgA was undetectable, while IgG and IgM were significantly lower than those of WT pigs (Supplementary Fig. 4a). In addition, B cells were not observed in mesentery tissues by immunohistostaining targeting cellular marker CD79 (Supplementary Fig. 4b). In all, the absence of or structurally abnormal immune organs and depletion of lymphocytes indicated SCID phenotype in RAG2/IL2RG deficient pigs, making these pigs a novel large animal model for the studies of viral pathogenesis and immunity in immunocompromised hosts.

**Increased and prolonged HuNoV shedding in SCID Gn pigs**

One RAG2/IL2RG deficient Gn pig was euthanized at 3 days of age due to general weakness rather than illness caused by pathogens; and one was used as a mock infection control. As HBGA type $A^+$ or $H^+$ hosts are more susceptible to HuNoV infection[25-27], all pigs (including a control group of WT Gn pigs) in this study were confirmed $A^+$ or $H^+$ (Supplementary Fig. 5 and Supplementary Table 1). The pigs were inoculated at 6 or 7 days of age with a HuNoV GII.4/2006b variant, which has been previously characterized in WT Gn pigs[16], and then euthanized on post inoculation day (PID) 3, PID10, or PID28. The effects of RAG2/IL2RG deficiency on HuNoV-induced

disease and infectivity were evaluated daily by comparing diarrhea parameters and fecal virus shedding to WT pigs.

As a self-limiting enteric virus, HuNoV shedding only lasted for 16 days in WT pigs, peaking on PID6 and PID10 (Fig. 3a). In contrast, HuNoV shedding could be detected for as long as 27 days in RAG2/IL2RG deficient pigs, peaking on PID2, PID11, and PID21-23 (Fig. 3a). RAG2/IL2RG deficient pigs had significantly longer duration of virus shedding than WT pigs on PID11-17 and PID18-28 (5.5 versus 1.2 days and 4.5 versus 0 days, respectively), and all RAG2/IL2RG deficient pigs had shedding on PID18-28 (Table 1), indicating prolonged HuNoV infection in SCID pigs. However, no significant difference in the incidence of diarrhea was observed for the two groups at any time points (Table 1), indicating that the prolonged HuNoV infection and fecal shedding in SCID pigs were not associated with increased duration of diarrhea, i.e., it was asymptomatic. Compared to WT pigs, the cumulative virus shedding in RAG2/IL2RG deficient pigs was significantly higher on PID1-3 and PID11-17 (Fig. 3b). There was also a trend for higher peak shedding titer on PID1-3 and significantly higher titer on PID11-17 (Fig. 3c), altogether indicating increased HuNoV replication in SCID pigs.

**HuNoV distribution in Gn pigs**

HuNoV (GII.4) antigen was observed previously in enterocytes of WT Gn pigs[15-17]. In this study, both WT and RAG2/IL2RG deficient pigs had confirmed HuNoV infection in enterocytes of duodenum and jejunum (Supplementary Fig. 6). Analysis of gut tissues indicated the existence of HuNoV genomes in all sections of the gastrointestinal tract of both WT and RAG2/IL2RG deficient pigs. Overall, virus titers in gut tissues of WT pigs peaked on PID3 and declined overtime as

expected, but virus titers remained consistent in RAG2/IL2RG deficient pigs from PID3 to PID10 (Figs. 4a, b). Specifically, in RAG2/IL2RG deficient pigs, virus titers were significantly higher in jejunum on PID3 (Fig. 4a), and significantly higher in jejunum and ileum on PID10 than in WT pigs (Fig. 4b). HuNoV genomes were detectable in 2 of 4 RAG2/IL2RG deficient pigs on PID28, but not in WT pigs (Fig. 4c). HuNoV genomes were present in many extraintestinal tissues, and the titers peaked on PID10 for both pig groups (Supplementary Fig. 7). Similar to the findings from clinical human samples[28], HuNoV genomes were consistently undetectable in cerebrospinal fluid (CSF) in this study, suggesting that HuNoV is blocked by the blood-brain barrier of WT and SCID hosts. Unlike WT pigs, HuNoV genomes were detected in liver of RAG2/IL2RG deficient pigs on PID10, presumably due to loss of protection following the depletion of lymphocytes.

The entire contents of small and large intestine were collected during necropsies and virus titers were determined. HuNoV titer was significantly higher in RAG2/IL2RG deficient pigs on PID10 compared to WT pigs (Fig. 4d). Transient HuNoV viremia was observed previously in Gn pigs and calves[14, 15]. In this study, virus titers in plasma were significantly higher in RAG2/IL2RG deficient pigs on PID3, PID10, and PID17, whereas HuNoV genomes were not detectable on PID28 from either group (Fig. 4e). Similarly, HuNoV genomes were detectable in whole blood cells, and the titer was significantly higher in RAG2/IL2RG deficient pigs on PID17 (Fig. 4f). Taken together, increased and prolonged HuNoV titers in intestinal tissues and contents and in blood demonstrated that RAG2/IL2RG deficiency promoted HuNoV infection of Gn pigs. Thus, B/T/NK lymphocytes are important in the control and clearance of HuNoV infection.

## Discussion

HuNoV gastroenteritis is characteristically acute and self-limiting with a duration of 24 to 72 hours, but in immunocompromised patients, the infection and disease can become persistent for weeks to years, and the chronic viral enteritis can become debilitating and life-threatening[22, 23]. There is currently no virus-specific therapy available for HuNoV infection, although such therapies are in greater demand in immunocompromised populations[29]. Balb/c RAG/IL2RG deficient mice support HuNoV infection, but the duration was only three days, and fecal virus shedding and gastrointestinal disease were not observed. Thus, this mouse model does not reflect HuNoV biology as in immunocompromised humans[30]. Among the related murine noroviruses (MNVs), MNV-1 can establish persistent infection in RAG1 deficient mice, which lack B and T cells[31]. Here, we demonstrated that RAG2/IL2RG deficient Gn pigs supported increased and prolonged HuNoV infection. Higher virus shedding was observed for the first 3 days, indicating SCID hosts were more susceptible to HuNoV infection at the initial stage. Furthermore, the prolonged HuNoV shedding in SCID pigs (after PID17) was asymptomatic and sporadic, which is similar to asymptomatic low virus shedding in immunosuppressed patients[32]. Fecal HuNoV shedding in WT Gn pigs had two clusters peaking on PID6 and PID10, but virus shedding in RAG2/IL2RG deficient Gn pigs had three clusters peaking on PID2, PID11, and PID21-23. The differences in kinetics might result from the higher susceptibility and rapid evolution of HuNoV in SCID hosts[23, 33], and the rapid evolution might also attribute to sporadic virus shedding after PID17, such as on PID27.

B cells were shown to be susceptible to HuNoV infection *in vitro* (human BJAB cell line) and in chimpanzees[13, 34, 35], but enterocytes are the only cell type that has been observed with

HuNoV infection in Gn pigs to date[15-17]. Unlike the reduced MNV-3 titers in RAG1 deficient mice and B cell deficient mice compared to WT mice[36], increased HuNoV titers were observed in RAG2/IL2RG deficient pigs in this study, suggesting that B cells might not be the target cell type of HuNoV in Gn pigs. HuNoV genomes were detected in stomach tissue in both groups with similar titers, presumably accumulating from duodenum-derived virions by reverse peristalsis rather than viral infection and replication in the stomach. HuNoV genomes were also detected in extraintestinal regions, but the titers peaked on PID10 for both groups and it is likely those are virions that translocated through circulating blood. The liver is a critical and unique organ populated with immune cells to eliminate pathogens in blood[37], the lack of lymphocytes may explain how HuNoV genomes were detected in SCID pigs, but were consistently negative in WT pigs. As HuNoV genomes were only detected at low levels in duodenum, ileum, and spleen from 2 of 4 SCID pigs on PID28, it is likely that HuNoV infection would not persist, and that fecal shedding afterward, if there were any, would be asymptomatic and sporadic with low viral loads.

Pig models, especially SCID models, are valuable in studying pathogenesis of human pathogens because of similarities in immunity and physiology between pigs and humans. The importance of these large animal models is increasingly being recognized by the biomedical research community[38, 39]. However, due to low efficiency in production and difficulty in housing the SCID pigs long-term for breeding, their application has been limited. In this study, we introduced a novel experimental platform to apply SCID pigs in pathogenesis study by using CRISPR/Cas9 and Gn systems. The CRISPR/Cas9 system allows us to generate multi-allelic mutant pigs without cloning or breeding, and the Gn system can protect the pigs from other pathogens. Through our study, we found that SCID Gn pigs infected with HuNoV had increased and prolonged

infection when compared to immunocompetent WT Gn pigs. The combination of the CRISPR/Cas9 system and gnotobiology demonstrates an ideal platform to use SCID pigs in biomedical research.

## Methods

**Virus.** Stool containing HuNoV GII.4/2006b variant 092895 (GenBank no. KC990829) was collected at Cincinnati Children's Hospital Medical Center from a child with norovirus gastroenteritis in 2008. The protocol for stool sample collection was approved by the institutional review boards of the Cincinnati Children's Hospital Medical Center (IRB number: 2008-1131), and informed consent was obtained from parents or child for future studies; the sample collection procedures were carried out in accordance with the approved guidelines. The stool was processed as inoculum and stored in our laboratory[16]. Inoculum was tested by culturing in thioglycollate medium and blood-agar plates to confirm sterility, and absence of other viruses was confirmed by a Virochip Microarray (University of California, San Francisco, Viral Diagnostics and Discovery Center).

**Gnotobiotic pigs and HuNoV inoculation.** Near-term WT and SCID pigs (Yorkshire cross breed) were derived via hysterectomy and maintained in Gn pig isolators. Sterility was monitored weekly by culturing feces from rectal swabs in thioglycollate medium and blood-agar plates as described previously[16, 40]. Pigs were orally inoculated at 6-7 days of age with 10 $ID_{50}$ of HuNoV ($2.74 \times 10^4$ viral RNA copies)[16]. Four ml of 200 mM sodium bicarbonate was given 15 min prior to inoculation to neutralize stomach acids. Clinical signs and virus shedding were monitored daily until

euthanasia on PID3, PID10, or PID28 for collection of blood, intestinal contents, and tissues. All animal experimental protocols were approved by the Institutional Animal Care and Use Committee at Virginia Tech (IACUC protocol: 14-108-CVM). All experimental procedures were carried out in accordance with federal and university guidelines.

**HBGA typing.** Pigs were blood-typed by PCR and/or immunofluorescence assay (Supplementary Fig. 5), HBGA type $A^-$ and $H^-$ pigs were excluded from this study. For PCR blood typing, genomic DNA was extracted from 20 µl whole blood using DNAzol Genomic DNA Isolation Reagent (Molecular Research Center) following the manufacturer's instructions. $A^+$ or $A^-$ was determined by a 500 bp PCR product using forward primer ABO4s and reverse primer ABO5a, while primers Pig5 and Pig3 were used as internal control[16]. For immunofluorescence assay[16], pig cheek swabs were collected and swirled in PBS, in which buccal cells were spun down and washed with PBS, and resuspended in 20 µl PBS. 2 µl buccal cell suspension was air dried on slides and fixed in cold acetone. HBGA phenotypes were measured by blood group A antigen antibody (sc-69951; Santa Cruz; 1:500), blood group H antigen antibody (sc-52369; Santa Cruz; 1:500), and AlexaFluor 488-labled secondary antibody (A-10680; Thermo Fisher Scientific; 1:500). Slides were mounted in Vectashield containing 4,6-diamidino-2-phenylindole (DAPI) to stain cell nuclei (Vector Laboratories).

**Isolation of MNC.** Ileum (40 cm) and blood (70 ml) were collected during necropsies for the isolation of MNC as described previously[20]. Briefly, segments of ileum were rinsed with wash medium and Hanks Balanced Salt Solution without $Ca^{2+}$ and $Mg^{2+}$ (HBSS/Modified; GE Healthcare),

and intraepithelial lymphocytes and epithelial cells were dislodged mechanically by horizontal rotation. Segments were minced, resuspended in RPMI-1640 medium containing 10% fetal bovine serum and 400 U $ml^{-1}$ of type 2 collagenase (Worthington Biochemical Co), and digested at 37℃ for 30 min with gentle shaking. The supernatants were then collected, and the remaining tissues were ground on an 80-mesh screen to obtain single cell suspensions. Cells pooled from supernatants and suspensions above were resuspended to a final concentration of 30% percoll (GE Healthcare) and centrifuged at 1800*g* for 20 min at 4℃ to remove mucous. Cell pellets were resuspended in 43% Percoll, underlaid with 70% Percoll, and centrifuged at 1800*g* for 30 min at 4℃. MNC were collected from the 43% to 70% Percoll interface. Blood was collected in 30% (vol/vol) acid citrate dextrose, and peripheral blood lymphocytes (PBL) were isolated by Ficoll-Paque PREMIUM (GE Healthcare) density gradient centrifugation at 1200*g* for 30 min. PBL were collected from the interface and washed in distilled $H_2O$ for 5 to 10 sec to lyse the remaining red blood cells.

**Flow cytometry.** For detecting $CD3^+$ and $CD3^-CD16^+$ lymphocytes, $2 \times 10^6$ of MNC were stained at 4℃ for 15 min in 100 µl of staining buffer with 2 µl mouse (IgG1) anti-pig CD3ε (4510-01; Southern Biotech) and 1 µl Phycoerythrin (PE) conjugated mouse (IgG1) anti-pig CD16 (MCA1971PE; AbDSerotec), followed by 1 µl Allophycocyanin conjugated rat (IgG1) anti-mouse IgG1 (A85-1; BD Pharmingen). Cells were fixed/permeabilized with BD cytofix/cytoperm™ buffer (BD pharmingen) at 4℃ for 30 min. One ml of staining buffer (prepared according to BD Pharmingen™ BrdU Flow Kits Instruction Manual) was used to wash cells between steps and cells were centrifuged at 500*g* for 5 min at 4℃. For detecting the frequencies of $CD79^+$ lymphocytes

among MNC, cells were first fixed/permeabilized with BD cytofix/cytoperm™ buffer at 4℃ for 30 min, then stained at 4℃ for 30 min in 100 µl of BD perm/wash buffer (BD pharmingen) with 0.5 µl mouse (IgG2b) anti-human CD79a (Vp-C366; Vector Laboratories), followed by stained at 4℃ for 30 min in 100 µl of BD perm/wash buffer with 0.5 µl PE-Cy7 goat anti-mouse IgG2b (1090-17, SouthernBiotech). One ml of BD perm/wash buffer was used to wash cells between steps and cells were centrifuged at 500*g* for 5 min at 4℃, followed by washing with 1 ml of staining buffer. At least 20,000 cells were acquired on a FACSAria flow cytometer (BD Biosciences). Flow cytometry data were analyzed using FlowJo 7.2.2 software (Tree Star, Ashland, Oregon). The absolute numbers of $CD3^+$, $CD3^-CD16^+$ and $CD79^+$ lymphocytes per tissue were calculated based on their frequencies among MNC and the total number of MNC isolated from each tissue.

**ELISA for total immunoglobulin.** Total immunoglobulin (Ig) titers in serum were measured by ELISA. 96-well plates were coated with goat anti-porcine IgM (01-14-03; KPL; 15 µg $ml^{-1}$), IgA (A100-102A; Bethyl; 18 µg $ml^{-1}$), or IgG (01-14-02; KPL; 3 µg $ml^{-1}$) antibody overnight at 4℃. Plates were washed twice with PBS containing 0.05% Tween-20 (PBST), blocked with PBST containing 2% non-fat milk at 37℃ for 2h, and washed twice with PBST. Sera were serially diluted with PBST containing 2% non-fat milk, and incubated on coated plates at 37℃ for 1h. After washing for four times, horseradish peroxidase-conjugated goat anti-porcine IgM (04-14-03; KPL; 1:5000), IgA (A100-102p; Bethyl; 1:5000), or IgG (A100-104p; Bethyl; 1:500) antibody was added and incubated at room temperature for 1h. Plates were washed four times with PBST and developed by ABTS substrate (KPL). The highest sample dilution that produced a mean absorbance ($A_{405}$)

greater than the cut-off value (mean $A_{405}$ of negative controls plus three times of standard deviation) was considered as the Ig titer.

**Detection of HuNoV by qRT-PCR.** HuNoV genomes were detected by a one-step TaqMan qRT-PCR, for which RNA templates from different samples were processed as follows. To assess virus shedding, pig feces were collected daily following HuNoV inoculation by rectal swab sampling, then rectal swabs were swirled in 1 ml PBS to release feces, after vortexing and centrifugation at 10000*g* for 5 min, 250 µl supernatant was prepared for total RNA isolation. Gut tissues were collected during necropsies and immediately frozen in liquid nitrogen; 40 to 60 mg of tissues were washed in PBS and homogenized in 0.2 ml TRIzol LS (Thermo Fisher Scientific) with 100 mg of 1.0 mm Zirconium Oxide beads (Next Advance) using Bullet Blender (Next Advance) for 10 min at maximum speed, and RNA was isolated by adding another 0.55 ml TRIzol LS. Intestinal contents were collected and the total volume was measured. Five ml were prepared as 10% solution using diluent #5 (Minimal Essential Medium with 1% penicillin-streptomycin and 1% HEPES), and RNA was isolated from 100 µl diluted intestinal contents. Plasma and whole blood cells were separated from blood containing ACD by centrifugation at 2000*g* for 5 min. Plasma from 250 µl blood was used for RNA isolation, and whole blood cells from 50 µl blood was washed in PBS and used for RNA isolation. MNC from ileum were isolated as described above and $2 \times 10^6$ cells were used for RNA isolation.

Samples processed above were isolated for total RNA using 750 µl TRIzol LS following the manufacturer's instructions. The RNA was dissolved in 40 µl DEPC-treated water, and 5 µl RNA was used for the 25 µl qRT-PCR reaction with a SensiFAST Probe No-ROX One-Step Kit (Bioline)

to detect HuNoV genomes. Primers COG2F, COG2R, and probe RING2 were adapted from a previous study[41]. Cycling conditions were: reverse transcription at 45℃ for 10 min, polymerase activation at 95℃ for 2 min, 40 cycles of denaturation at 95℃ for 5s and annealing and extension at 58℃ for 20s. A standard curve was obtained by using COG2 amplicon-containing plasmid in serially diluted tenfold from $10^7$ to 1 genomic copy. Amplification was performed on CFX96 Real-Time System (Bio-Rad), and data were collected and analyzed with Bio-Rad CFX Manager 2.0.

**Assessment of HuNoV diarrhea.** Daily rectal swabs were collected following HuNoV inoculation, fecal consistency was scored based on our previous system[16]. From PID1 to PID17, pigs were scored as follows: 0, solid; 1, semisolid; 2, pasty; 3, semiliquid; and 4, liquid. From PID18 to PID28, pigs were scored based on a more stringent system since the feces from older pigs were looser: 0, solid; 1, pasty; 2, semiliquid; and 3, liquid. Pigs with daily fecal scores of 2 or greater were considered diarrheic.

**Immunohistostaining.** Sections of intestinal tissues were collected during necropsies, fixed overnight in 10% neutral formalin, embedded in paraffin, and sectioned 5 μm on positively charged glass slides. For immunostaining, slides were deparaffinized and rehydrated via graded ethanol series. Enzymatic antigen retrieval was performed by digesting sections in proteinase K solution (80 μg $ml^{-1}$, Sigma Aldrich) at 37 ℃ for 30 min. Slides were incubated in blocking buffer (tris-buffered saline (TBS) with 10% normal pig serum and 1% bovine serum albumin (BSA)) at room temperature for 2 h. For immunostaining of duodenum and jejunum, the staining procedure consisted of incubation with a goat anti-HuNoV GII.4 VLP polyclonal antibody diluted

in TBS containing 1% BSA overnight at 4 ℃, washing with TBS containing 0.025% Triton X-100, and incubation with Alexa Fluor 488-labeled donkey anti-goat secondary antibody (A-11055; Thermo Fisher Scientific; 1:500) diluted in TBS containing 1% BSA at room temperature for 1 h. For immunostaining of mesentery, mouse anti-CD79 (VP-C366; Vector Laboratories; 1:1000) and Alexa Fluor 546-labeled donkey anti-mouse secondary antibody (A10036; Thermo Fisher Scientific; 1:500) were used in the two incubation steps above. Slides were washed in TBS and mounted in Vectashield containing DAPI to stain cell nuclei (Vector Laboratories). Images were acquired on a Zeiss LSM 880 confocal laser scanning microscope with Zen software (Zeiss).

**Statistics.** All pigs infected with HuNoV were randomly assigned to be euthanized on PID3, PID10, or PID28. For virus shedding, diarrhea scores, and virus in blood, pigs euthanized on PID28 contributed data to PID3 and PID10 subgroups, as did PID10 contributed data to PID3 subgroup. Statistical analysis (Mann-Whitney test or Student's *t*-test as specified) was performed using GraphPad Prism 6.0 (GraphPad Software). *P* value < 0.05 was considered statistically significant.

## Acknowledgements

We thank X.J. Meng, B. Coulson, X. Wang, and N. Nanthakumar for critical discussion. We thank K. DeCourcy for assisting on confocal microscope, K. Pelzer for veterinary service, K. Young, K. Allen, K. Hall, S. Viers, and J. Park for animal care. This work was supported by NIH grant R01AI089634 (to LY) and R21OD019934 (to KL and LY).

## Author contributions

K.L. and L.Y. designed and supervised the project. S.L. and J.R. performed most of the experiments and analyzed data. K.W. performed flow cytometry and analyzed data. E.T., T.B., A.R., M.W., G.L., and H.S. performed experiments. S.C. performed embryo transfer and provided veterinary services. X.J. contributed materials. S.L., K.L., and L.Y. wrote the manuscript. All authors reviewed the manuscript.

## Additional Information

**Competing financial interests:** The authors declare no competing financial interests.

## References


1. Walters, E.M. & Prather, R.S. Advancing swine models for human health and diseases. *Mo Med* **110**, 212-5 (2013).
2. Suzuki, S. et al. Il2rg gene-targeted severe combined immunodeficiency pigs. *Cell Stem Cell* **10**, 753-8 (2012).
3. Gaj, T., Gersbach, C.A. & Barbas, C.F., 3rd. ZFN, TALEN, and CRISPR/Cas-based methods for genome engineering. *Trends Biotechnol* **31**, 397-405 (2013).
4. Ramani, S., Atmar, R.L. & Estes, M.K. Epidemiology of human noroviruses and updates on vaccine development. *Curr Opin Gastroenterol* **30**, 25-33 (2014).
5. Hemming, M. et al. Major reduction of rotavirus, but not norovirus, gastroenteritis in children seen in hospital after the introduction of RotaTeq vaccine into the National Immunization Programme in Finland. *Eur J Pediatr* **172**, 739-46 (2013).
6. Karve, S., Krishnarajah, G., Korsnes, J.S., Cassidy, A. & Candrilli, S.D. Burden of acute gastroenteritis, norovirus and rotavirus in a managed care population. *Hum Vaccin Immunother* **10**, 1544-56 (2014).
7. Patel, M.M. et al. Systematic literature review of role of noroviruses in sporadic gastroenteritis. *Emerg Infect Dis* **14**, 1224-31 (2008).
8. Hall, A.J. et al. Norovirus disease in the United States. *Emerg Infect Dis* **19**, 1198-205 (2013).
9. Gastanaduy, P.A., Hall, A.J., Curns, A.T., Parashar, U.D. & Lopman, B.A. Burden of norovirus gastroenteritis in the ambulatory setting--United States, 2001-2009. *J Infect Dis* **207**, 1058-65 (2013).
10. Karst, S.M. Pathogenesis of noroviruses, emerging RNA viruses. *Viruses* **2**, 748-81 (2010).
11. Tan, M. & Jiang, X. Vaccine against norovirus. *Hum Vaccin Immunother* **10**, 1449-56 (2014).
12. Kocher, J. & Yuan, L. Norovirus vaccines and potential antinorovirus drugs: recent advances and future perspectives. *Future Virol* **10**, 899-913 (2015).
13. Bok, K. et al. Chimpanzees as an animal model for human norovirus infection and vaccine development. *Proc Natl Acad Sci U S A* **108**, 325-30 (2011).
14. Souza, M., Azevedo, M.S., Jung, K., Cheetham, S. & Saif, L.J. Pathogenesis and immune responses in gnotobiotic calves after infection with the genogroup II.4-HS66 strain of human norovirus. *J Virol* **82**, 1777-86 (2008).
15. Cheetham, S. et al. Pathogenesis of a genogroup II human norovirus in gnotobiotic pigs. *J Virol* **80**, 10372-81 (2006).
16. Bui, T. et al. Median infectious dose of human norovirus GII.4 in gnotobiotic pigs is decreased by simvastatin treatment and increased by age. *J Gen Virol* **94**, 2005-16 (2013).
17. Jung, K. et al. The effects of simvastatin or interferon-alpha on infectivity of human norovirus using a gnotobiotic pig model for the study of antivirals. *PLoS One* **7**, e41619 (2012).
18. Ball, R.O., House, J.D., Wykes, L.J. & Pencharz, P.B. in Advances in Swine in Biomedical Research (eds. Tumbleson, M.E. & Schook, L.B.) 713-731 (Plenum Press, New York, 1996).
19. Kocher, J. et al. Intranasal P particle vaccine provided partial cross-variant protection against human GII.4 norovirus diarrhea in gnotobiotic pigs. *J Virol* **88**, 9728-43 (2014).
20. Yuan, L., Ward, L.A., Rosen, B.I., To, T.L. & Saif, L.J. Systematic and intestinal antibody-secreting cell responses and correlates of protective immunity to human rotavirus in a gnotobiotic pig model of disease. *J Virol* **70**, 3075-83 (1996).
21. Karst, S.M., Wobus, C.E., Goodfellow, I.G., Green, K.Y. & Virgin, H.W. Advances in norovirus biology. *Cell Host Microbe* **15**, 668-80 (2014).

22. Green, K.Y. Norovirus infection in immunocompromised hosts. *Clin Microbiol Infect* **20**, 717-23 (2014).
23. Bok, K. & Green, K.Y. Norovirus gastroenteritis in immunocompromised patients. *N Engl J Med* **367**, 2126-32 (2012).
24. Lei, S. et al. Increased and prolonged human norovirus infection in RAG2/IL2RG deficient gnotobiotic pigs with severe combined immunodeficiency. *Sci Rep* **6**, 25222 (2016).
25. Tan, M. & Jiang, X. Norovirus and its histo-blood group antigen receptors: an answer to a historical puzzle. *Trends Microbiol* **13**, 285-93 (2005).
26. Cheetham, S. et al. Binding patterns of human norovirus-like particles to buccal and intestinal tissues of gnotobiotic pigs in relation to A/H histo-blood group antigen expression. *J Virol* **81**, 3535-44 (2007).
27. Tian, P. et al. Binding of recombinant norovirus like particle to histo-blood group antigen on cells in the lumen of pig duodenum. *Res Vet Sci* **83**, 410-8 (2007).
28. Takanashi, S. et al. Detection, genetic characterization, and quantification of norovirus RNA from sera of children with gastroenteritis. *J Clin Virol* **44**, 161-3 (2009).
29. Kaufman, S.S., Green, K.Y. & Korba, B.E. Treatment of norovirus infections: moving antivirals from the bench to the bedside. *Antiviral Res* **105**, 80-91 (2014).
30. Taube, S. et al. A mouse model for human norovirus. *MBio* **4**, e00450-13 (2013).
31. Karst, S.M., Wobus, C.E., Lay, M., Davidson, J. & Virgin, H.W.t. STAT1-dependent innate immunity to a Norwalk-like virus. *Science* **299**, 1575-8 (2003).
32. Ludwig, A., Adams, O., Laws, H.J., Schroten, H. & Tenenbaum, T. Quantitative detection of norovirus excretion in pediatric patients with cancer and prolonged gastroenteritis and shedding of norovirus. *J Med Virol* **80**, 1461-7 (2008).
33. Mai, H. et al. GII.4 Sydney_2012 norovirus infection in immunocompromised patients in Beijing and its rapid evolution in vivo. *J Med Virol* **88**, 224-33 (2016).
34. Jones, M.K. et al. Enteric bacteria promote human and mouse norovirus infection of B cells. *Science* **346**, 755-9 (2014).
35. Jones, M.K. et al. Human norovirus culture in B cells. *Nat Protoc* **10**, 1939-47 (2015).
36. Zhu, S. et al. Identification of immune and viral correlates of norovirus protective immunity through comparative study of intra-cluster norovirus strains. *PLoS Pathog* **9**, e1003592 (2013).
37. Jenne, C.N. & Kubes, P. Immune surveillance by the liver. *Nat Immunol* **14**, 996-1006 (2013).
38. Harding, J., Roberts, R.M. & Mirochnitchenko, O. Large animal models for stem cell therapy. *Stem Cell Res Ther* **4**, 23 (2013).
39. Plews, J.R., Gu, M., Longaker, M.T. & Wu, J.C. Large animal induced pluripotent stem cells as pre-clinical models for studying human disease. *J Cell Mol Med* **16**, 1196-202 (2012).
40. Meyer, R.C., Bohl, E.H. & Kohler, E.M. Procurement and Maintenance of Germ-Free Seine for Microbiological Investigations. *Appl Microbiol* **12**, 295-300 (1964).
41. Kageyama, T. et al. Broadly reactive and highly sensitive assay for Norwalk-like viruses based on real-time quantitative reverse transcription-PCR. *J Clin Microbiol* **41**, 1548-57 (2003).

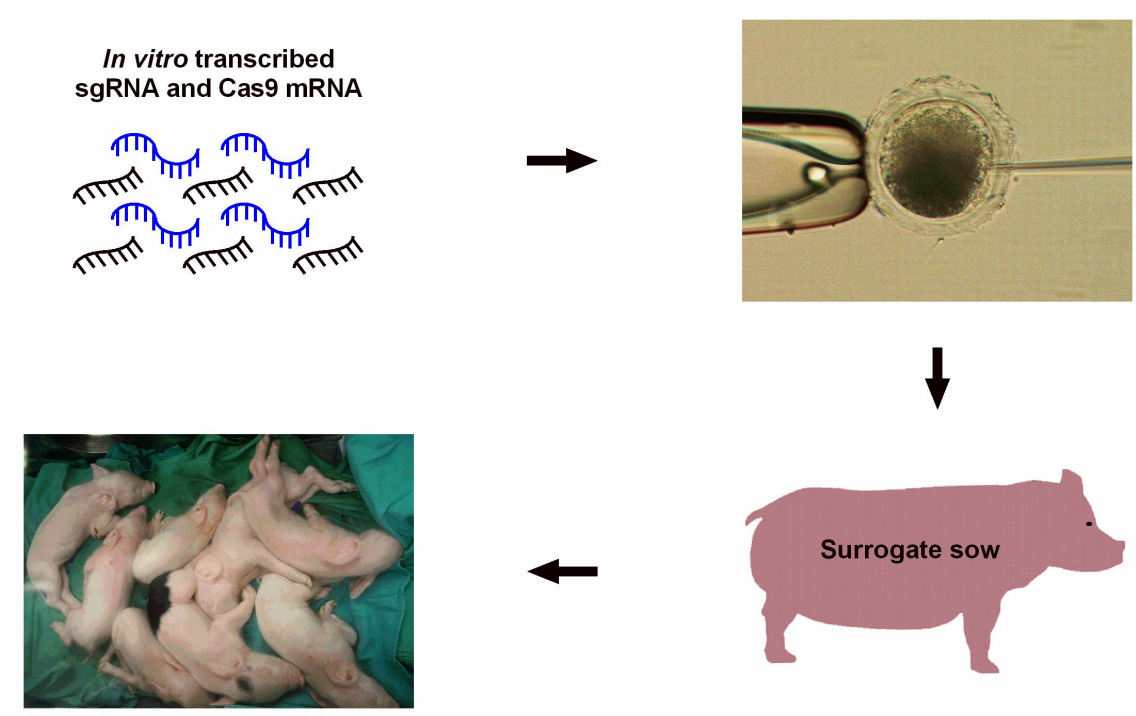


**Figure 1. Use of CRISPR/Cas9 system to generate RAG2/IL2RG deficient pigs.** RNA form of sgRNA and Cas9 were injected into presumable zygotes at an optimized concentration. Then the injected embryos were transferred into surrogate sows. Piglets were derived by hysterectomy and maintained in Gn isolators.

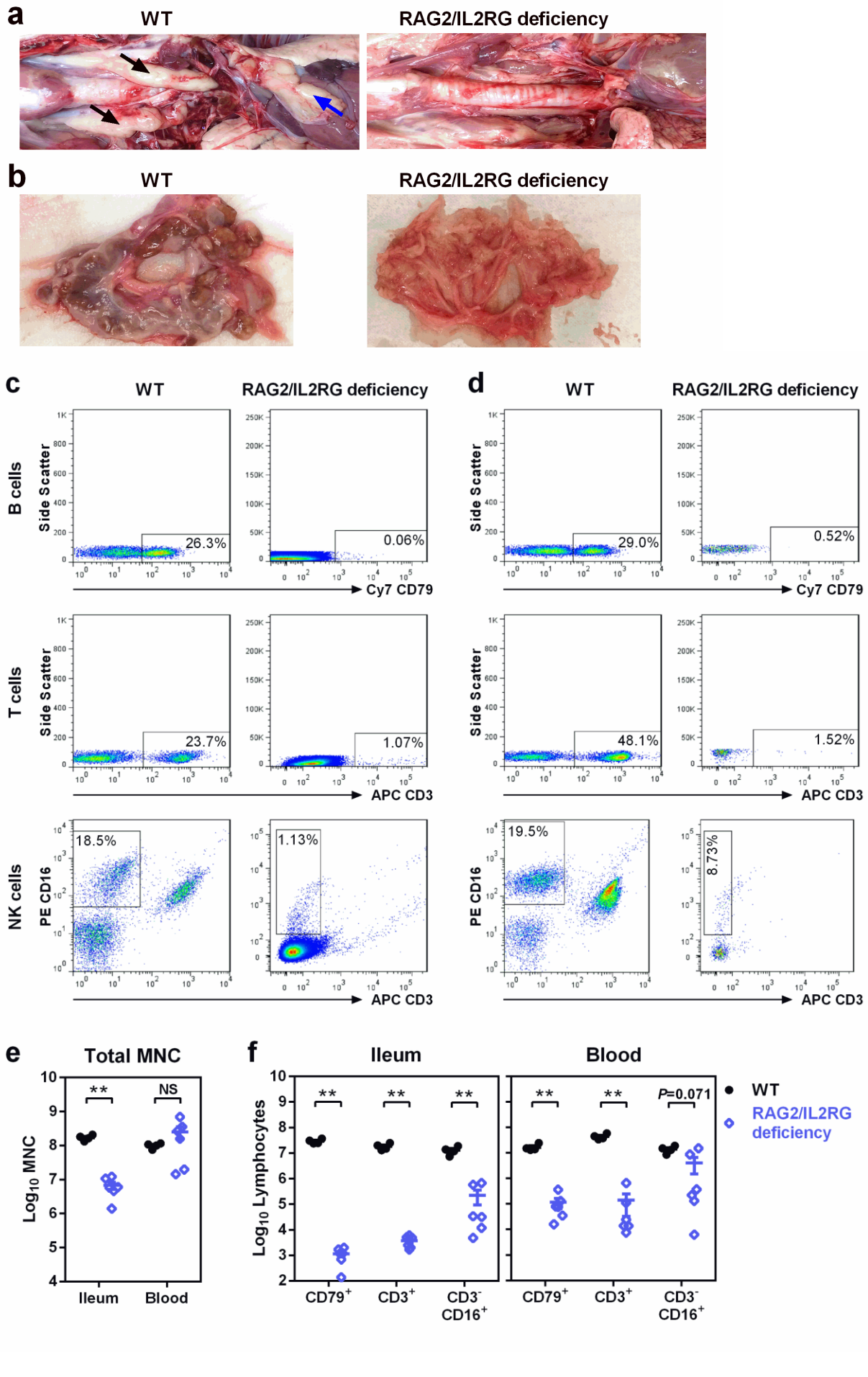
a
WT
RAG2/IL2RG deficiency
b
WT
RAG2/IL2RG deficiency
c
WT
RAG2/IL2RG deficiency
B cells
Side Scatter
26.3%
0.06%
Cy7 CD79
T cells
23.7%
1.07%
APC CD3
NK cells
PE CD16
18.5%
1.13%
d
WT
RAG2/IL2RG deficiency
29.0%
0.52%
48.1%
1.52%
19.5%
8.73%
e
Total MNC
Log10 MNC
**
NS
Ileum
Blood
f
Ileum
Blood
Log10 Lymphocytes
**
P=0.071
CD79+
CD3+
CD3-CD16+
WT
RAG2/IL2RG deficiency

**Figure 2. SCID phenotype of RAG2/IL2RG deficient pigs at 34 days of age.** (**a**) Representative images showing thoracic thymus (black arrows) and cervical thymus (blue arrow) in WT pigs, while thoracic and cervical thymus were lacking in some RAG2/IL2RG pigs. (**b**) Representative images of the mesentery showing the lack of MLN in some RAG2/IL2RG pigs. Representative flow cytometry of MNC from ileum (**c**) and blood (**d**) showing a significant reduction of B cells ($CD79^+$), T cells ($CD3^+$), and NK cells ($CD3^-CD16^+$), as indicated by dot plots gated within lymphocytes. Cy7, cyanine 7; APC, allophycocyanin; PE, phycoerythrin. (**e**) Total number of MNC from 40 cm ileum and 70 ml blood were isolated and quantified for WT (*n* = 4) and RAG2/IL2RG deficient pigs (*n* = 6). (**f**) Lymphocytes in ileum and blood were quantified based on the total number of MNC and the proportion of cells within MNC (Supplementary Fig. 3). Data are presented as means ± s.e.m. with individual animal data points (**e**-**f**). Statistical significance was determined by Mann-Whitney test. NS, not significant, $^{**}P<0.01$.

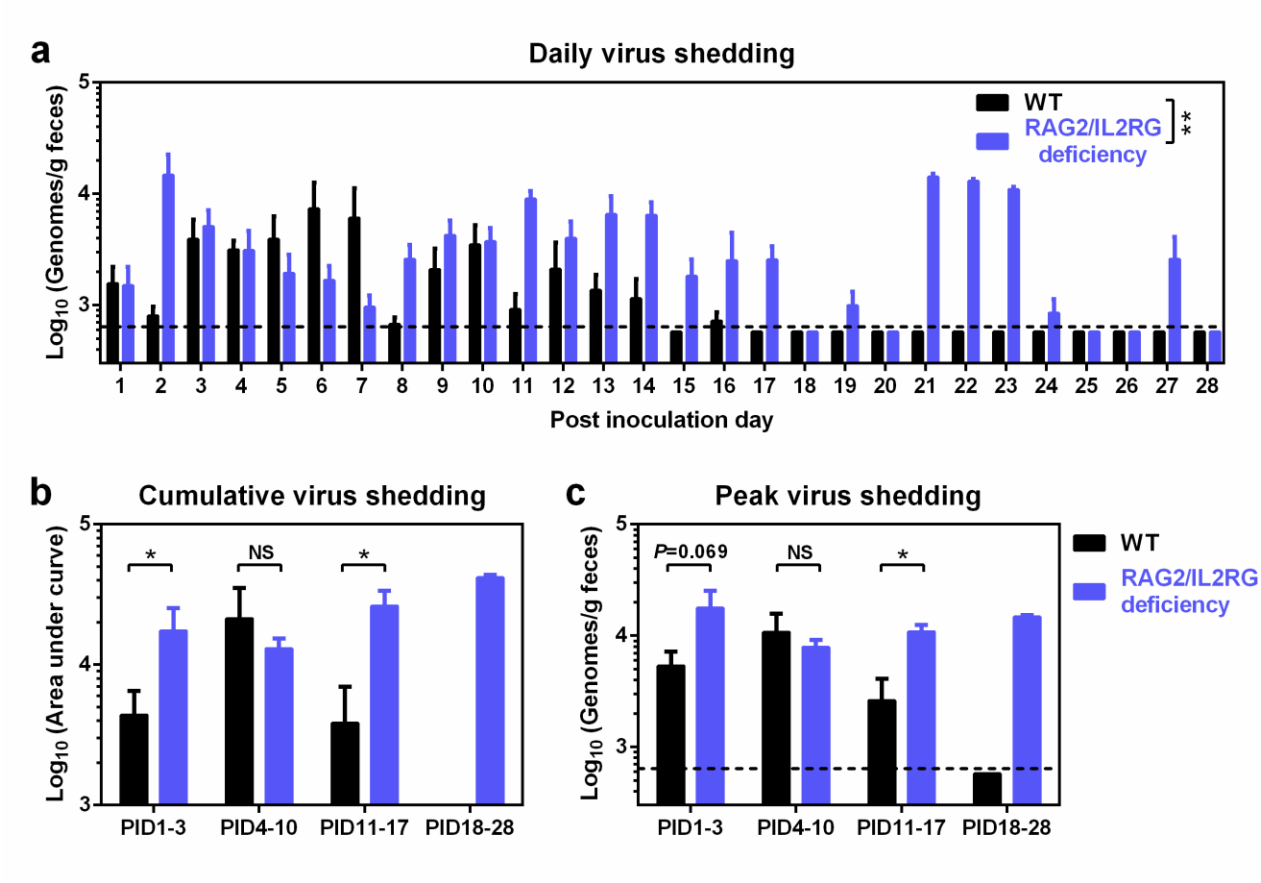


**Figure 3. Increased and prolonged fecal HuNoV shedding in RAG2/IL2RG deficient pigs.** (**a**) Daily virus shedding was monitored from PID1 to PID28 by rectal swab sampling of feces and quantitative reverse transcription polymerase chain reaction (qRT-PCR) to quantify the HuNoV genomes. (**b**) Individual pigs' cumulative virus shedding was presented as area under curve from **a**. (**c**) Peak virus shedding titers from PID1 to PID3, PID4 to PID10, PID11 to PID17, and PID18 to PID28 in individual pigs. Sample sizes are shown in **Table 1**. Dashed line indicates limit of detection. Data are presented as mean ± s.e.m. Statistical significance was determined by two-way analysis of variance (ANOVA) (**a**) or Mann-Whitney test (**b**-**c**). NS, not significant, **P*<0.05, ***P*<0.01.

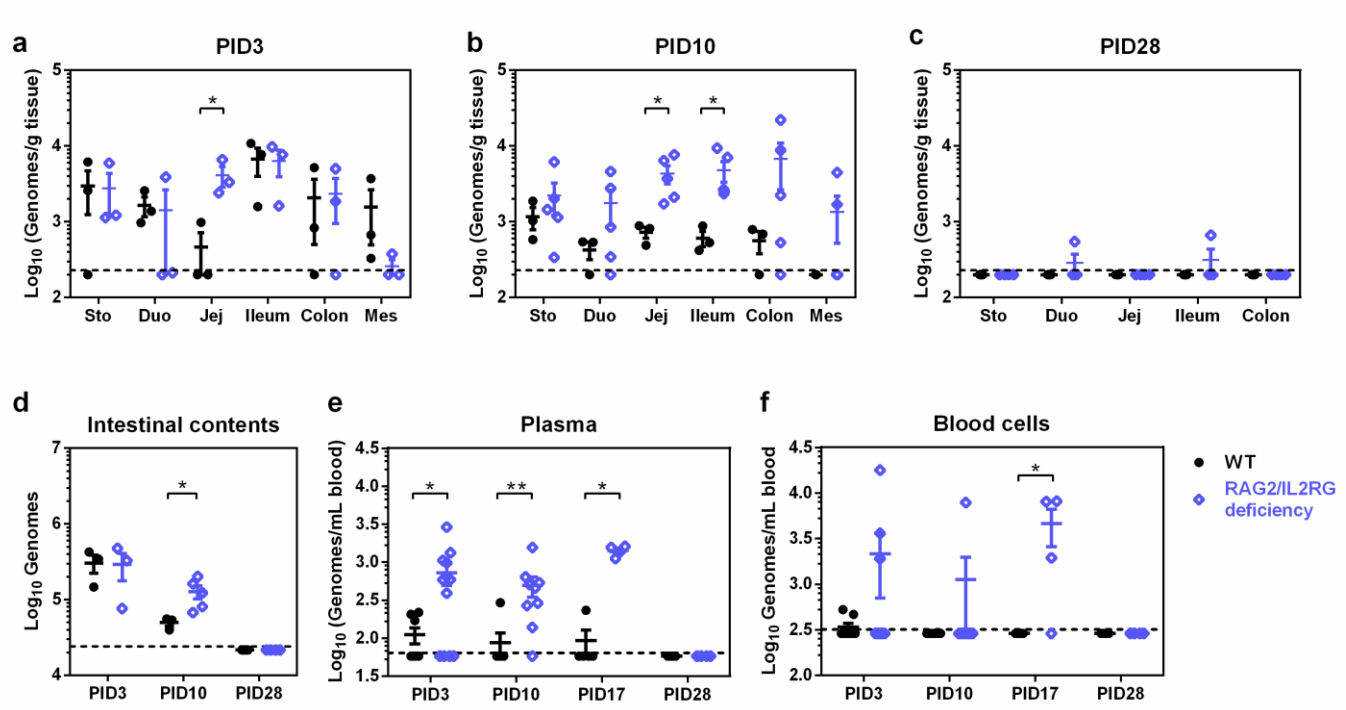


**Figure 4. HuNoV distribution in Gn pigs.** HuNoV genomes in stomach (Sto), duodenum (Duo), jejunum (Jej), ileum, and mesentery (Mes) from pigs euthanized on PID3 (**a**), PID10 (**b**), and PID28 (**c**) were measured by qRT-PCR. (**d**) Total HuNoV genomes in intestinal contents were measured by qRT-PCR. HuNoV genomes in plasma (**e**) and whole blood cells (**f**) were measured by qRT-PCR. (**a**-**d**) WT groups, PID3 *n*=3, PID10 *n*=3, PID *n*=5; RAG2/IL2RG deficiency groups, PID3 *n*=3, PID10 *n*=5, PID *n*=4. (**e**-**f**) Sample sizes are shown in **Table 1**. Dashed line indicates limit of detection. Data are presented as mean ± s.e.m. with individual animal data points. Statistical significance was determined by Student's *t*-test (**a**) or Mann-Whitney test (**b**-**f**). **P*<0.05, ***P*<0.01.

| Group | Time | *n* | Diarrhea | | Virus shedding | |
|---|---|---|---|---|---|---|
| | | | Pigs with diarrhea (%)* | Mean duration days (SEM)** | Pigs shedding virus (%)* | Mean duration days (SEM)** |
| WT | PID1–3 | 11 | 8 (73%) | 1.0 (0.3) | 9 (82%) | 1.5 (0.3) |
| RAG2/IL2RG deficiency | | 12 | 6 (50%) | 0.8 (0.3) | 11 (92%) | 1.3 (0.2) |
| WT | PID4–10 | 8 | 7 (88%) | 2.8 (0.6) | 7 (88%) | 3.0 (0.7) |
| RAG2/IL2RG deficiency | | 9 | 6 (67%) | 1.7 (0.6) | 9 (100%) | 3.4 (0.3) |
| WT | PID11–17 | 5 | 5 (100%) | 2.6 (1.0) | 2 (40%) | 1.2 (1.0)$^{A}$ |
| RAG2/IL2RG deficiency | | 4 | 4 (100%) | 4.5 (1.2) | 4 (100%) | 5.5 (0.6)$^{B}$ |
| WT | PID18–28 | 5 | 1 (20%) | 0.4 (0.4) | 0$^{A}$ | 0$^{A}$ |
| RAG2/IL2RG deficiency | | 4 | 2 (50%) | 0.8 (0.5) | 4 (100%)$^{B}$ | 4.5 (0.3)$^{B}$ |

**Table 1. Incidence of clinical signs and fecal virus shedding in Gn pigs.** Gn pigs were inoculated with a HuNoV GII.4 2006b variant 092895 at 6-7 days of age. Rectal swabs were collected daily after inoculation to determine diarrhea and virus shedding. SEM, standard error of the mean. *Fisher's exact test or **Mann-Whitney test was used for statistical analysis. Groups with significant differences ($P$<0.05) were indicated with letters A and B.

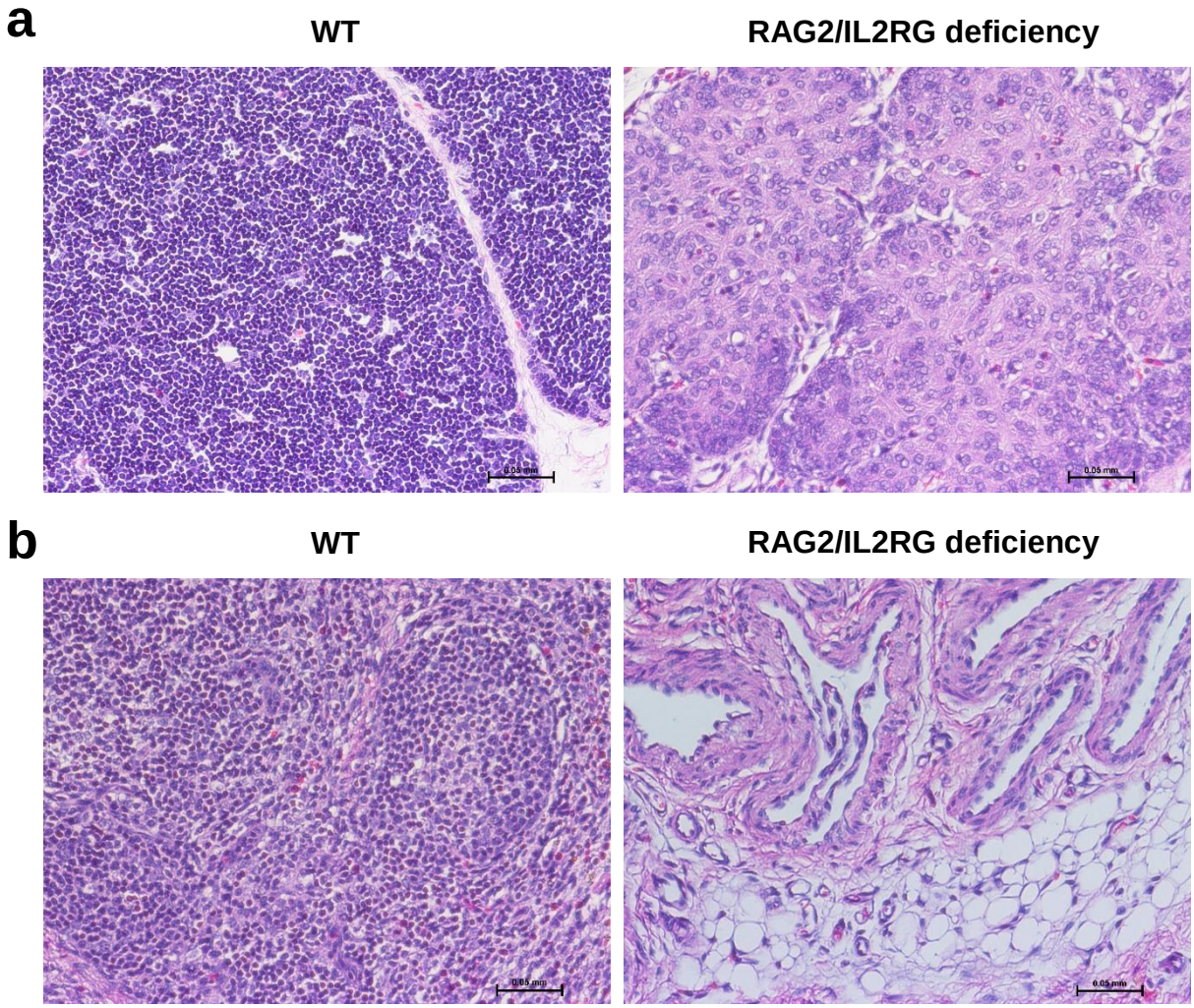


**Supplementary Figure 1. Lack of lymphocytes in thymus and mesentery in some RAG2/IL2RG deficient pigs.** (**a**) Representative images of H&E stained sections showing lack of lymphocytes within observed thymus in a RAG2/IL2RG deficient pig (right), while thymuses were populated with lymphocytes in WT pigs (left). (**b**) Representative images of H&E stained sections showing lack of lymphocytes within mesenteric tissue in a RAG2/IL2RG deficient pig (right), while mesenteric lymph nodes were populated with lymphocytes in WT pigs (left). Scale bar, 50 µm.

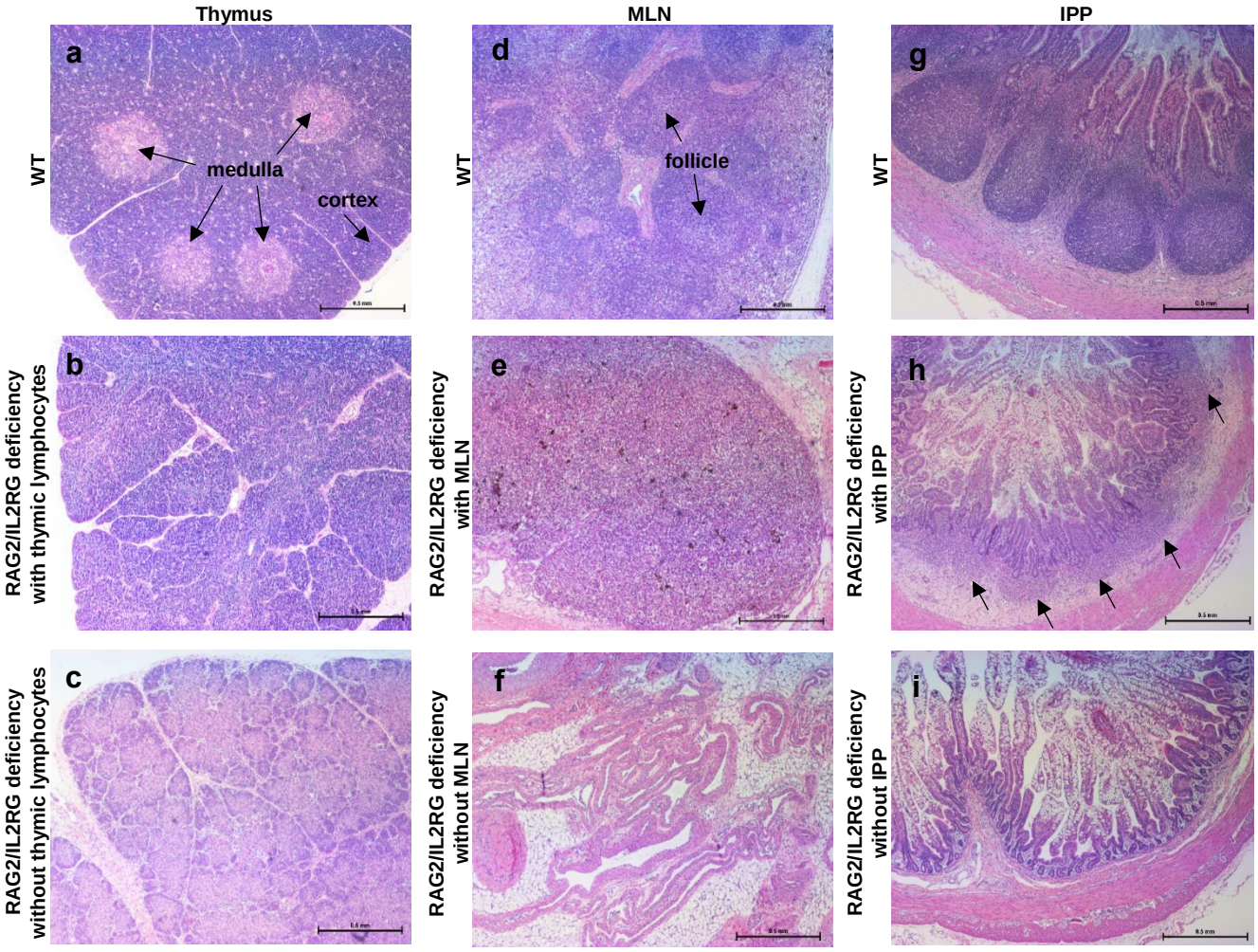


**Supplementary Figure 2. Abnormal morphology of thymus, MLN, and IPP in RAG2/IL2RG deficient pigs.** Representative images of H&E stained sections showing abnormal structure of thymus (left panel), MLN (middle panel), and IPP (right panel) in RAG2/IL2RG deficient pigs at 34 days of age. (**a**) Histologically normal thymus from a WT pig with defined cortex and medulla. Thymus from RAG2/IL2RG deficient pigs with lymphocytes but no distinction between cortex and medulla (**b**) or without lymphocytes (**c**). (**d**) Histologically normal MLN from a WT pig. **(e**) MLN from RAG2/IL2RG deficient pigs without defined cortical or medullary lymphoid tissue. (**f**) Mesentery without MLN from a RAG2/IL2RG deficient pig. (**g**) Normal IPP from WT pigs. (**h**) Poorly developed and unstructured small IPP indicated by arrows in RAG2/IL2RG deficient pigs. (**i**) Ileum without IPP from a RAG2/IL2RG deficient pig. Scale bar, 0.5 mm.

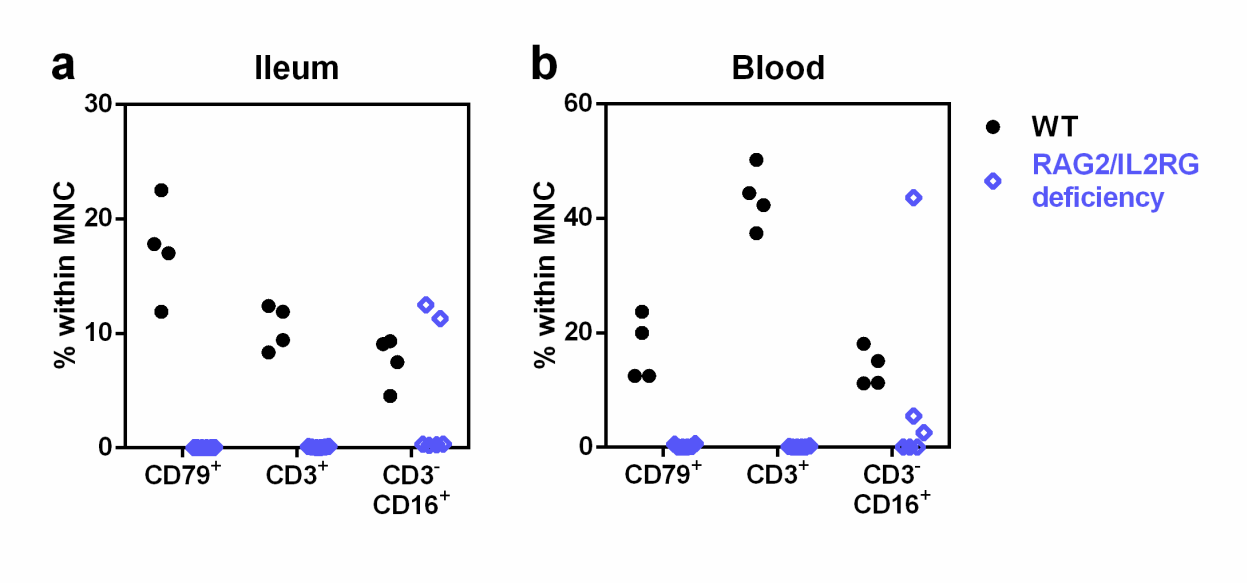


**Supplementary Figure 3. Proportion of B cells ($CD79^+$), T cells ($CD3^+$), and NK cells ($CD3^-CD16^+$) within MNC.** The frequency of B cells, T cells, and NK cells within MNC from ileum (**a**) and blood (**b**) were quantified by flow cytometry for WT (*n* = 4) and RAG2/IL2RG deficient pigs (*n* = 6). Data are presented as individual animal data points.

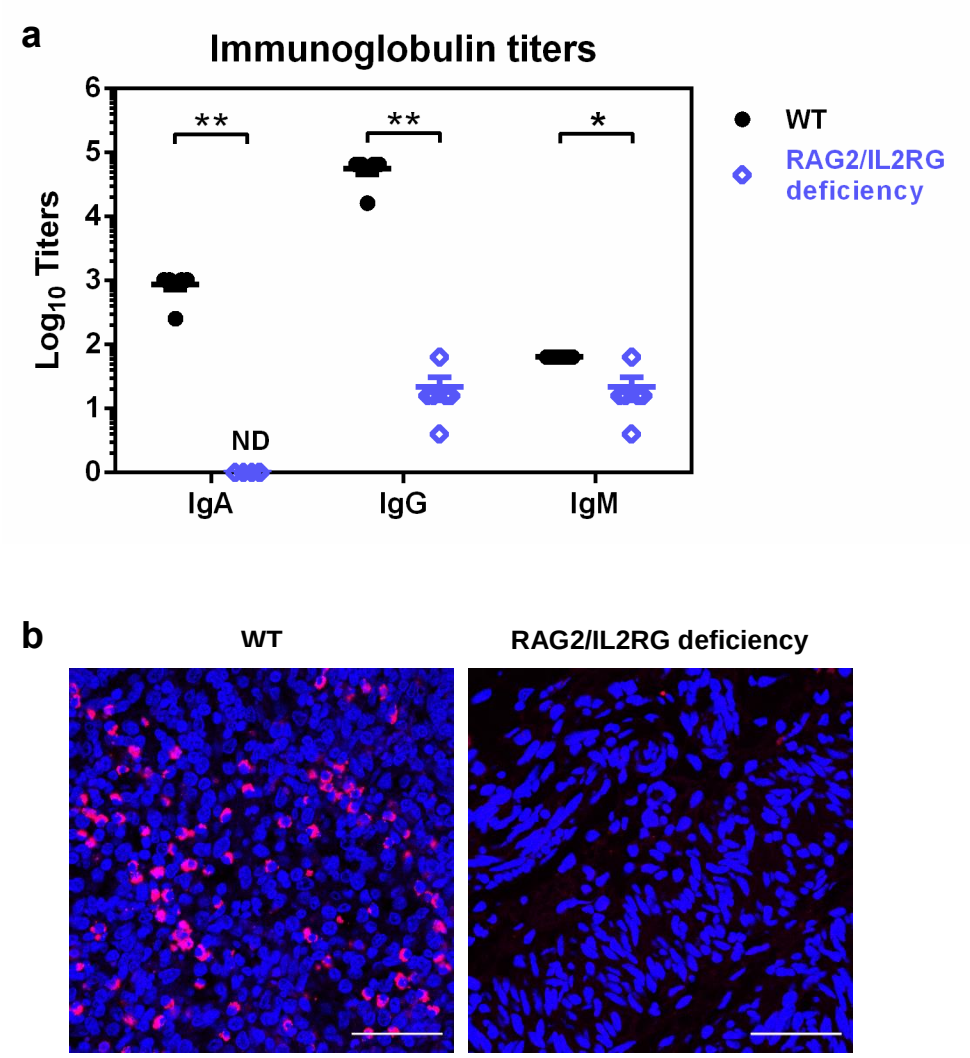


**Supplementary Figure 4. Depletion of B cells in RAG2/IL2RG deficient pigs at 34 days of age.** (**a**) Immunoglobulin titers in serum were determined by ELISA in WT (*n* = 5) and RAG2/IL2RG deficient pigs (*n* = 6). Data are presented as means ± s.e.m. with individual animal data points. Statistical significance was determined by Mann-Whitney test. **P*<0.05, ***P*<0.01. **(b)** Mesentery tissue sections from WT and RAG2/IL2RG deficient pigs were stained to detect B cells ($CD79^+$, red) with counter staining of cell nuclei (DAPI, blue). Scale bar, 50 µm.

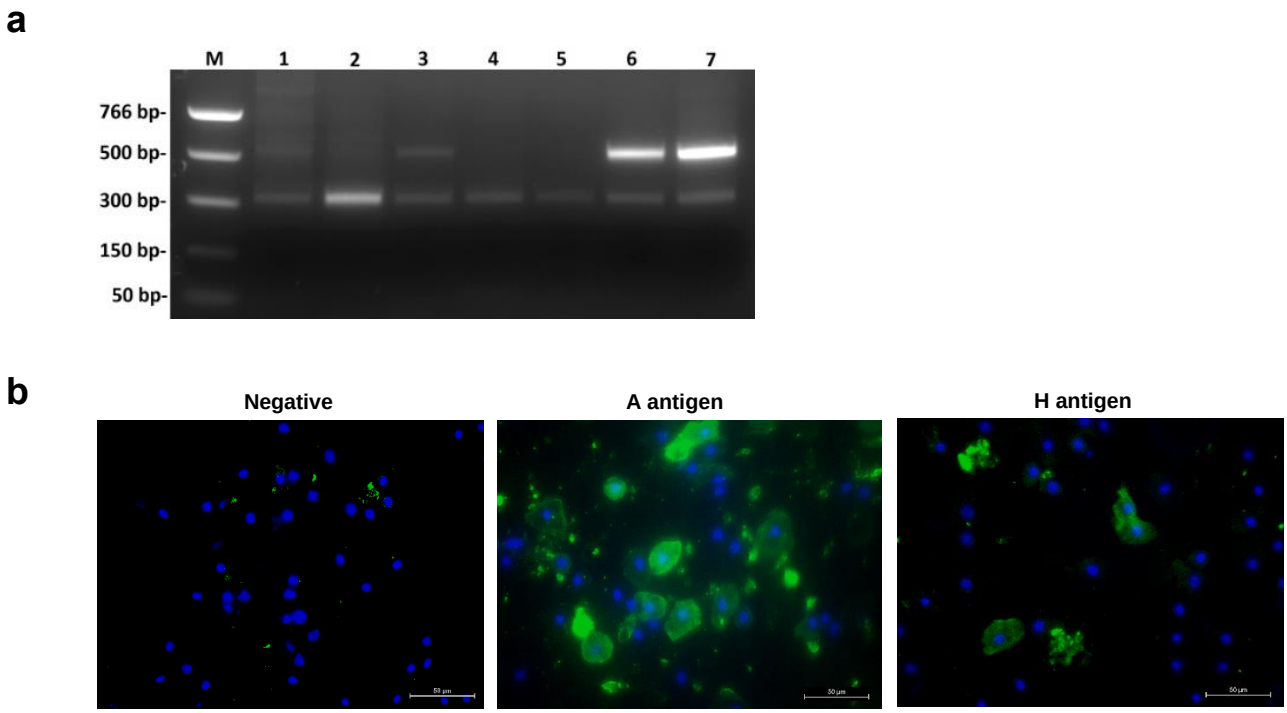


**Supplementary Figure 5. HBGA typing of Gn pigs by PCR and immunofluorescence assay.** (**a**) Pigs were determined to be $A^+$ or $A^-$ by PCR using genomic DNA from blood. Representative gel image showing $A^+$ samples with a 500 bp PCR product in addition to a 300 bp PCR internal control (Lane 1, 3, 6, 7). (**b**) Buccal cells were fixed on glass slides and stained for A or H antigen (FITC, green) and nuclei (DAPI, blue). Representative images indicate HBGA $A^-$ and $H^-$, $A^+$, and $H^+$ pigs. Scale bar, 50 μm.

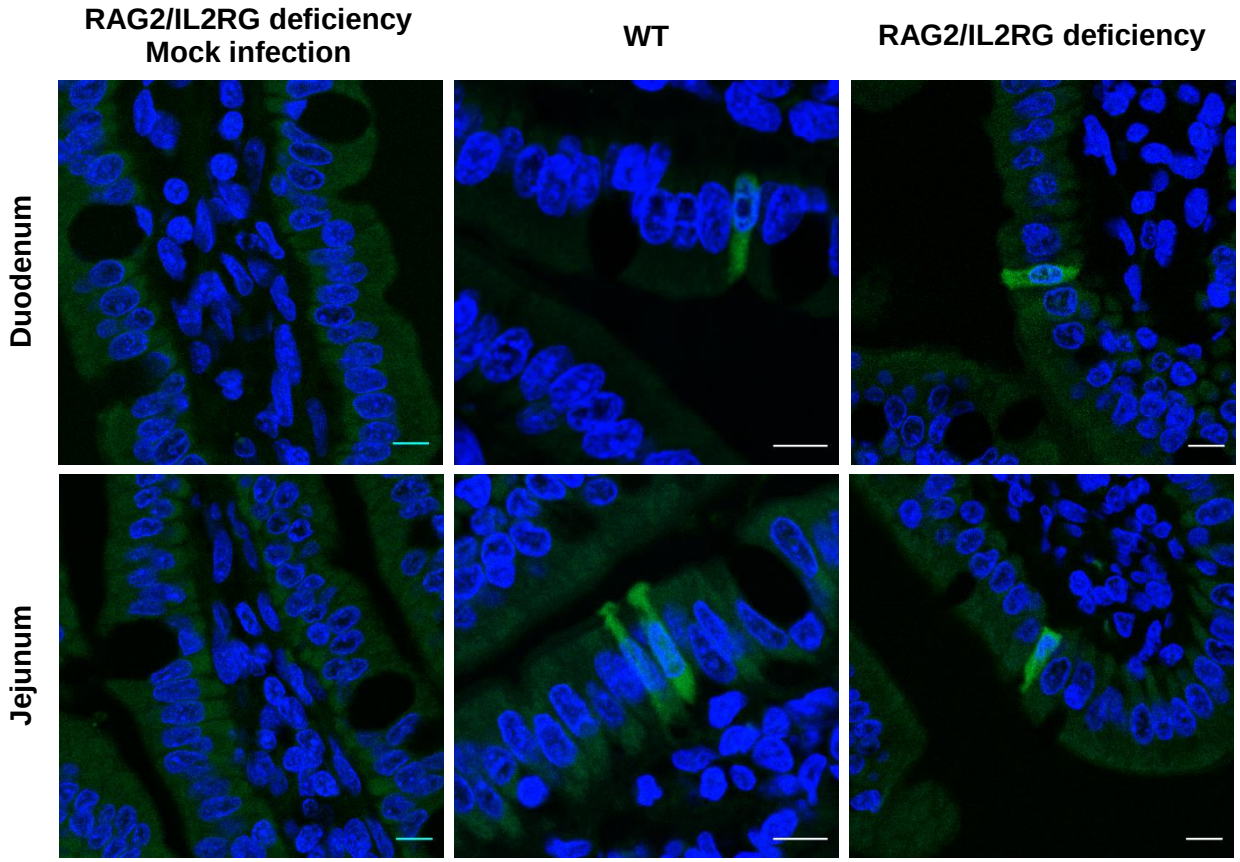


**Supplementary Figure 6. HuNoV infection of enterocytes in Gn pigs.** Immunohistochemistry of duodenum (upper panel) and jejunum (lower panel) from pigs euthanized on PID3 for HuNoV capsid protein (bright green) and cell nuclei (blue). Representative images showing HuNoV infection of enterocytes in WT and RAG2/IL2RG deficient pigs. Scale bar, 10 µm.

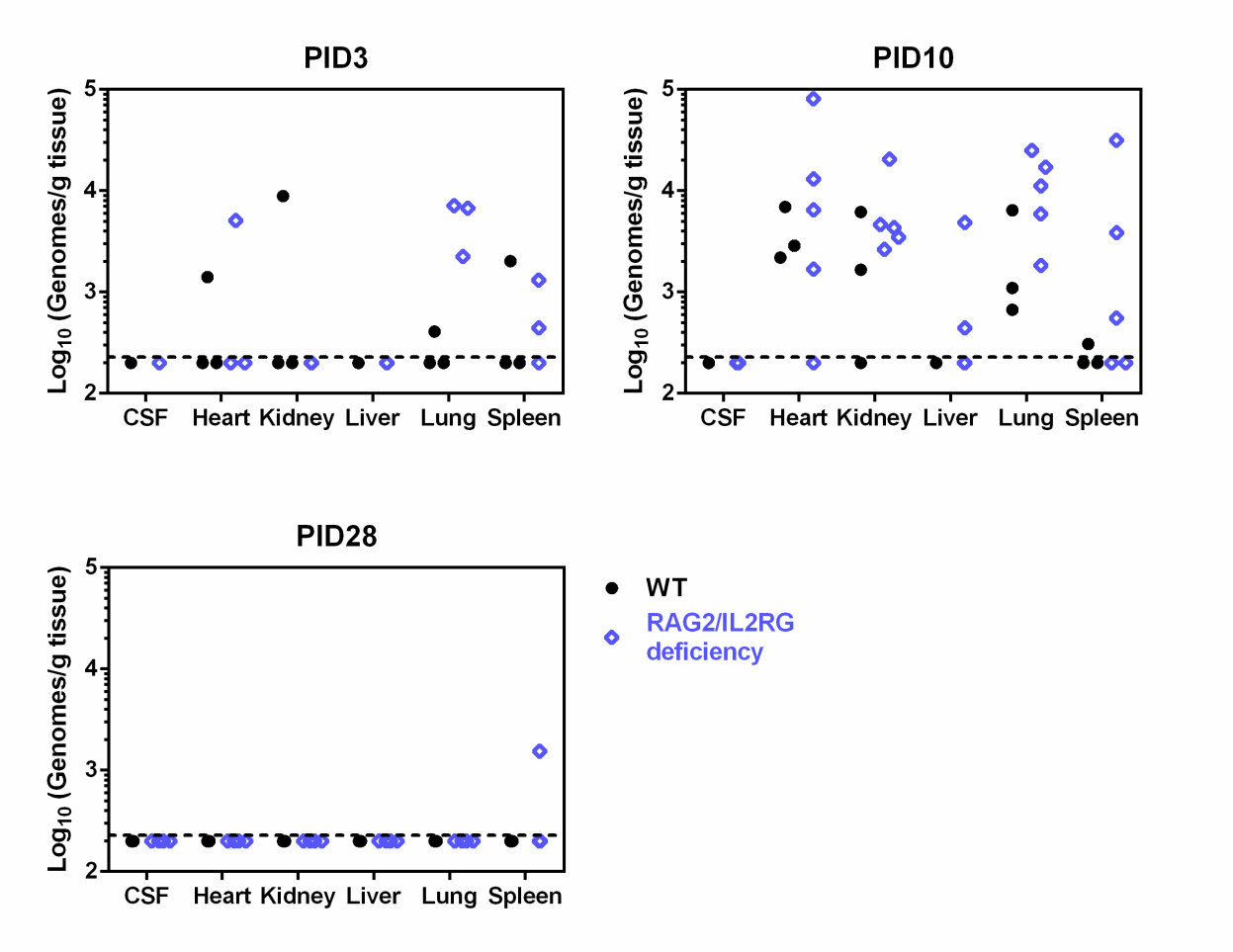


**Supplementary Figure 7. HuNoV genomes in extraintestinal tissues in Gn pigs.** HuNoV genomes in CSF (cerebrospinal fluid), heart, kidney, liver, lung, and spleen in WT and RAG2/IL2RG deficient pigs euthanized on PID3, PID10, and PID28 were measured by qRT-PCR. WT groups, PID3 *n*=3, PID10 *n*=3, PID *n*=5; RAG2/IL2RG deficiency groups, PID3 *n*=3, PID10 *n*=5, PID *n*=4. Dashed line indicates limit of detection. Data are presented as individual animal data points

**Supplementary Table 1. Genotypes and phenotypes of RAG2/IL2RG deficient pigs.**

| Pig ID | Gender | *RAG2* | *IL2RG* | Thoracic thymus[a] | Cervical thymus[a] | MLN[b] | IPP[c] | HBGA type[d] | General health | Age on euthanasia |
|---|---|---|---|---|---|---|---|---|---|---|
| Gp5-2-15* | M | Homozygous[#] | Hemizygous[#] | + | - | ++ | + | H | Normal | 9 days (PID3) |
| Gp5-3-15* | M | Homozygous | Hemizygous[#] | - | - | ++ | + | H | Normal | 9 days (PID3) |
| Gp5-4-15* | F | Homozygous | Biallelic | - | +, ND[e] | - | - | A | Normal | 9 days (PID3) |
| Gp5-5-15* | F | Mosaic | Homozygous | - | - | - | - | H | Normal | 16 days (PID10) |
| Gp5-7-15* | M | Biallelic | Mosaic[#] | ++ | - | ++ | + | H | Normal | 16 days (PID10) |
| Gp5-8-15* | F | Homozygous | Homozygous | - | - | - | - | A | Normal | 9 days (mock) |
| Gp7-1-15* | M | Homozygous | Hemizygous | +, ND | ++, ND | - | - | A | Normal | 34 days (PID28) |
| Gp7-2-15* | M | Biallelic | Mosaic | ++, ND | ++, ND | - | - | H | Normal | 34 days (PID28) |
| Gp7-3-15* | F | Biallelic[#] | Biallelic | +, ND | +, ND | - | - | A | Normal | 34 days (PID28) |
| Gp7-4-15* | F | Homozygous | Biallelic[#] | ++ | ++ | + | + | H | Normal | 34 days (PID28) |
| Gp7-5-15* | F | Biallelic[#] | Biallelic[#] | ++ | + | + | + | A | Normal | 17 days (PID10) |
| Gp7-6-15* | F | Homozygous | Homozygous[#] | ++ | + | + | + | H | Normal | 17 days (PID10) |
| Gp7-7-15* | M | Biallelic[#] | Hemizygous | - | - | - | - | H | Normal | 17 days (PID10) |
| Gp5-1-15 | F | Biallelic | Homozygous | - | +, ND | - | - | | Normal | 9 days (PID3) |
| GP5-6-15 | M | Biallelic | Hemizygous | - | - | - | - | | Failure to thrive | 3 days |
| Gp8-1-15 | F | Biallelic | Biallelic | - | +, ND | - | - | | Normal | 34 days (PID28) |
| Gp8-2-15 | F | Homozygous | Biallelic[#] | ++ | + | ++ | - | | Normal | 34 days (PID28) |

* Pigs used in this HuNoV infection study. [#] Pre-mature stop codon was not generated on at least one allele based on genotyping.

[a] -, not observed; +, smaller than wild type pigs (≤ 15 mm); ++, similar to wild type pigs (15 mm to 25 mm).

[b] MLN, mesenteric lymph nodes; -, not observed; +, less than wild type pigs; ++, similar to wild type pigs.

[c] IPP, ileal Peyer's patches; -, not observed; +, poorly developed and unstructured small IPP.

[d] Pigs used in this study were blood-typed as $A^+$ or $H^+$ by PCR and/or immunofluorescence assay.

[e] ND, lymphocytes were not detected in thymus as indicated by H&E staining, only epithelial components were observed.

# Chapter 4

## High protective efficacy of probiotics and rice bran against human norovirus infection and diarrhea in gnotobiotic pigs

Shaohua Lei[1], Ashwin Ramesh[1], Erica Twitchell[1], Ke Wen[1], Tammy Bui[1], Mariah Weiss[1], Xingdong Yang[1], Jacob Kocher[1], Guohua Li[1], Ernawati Giri-Rachman[1,2], Nguyen Van Trang[3], Xi Jiang[4], Elizabeth P. Ryan[5], Lijuan Yuan[1,*]

[1]Department of Biomedical Sciences and Pathobiology, Virginia-Maryland College of Veterinary Medicine, Virginia Tech, Blacksburg, VA, USA.

[2]School of Life Science and Technology, Institut Teknologi, Bandung, West Java, Indonesia.

[3]National Institute of Hygiene and Epidemiology, Hanoi, Vietnam.

[4]Division of Infectious Diseases, Cincinnati Children's Hospital Medical Center, Cincinnati, OH, USA.

[5]Department of Environmental and Radiological Health Sciences, College of Veterinary Medicine and Biomedical Sciences, Colorado State University, Fort Collins, CO, USA.

*Correspondence: Lijuan Yuan. E-mail: lyuan@vt.edu

Running title: Probiotics and rice bran against HuNoV

---

Published in *Frontiers in Microbiology*. 2016 Nov 2; 7:1699. Used with permission.

## Abstract

Probiotics have been recognized as vaccine adjuvants and therapeutic agents to treat acute gastroenteritis in children. We previously showed that rice bran reduced human rotavirus diarrhea in gnotobiotic pigs. Human noroviruses (HuNoVs) are the major pathogens causing nonbacterial acute gastroenteritis worldwide. In this study, *Lactobacillus rhamnosus* GG (LGG) and *Escherichia coli* Nissle 1917 (EcN) were first screened for their ability to bind HuNoV P particles and virions derived from clinical samples containing HuNoV genotype GII.3 and GII.4, then the effects of LGG+EcN and rice bran on HuNoV infection and diarrhea were investigated using the gnotobiotic pig model. While LGG+EcN colonization inhibited HuNoV shedding, probiotic cocktail regimens in which rice bran feeding started 7 days prior to or 1 day after viral inoculation in the LGG+EcN colonized gnotobiotic pigs exhibited high protection against HuNoV diarrhea and shedding, characterized by significantly reduced incidence (89% versus 20%) and shorter mean duration of diarrhea (2.2 versus 0.2 days), as well as shorter mean duration of virus shedding (3.2 versus 1.0 days). In both probiotic cocktail groups, the diarrhea reduction rates were 78% compared with the control group, and diarrhea severity was reduced as demonstrated by the significantly lower cumulative fecal scores. The high protective efficacy of the probiotic cocktail regimens was attributed to stimulation of IFN-$\gamma^+$ T cell responses, increased production of intestinal IgA and IgG, and maintenance of healthy intestinal morphology (manifested as longer villi compared with the control group). Therefore, probiotic cocktail regimens containing LGG+EcN and rice bran may represent highly efficacious strategies to prevent and treat HuNoV gastroenteritis, and potentially other human enteric pathogens.

**Keywords:** probiotics, rice bran, human norovirus, diarrhea, gnotobiotic pigs

## Introduction

Human noroviruses (HuNoVs), non-enveloped viruses with a positive-strand RNA genome, are the major pathogens causing nonbacterial acute gastroenteritis worldwide[1]. In the United States, HuNoVs have replaced human rotaviruses (HRVs) as the single most common cause of viral gastroenteritis in children and adults[2, 3]. After approximately 1.2 days of incubation[4], HuNoV gastroenteritis generally lasts for 2-3 days and consists of nausea, vomiting, and diarrhea[5]. More severe and prolonged illness can occur in specific risk groups, including infants, the elderly, and immunocompromised patients[6-8]. Given the tremendous disease burden and economic loss associated with HuNoVs infection[9, 10], vaccines and therapeutics are in great demand to prevent and treat these infections. However, due to the lack of a robust culturing system and a suitable small-animal model, HuNoVs vaccine development and antiviral research have long been hampered. Promising vaccines have focused on recombinant capsid proteins, including virus-like particles (VLPs) and P particles[11]. Appropriate animal models are essential tools to facilitate investigation of vaccine candidates and therapeutic strategies. Neonatal gnotobiotic (Gn) pigs recapitulate the pathologic hallmarks of enteric viral infection and associated immune responses in the gastrointestinal tract of young children[12]. Currently, as the only animal model that supports the oral route of HuNoV infection, develops diarrhea, and sheds virus in feces, Gn pigs are used to evaluate viral pathogenesis and vaccine efficacy with high translational validity to humans[13-15].

Probiotic bacteria are increasingly recognized as vaccine adjuvants and therapeutic agents to treat acute gastroenteritis in children[16, 17]. The potential mechanisms include competing with pathogens for nutrients and colonization sites, producing antimicrobial

metabolites, enhancing protective immune responses, and reducing intestinal permeability[18]. Notably, Gram-positive probiotics *Lactobacillus* spp. have been extensively evaluated for their beneficial effects against viral infection and diseases. These include reducing HRV and vesicular stomatitis virus infection in cell cultures[19, 20] and promoting HRV-specific immune responses, which contribute to shortened HRV-induced diarrhea in animal models[21-23] and human clinical trials[24-26]. Gram-negative *Escherichia coli* Nissle 1917 (EcN) is also a well-characterized probiotic used to treat diarrhea in infants and young children[27, 28], as well as in neonatal large animals[29, 30]. The beneficial health effects are mediated via improving intestinal barrier function[31] or moderating inflammatory responses[32], which could protect Gn piglets from lethal infection of *Salmonella* Typhimurium[32]. In addition, EcN was recently shown to have HRV-binding and immunomodulatory properties, resulting in significantly reduced HRV infection and diarrhea in Gn pigs[33]. Probiotics can act as adsorbents for HuNoV P particles, and the presence of *L. casei* BL23 and EcN might inhibit P particle attachment to epithelial cells[34]. *Enterobacter cloacae* (EC) is a commensal bacterium that can bind to HuNoV by surface histo-blood group antigen (HBGA) and inhibit HuNoV infectivity in Gn pigs[35, 36]. Taken together, diarrhea-reducing probiotics may inhibit HuNoV infectivity *in vivo*, most likely by the binding between bacteria and virions.

Rice bran (RB), an underutilized by-product of rice milling, contains a variety of prebiotic and bioactive components that modulate gut microbiota and potentially prevent chronic diseases, including diabetes, cancer, metabolic syndrome, and cardiovascular disease[37]. In mouse studies, dietary RB feeding increased production of fecal and serum IgA[38], and RB glycoproteins ameliorated cyclophosphamide-induced immunosuppression by restoring splenic lymphocytes[39], indicating that RB promoted the development of mucosal and systemic adaptive immunity.

Chemically engineered RB glucans possessed anti-cytomegalovirus activity by blocking viral entry of target cells[40]. Recently, therapeutic effects of RB in inhibiting enteric infections and reducing diarrhea have been gaining attention. In a clinical trial, Biobran (modified arabinoxylan rice bran) improved irritable bowel syndrome symptoms, presumably resulting from its anti-inflammatory and/or immunomodulatory effects[41]. In our previous Gn pig studies, dietary RB feeding significantly enhanced HRV vaccine immunogenicity and reduced HRV-induced diarrhea[42]. RB could also protect against HRV diarrhea in the presence of probiotics by preventing intestinal epithelial damage and promoting innate immune responses[43]. Therefore, its beneficial effects on gastrointestinal health support RB as a promising agent against HuNoV infection.

In this study, aiming to develop an effective and ready-to-use anti-HuNoV therapeutic strategy, we first screened a group of probiotics to identify the virus-binding bacteria using HuNoV P particles and native virions. Subsequently, probiotics and RB were evaluated individually or combined as cocktail regimens for their effects on HuNoV infection and diseases in the well-established Gn pig model[13]. Finally, the mechanisms of antiviral and diarrhea-reducing activities from those treatments were explored.

## Materials and methods

**Viruses and bacteria.** A human stool sample containing the HuNoV GII.4/2006b variant 092895 (GenBank KC990829) was collected in 2008 at the Cincinnati Children's Hospital Medical Center from a child with norovirus gastroenteritis. The sample pool was processed as an oral inoculum for HuNoV infection studies in Gn pigs[13]. A human stool sample containing the HuNoV GII.3/20110200 (GenBank KX355506) was collected in 2011 at the Thai Binh Pediatric Hospital

(Thai Binh province, Vietnam) from a female child with norovirus gastroenteritis. *L. reuteri* (ATCC 23272), *L. acidophilus* (strain NCFM), *L. rhamnosus* GG (ATCC 53103), and *L. bulgaricus (*ATCC 11842) were cultured in lactobacilli MRS broth (Neogen Corporation) anaerobically using BBL™ GasPak™ jar system with Anaerobe Sachets (BD) under static condition at 37°C. *Escherichia coli* Nissle 1917 (a gift from Dr. Jun Sun, Rush University, Chicago, IL) and *Enterobacter cloacae* (ATCC 13047) were cultured in Luria Bertani medium at 37°C and in nutrient broth at 30°C, respectively, with shaking at 250 rpm.

**Purification of HuNoVs and VP1 sequencing.** The pooled human stools containing HuNoVs were diluted 10-fold with diluent #5 (Minimal Essential Medium with 1% penicillin-streptomycin and 1% HEPES) and mixed thoroughly with an equal volume of Vertrel XF (Miller-Stephenson), and viruses were purified by CsCl gradient centrifugation as described previously[44]. VP1 of GII.4/2006b variant 092895 was cloned and sequenced previously[14]. GII.3/20110200 viral RNA was extracted from the purified virus by TRIzol LS and reverse transcribed by SuperScript III Reverse Transcriptase (Thermo Fisher Scientific) using universal GII.3 reverse primer 5'-TAG CCC CTG CAT TAA CTA-3' and following the manufacturer's instructions. The GII.3 VP1 was cloned by a nested PCR with primer set 1 (forward: 5'-TGA GCA CGT GGG AGG GCG-3' and reverse: 5'-TAG CCC CTG CAT TAA CTA-3') and primer set 2 (forward: 5'-CAC CAT GAA GAT GGC GTC GAA T-3' and reverse: 5'-TTA TTG AAT CCT TCT ACG CC-3') into pENTR directional TOPO vector (Thermo Fisher Scientific). The GII.3 VP1 fragment in the recombinant plasmids were sequenced by Virginia Bioinformatics Institute at Virginia Tech, and the predominant sequence was used for the preparation of P particles.

**P particles and transmission electron microscopy.** The region coding for the P domain was amplified from the recombinant plasmids containing VP1 capsid gene of HuNoV GII.3 or GII.4 as described above. The P domains were cloned into prokaryotic expression vector pET21a (EMD Millipore) as previously described[34]. A 6×His-Tag was incorporated to the N-terminus of P proteins by forward primers, and a cysteine-rich peptide CDCRGDCFC was incorporated to the C-terminus of P proteins by reverse primers to enhance the P particle stability[45]. P proteins were expressed in *E. coli* strain BL21 (New England Biolabs) and purified via HisPur Ni-NTA Spin Columns (Thermo Fisher Scientific) following the manufacturer's instructions. Protein production was monitored by SDS-PAGE and InVision His-tag In-gel Stain (Thermo Fisher Scientific). Protein concentrations were measured spectroscopically by Quick Start™ Bradford protein assay (Bio-Rad). Electron microscopy formvar carbon square grids (Electron Microscopy Sciences) were pretreated with 1% aqueous Alcian blue for 5 min. After washes, P particles of genotype GII.3 or GII.4 were diluted in PBS to 5 μg/ml and absorbed to the grids for 1 min. The grids were stained with 3% phosphotungstic acid pH 7.0 for 1 min and viewed with a JEOL JEM 1400 transmission electron microscope.

**Binding of P particles and virions to bacteria.** After the initial inoculation into fresh culture medium, bacteria were grown overnight and sub-cultured at 1:50 for 2-3 hours until $OD_{600}$ reached 0.4-1.0, which was the log phase of growth. Bacteria were washed three times and resuspended with PBS to an $OD_{600}$ of 1.0. Then 10 μg P particles or $10^6$ viral genome copies of purified HuNoVs were incubated with 1 ml bacteria for 1h at 37°C, then the mixture was centrifuged and washed three times with PBS. To measure the remaining P particles attached to

bacteria, the bacterial pellets were resuspended with 100 µl Laemmli sample buffer (Bio-Rad) and boiled for 10 min, and 20 µl of sample was loaded to 10% SDS-PAGE gel and analyzed by Western Blot using HRP conjugated anti-His-Tag antibody (MA1-21315-HRP, Thermo Fisher Scientific). To measure the remaining virions, the total RNA of the bacterial pellets was extracted by 750 µl TRIzol LS, and HuNoV genomes were detected by a one-step TaqMan qRT-PCR with primers targeting all GII viruses[46, 47]. For controls, *Enterobacter cloacae* were heat-killed at 65°C for 40 min, then blocked with 5 µl of A antigen antibody (sc-69951, Santa Cruz) and H antigen antibody (sc-52369, Santa Cruz) at 37°C for 20 min before adding P particles or virions.

**Gnotobiotic pigs and treatment groups.** Near-term Yorkshire cross-breed pigs were derived via hysterectomy by veterinarians and maintained in sterile isolator units as described previously[48]. Neonatal Gn pigs (male and female) were randomly assigned to the five treatment groups upon derivation: Cocktail-7d (*n* = 5), Cocktail+1d (*n* = 5), RB-7d (*n* = 4), LGG+EcN (*n* = 5), Control (*n* = 9). To initiate the colonization of LGG and EcN, $10^4$ CFU of each were mixed in five ml of Minimal Essential Medium and administered orally to pigs on post-partum day (PPD) 3, 5, and 7. The low dosage was chosen on purpose to be well below the therapeutic practice ($10^9$ to $10^{12}$ CFU). LGG and EcN fecal shedding were determined by rectal swab sampling of pig feces and enumeration of colonies grown on media agar plates as described previously[43]. For RB feeding of pigs, heat-stabilized and gamma-irradiated RB (Calrose variety) was added to pigs' milk diet by replacing 10% daily calorie intake [43]. Daily feeding started 7 days prior to or 1 day after HuNoV inoculation until euthanasia. All pigs were orally inoculated on PPD33 with $6.43 \times 10^5$ viral genome copies of HuNoV GII.4/2006b variant 092895. To reduce gastric acidity, four ml 200 mM sodium

bicarbonate were given to pigs 15 min prior to inoculation. Fecal consistency and virus shedding were assessed daily until euthanasia on PPD40 where blood, tissues, and intestinal contents were collected. Fecal consistency scores were obtained based on previous scaling system[13], and fecal virus shedding was measured by a one-step TaqMan qRT-PCR as described previously[47].

**Flow cytometry analysis.** Mononuclear cells (MNCs) were isolated from the duodenum, ileum, spleen, and blood as described previously[49]. $2 \times 10^6$ of MNCs were restimulated *in vitro* with P particle (12μg/ml for the spleen and 6μg/ml for others), positive control PHA (10μg/ml), or mock control in E-RPMI media for 17h at 37°C. Brefeldin A (B6542, Sigma-Aldrich, 5μg/ml) and anti-CD49d monoclonal antibody (561892, BD Biosciences, 1μl/ml) were added at 12h post incubation to block the secretion of cytokines and enhance the stimulation, respectively. IFN-$\gamma^+$ $CD4^+$ and $CD8^+$ T cells were quantified by flow cytometry as described previously[49]. Isotype matched irrelevant antibodies were included as negative gate controls. Mock-stimulated samples indicate the total IFN-$\gamma^+$ T cells, while the increased cell populations of P particle-stimulated over mock-stimulated samples indicate HuNoV-specific IFN-$\gamma^+$ T cells.

**ELISA for total immunoglobulin and IFN-γ.** The total immunoglobulin (Ig) titers in intestinal contents were determined by ELISA as described previously[47]. Intestinal IFN-γ titers were measured by Swine IFN-γ VetSet™ ELISA development Kit (Kingfisher Biotech) following the manufacturer's instructions.

**Jejunum histopathology.** Jejunum tissue was collected after pig euthanasia, fixed in 4% paraformaldehyde for 12-16h, paraffin embedded, sectioned into 5µm slices and placed on positively charged slides, for routine H&E staining. A pathologist who was blinded to the sample identifications evaluated the villus length using an ocular micrometer under a light microscope.

**Ethical statement.** Stool collection protocols were approved by the Institutional Review Boards of the Cincinnati Children's Hospital Medical Center (IRB#: 2008-1131) and the National Institute of Hygiene and Epidemiology - Vietnam (IRB#: 15-IRB), written consent was provided by parents or guardians of the children. Animal experimental protocols were approved by the Institutional Animal Care and Use Committee at Virginia Tech (IACUC protocol: 13-187-CVM and 14-108-CVM). All sample collection and experimental procedures were conducted in accordance with the approved guidelines.

**Statistics.** Statistics were performed using GraphPad Prism 6.0 (GraphPad Software) with analyses indicated in table notes and figure legends. Statistical significance was determined at the level of $P < 0.05$.

## Results

### Probiotic bacteria bind to HuNoVs

Although HuNoV genotype GII.4 accounts for the most global acute gastroenteritis outbreaks[1], GII.3 is emerging and becoming predominant in some underdeveloped areas[50-52]. To explore the interactions between HuNoVs and probiotics, we first cloned the capsid VP1 genes

of GII.3 and GII.4 from clinical stool samples, then the P-domains were cloned and proteins were expressed with N-terminal 6×His-Tag to facilitate their detection and purification (**Figure 1A**). The formation of P particles was not compromised as indicated by a negative staining electron microscopy (**Figure 1B**).

P particles were first used as a model to determine HuNoVs interactions with probiotics, including a Gram-negative strain EcN and four Gram-positive lactobacilli strains, i.e., *L. reuteri* (LR), *L. acidophilus* (LA), *L. rhamnosus* GG (LGG), and *L. bulgaricus (*LB). Since EC can bind to HuNoVs specifically by surface HBGA[35], native EC was used as a positive control and HBGA A&H antibodies-blocked EC was a negative control in the binding assays. After incubation of P particles and bacteria, the P particles remaining on the bacterial surface were quantified by Western Blot using anti-His-Tag antibody. The results showed that all the tested bacteria were able to bind to both GII.3 and GII.4 P particles, and lactobacilli strains had significantly higher binding capacity than those of EcN and EC (**Figure 1C**). Additionally, LA was stronger than LR in binding to GII.3 P particle, while EcN was weaker than EC. The four lactobacilli strains did not differ from each other in binding to GII.4 P particle, and neither did EcN and EC (**Figure 1C**). Similarly, the binding assays were performed using HuNoV virions purified from stool samples. Unlike the P particles, GII.3 virions had comparable binding to all tested bacteria except for the higher binding to LGG, whereas GII.4 virions shared the binding pattern with P particle except for the lower binding to LGG and higher binding to LB (**Figure 1D**). These data suggest that probiotic bacteria can bind to HuNoVs.

**LGG+EcN inhibited HuNoV shedding and RB reduced diarrhea in Gn pigs**

To develop a ready-to-use anti-HuNoV therapeutic strategy, LGG and EcN were chosen for the evaluation of their potential antiviral effects in the Gn pig model of HuNoV infection and diarrhea, since they could bind HuNoVs *in vitro* and are commercially available as diarrhea-reducing probiotics. Previous study showed that RB protected against HRV-induced diarrhea in the presence of LGG and EcN [43], we tested RB feeding and/or LGG+EcN co-colonization in five treatment groups in this study: Cocktail-7d (*n* = 5), pigs were pre-colonized with LGG and EcN, RB feeding started 7 days prior to HuNoV inoculation; Cocktail+1d (*n* = 5), pigs were pre-colonized with LGG and EcN, RB feeding started 1 day after virus inoculation; RB-7d (*n* = 4), RB feeding started 7 days prior to inoculation; LGG+EcN (*n* = 5), pigs were colonized with LGG and EcN only; Control (*n* = 9), non-RB fed and non-LGG+EcN colonized. All pigs were inoculated with a HuNoV GII.4/2006b variant 092895 on PPD33/PID0 and euthanized on PID7 (**Figure 2A**).

Fecal consistency and virus shedding were assessed daily after the HuNoV inoculation (Supplementary Figure 1). The results summarized in **Table 1** showed that compared to the control group, LGG+EcN group had similar rates of HuNoV diarrhea (89% versus 60%), yet undetectable HuNoV shedding. RB-7d group had a slightly shorter mean duration of diarrhea (2.2 versus 1.3 days) and significantly delayed shedding onset (2.8 versus 6.3 days). More importantly, cocktail-7d and cocktail+1d groups had a significantly lower incidence (20%), delayed onset (3.9 versus 7.0 and 7.2 days, respectively), shorter mean duration of diarrhea (2.2 versus 0.2 days), and shorter mean duration of virus shedding (3.2 versus 1.0 days). In both cocktail groups, the diarrhea reduction rates were 78% [1 - (% of treated pigs with diarrhea / % of control pigs with diarrhea)], and the reduced severity of diarrhea was also shown by the significantly lower

cumulative fecal scores (**Figure 2B**). Interestingly, only the LGG+EcN group had significantly reduced cumulative and peak virus shedding compared to the control group. RB feeding with or without LGG+EcN colonization did not significantly alter virus shedding pattern, except that shedding in the cocktail+1d group trended lower when compared to the other RB fed groups and the controls (**Figures 2C and 2D**).

**RB promoted the colonization of EcN but not LGG in Gn pigs**

The colonization of LGG and EcN in Gn pigs was confirmed by their fecal shedding on PPD26 (**Figures. 3A and 3B**). After the beginning of RB feeding on PPD26 in the cocktail-7d group and on PPD34 in the cocktail-1d group, LGG fecal shedding appeared to decrease in both groups, however, statistical significance was not observed for these differences (**Figure 3A**). On the other hand, RB feeding significantly increased EcN fecal shedding in the cocktail-7d group and slightly in the cocktail-1d group (**Figure 3B**). Taken together, these results indicate the differential effects of RB on the co-colonization of probiotic bacteria.

**LGG+EcN and RB stimulated the production of IFN-$\gamma^+$ T cells**

To elucidate the mechanisms of the inhibitory effects of LGG+EcN and RB on HuNoV infection and diarrhea, their immunomodulatory roles were first assessed regarding effector T cells. After euthanasia on PID7, MNCs were isolated from both intestinal and systemic lymphoid tissues, and the frequencies of IFN-$\gamma^+$ $CD4^+$ and $CD8^+$ T cells were determined by flow cytometry (**Figure 4A**). MNCs were stimulated with P particle to detect HuNoV-specific IFN-$\gamma^+$ T cells, which was the increased frequency compared to the mock stimulated sample. For pigs in the control,

LGG+EcN, and RB-7d groups, no significant increase of IFN-γ$^+$ T cells was observed in P particle stimulated MNCs (**Figure 4A** and data not shown), suggesting low or short-term HuNoV-specific IFN-γ$^+$ T cell responses. However, compared with control pigs, both LGG+EcN colonization and RB feeding significantly increased frequencies of non-specific total IFN-γ$^+$ T cells (**Figure 4B**). In addition, compared with the LGG+EcN group, the RB-7 group had significantly higher frequencies of IFN-γ$^+$ CD8$^+$ T cell population in ileum and IFN-γ$^+$ CD4$^+$ T cell population in all assayed lymphoid tissues (duodenum, ileum, spleen, and blood) (**Figure 4B**), indicating that RB has strong stimulatory effects on total IFN-γ$^+$ T cell responses, which may contribute to the reduction of HuNoV diarrhea in Gn pigs.

**Probiotics plus RB cocktail regimens enhanced gut immunity**

The immunomodulatory roles of LGG+EcN and RB on gut immunity were evaluated by testing total intestinal IgA, IgG, and IFN-γ levels, since PID 7 is too early to detect virus-specific IgA and IgG antibody responses. Compared with the control group, the cocktail-7d, cocktail+1d, and LGG+EcN groups had significantly higher IgA titers in both small and large intestinal contents (SIC and LIC), but the increase was not observed in the RB-7d group (**Figure 5A**), indicating that LGG+EcN but not RB enhanced the production of IgA. The cocktail-7d and cocktail+1d groups had significantly higher IgG titers in both SIC and LIC, whereas no differences were observed in either the LGG+EcN or RB groups (**Figure 5B**). Consistent with the strong stimulation of RB on total IFN-γ$^+$ T cells (**Figure 4B**), significantly higher IFN-γ concentrations were detected in LIC from the cocktail-7d, cocktail+1d, and RB-7d groups (**Figure 5C**). In all, cocktail regimens remarkably

enhanced gut immunity in Gn pigs by secretion of intestinal immunoglobulins and interferon, which might provide protection against HuNoV infection.

**Probiotics plus RB cocktail regimens increased jejunal villi length**

Villus blunting is a major manifestation of impaired intestinal health, such as in Crohn's disease[53], celiac disease[54], and virus-induced gastroenteritis[55]. To examine the beneficial effects of LGG+EcN and RB on the health of small intestine in Gn pigs, sections of jejunum were stained with H&E and evaluated for all the treatment groups after euthanasia. Compared with control, both LGG+EcN colonization and RB feeding were associated with significantly longer jejunal villus length. Their stimulatory roles might be additive as the two cocktail groups displayed greater villus length than either single treatment (**Figure 6**). These data indicate that the cocktail regimens promote the growth and health of intestinal epithelium, which might contribute to the protection of HuNoV-induced disease.

## Discussion

Robust cell culture and animal models have long been lacking for HuNoV propagation, as a result, clinical stool samples from patients are the only resource for HuNoV infection studies. P particles are promising surrogates as they exhibit surface conformation and receptor-binding profiles similar to the corresponding VLPs[56], and they have been validated as an *in vitro* model to evaluate viral binding with probiotics[34]. In this study, we first prepared HuNoV GII.3 and GII.4 P proteins, which displayed double bands as expected (**Figures. 1A and 1C**)[34]. The P particle structures were observed under electron microscopy. The binding assays with both P particles

and native virions showed that their binding capacity with Gram-negative EcN was lower than that with Gram-positive lactobacilli, EcN was still included in this study due to its commercial availability, diarrhea-reducing properties on enteric pathogens such as HRV[33], and potential inhibition of HuNoV attachment to epithelial cells[34]. It is likely that differential cell surface composition of Gram-negative and Gram-positive bacteria determines the observed differences, although surface components that are responsible for viral binding remain to be identified.

Bacterial microbiota was shown to facilitate persistent and acute murine norovirus (MuNoV) infection in mice[57, 58], but the effects of different bacteria on MuNoV infectivity might vary as lactobacilli could inhibit MuNoV infection *in vitro* using RAW264.7 cell culture model and vitamin A inhibited MuNoV replication in mice by upregulating lactobacilli in gut microbiota[59]. In this study, after HuNoV inoculation in Gn pigs colonized with LGG+EcN, virus fecal shedding was below the limit of detection, indicating significant inhibition on HuNoV infection by their colonization. Similar to the reduced virus shedding but unaffected incidence of diarrhea observed in EC colonized Gn pigs in the previous study[36], LGG+EcN colonization did not alter the occurrence of diarrhea, suggesting that HuNoV gastroenteritis could be induced by extremely low viral loads and that anti-HuNoV agents inhibiting viral replication may have insufficient efficacy in reducing the disease. Given that bacterial anti-HuNoV capacity might depend on the extent of viral retention ability, it is likely that LGG plays a more important role on the inhibition of HuNoV infectivity than EcN, since LGG has a greater HuNoV-binding ability, but further investigations will be required to clarify the effects of LGG or EcN mono-colonization on HuNoV infection. Nevertheless, cocktail regimens containing LGG and EcN offer great promise to simultaneously protect against HuNoV and HRV infection[33].

Although RB was shown to promote the colonization of lactobacilli in mice[38], LGG fecal shedding was lower after RB feeding in cocktail groups in this study. When colonized together with EcN in Gn pigs, LGG fecal shedding and concentration in intestinal tissues trended toward lower than those of single colonization[33], suggesting that the presence of EcN might inhibit the growth of LGG. Thus, it is likely that higher growth of EcN led to lower growth of LGG after RB feeding, and underlying mechanisms utilized by EcN need to be identified, such as competing for the nutrients and colonization sites, improving intestinal barrier, and modulating immune responses[31, 32]. In all, higher protective efficacy against HuNoV shedding and diarrhea might be achieved only if rice bran and LGG are given.

Effector T cells are a crucial immune component to eliminate viral infected cells, and their responses in the small intestine are associated with protective immunity against HRV[49]. However, HuNoV infection or P particle vaccination did not significantly stimulate virus-specific IFN-$\gamma^+$ $CD4^+$ or $CD8^+$ T cell responses[14], and neither did LGG+EcN colonization nor RB feeding in this study. Still, significantly increased frequencies of non-specific IFN-$\gamma^+$ T cells were observed especially after RB feeding, which might be correlated with the diarrhea-reducing property of RB, but a significant reduction in virus shedding was not observed along with the enhanced T cell responses in the RB-7d group, which was similar to our previous study on HRV[42]. For the cocktail regimens, the intestinal IgA was increased by LGG+EcN alone, while the increased intestinal IgG might have been induced by the synergism between LGG+EcN and RB. The additive effects of the probiotics and RB appeared to be associated with longer jejunal villus length.

In this study, the cocktail-7d group displayed a 78% reduction of diarrhea, as well as significantly shortened duration of diarrhea and virus shedding after HuNoV challenge, indicating

the regimen is an effective preventive measure. In addition, similar effects in reducing diarrhea and virus shedding were observed in the cocktail+1d group, in which RB feeding started 1 day after HuNoV challenge, thus this regimen could be considered as a therapeutic strategy to treat HuNoV gastroenteritis. The first HuNoV vaccine candidate evaluated in clinical trials was an adjuvanted monovalent GI.1 VLP, which provided 47% and 26% protection against Norwalk virus gastroenteritis and infection compared with the placebo group, respectively[60]. A bivalent VLP-based vaccine containing both GI.1 and GII.4 components is under development as well, and human clinical trials showed a 52% reduction in vomiting and/or diarrhea compared with the control after challenge[61]. Our previous evaluations of adjuvanted GII.4 VLP and P particle vaccines in Gn pigs demonstrated reductions of diarrhea by 60% and 47%, respectively[14]. Therefore, the probiotics plus RB cocktail regimens may provide an alternative strategy with better anti-HuNoV effects than the current vaccine candidates.

In summary, lactobacilli and EcN could bind to HuNoV P particles and virions derived from GII.3 and GII.4 clinical samples. Colonization with LGG+EcN completely inhibited HuNoV fecal shedding in Gn pigs. The two cocktail regimens had RB feeding started either 7 days prior to or 1 day after viral inoculation in the LGG+EcN colonized Gn pigs, and both regimens exhibited dramatic anti-HuNoV effects, including reduced incidence and shorter duration of diarrhea, as well as shorter duration of virus fecal shedding. The anti-HuNoV effects of the cocktail regimens were associated with the stimulated IFN-$\gamma^+$ T cell responses, increased production of intestinal IgA and IgG, and longer villus length. Considering the natural source and commercial availability of probiotics and RB, the cocktail regimens may represent a novel, safe and ready-to-use strategy against diarrhea and infection caused by HuNoV infection and other enteric pathogens.

## Abbreviations:

EC, *Enterobacter cloacae*; EcN, *Escherichia coli* Nissle 1917; Gn, gnotobiotic; HBGA, histo-blood group antigen; HRV, human rotavirus; HuNoV, human norovirus; LA, *Lactobacillus acidophilus*; LB, *Lactobacillus bulgaricus*; LGG, *Lactobacillus rhamnosus* GG; LR, *Lactobacillus reuteri*; MuNoV, murine norovirus; PID, post-infection day; PPD, post-partum day; RB, rice bran; VLP, virus-like particle.


## Acknowledgements

This work was supported by the Bill and Melinda Gates Foundation grant OPP1043255 to EPR with G-6289 subcontract to LY and a NIH grant R01AI089634 to LY. We gratefully thank X.J. Meng, X. Wang, and N. Nanthakumar for critical discussion on the project. We thank K. Pelzer and S. Clark-Deener for veterinary services, TRACSS staff members for animal care, M. Makris for operating flow cytometry, and K. Lowe for assistance in electron microscopy.


## Author contributions

SL and LY conceived the project and designed the experiments. SL performed most experiments and analyzed data. AR, ET, KW, TB, MW, XY, JK, GL, and EG-R assisted with experiments. NVT, XJ, and EPR contributed key materials and/or reagents. SL and LY wrote the manuscript. All authors reviewed the manuscript before submission.

## Conflict of Interest Statement

The authors declare that the research was conducted in the absence of any commercial or financial relationships that could be construed as a potential conflict of interest.

## References


1. Pringle, K. et al. Noroviruses: epidemiology, immunity and prospects for prevention. *Future Microbiol* **10**, 53-67 (2015).
2. Payne, D.C. et al. Norovirus and medically attended gastroenteritis in U.S. children. *N Engl J Med* **368**, 1121-30 (2013).
3. Bresee, J.S. et al. The etiology of severe acute gastroenteritis among adults visiting emergency departments in the United States. *J Infect Dis* **205**, 1374-81 (2012).
4. Lee, R.M. et al. Incubation periods of viral gastroenteritis: a systematic review. *BMC Infect Dis* **13**, 446 (2013).
5. Lopman, B.A., Reacher, M.H., Vipond, I.B., Sarangi, J. & Brown, D.W. Clinical manifestation of norovirus gastroenteritis in health care settings. *Clin Infect Dis* **39**, 318-24 (2004).
6. Murata, T. et al. Prolonged norovirus shedding in infants <or=6 months of age with gastroenteritis. *Pediatr Infect Dis J* **26**, 46-9 (2007).
7. Hall, A.J., Curns, A.T., McDonald, L.C., Parashar, U.D. & Lopman, B.A. The roles of Clostridium difficile and norovirus among gastroenteritis-associated deaths in the United States, 1999-2007. *Clin Infect Dis* **55**, 216-23 (2012).
8. Green, K.Y. Norovirus infection in immunocompromised hosts. *Clin Microbiol Infect* **20**, 717-23 (2014).
9. Patel, M.M. et al. Systematic literature review of role of noroviruses in sporadic gastroenteritis. *Emerg Infect Dis* **14**, 1224-31 (2008).
10. Ahmed, S.M. et al. Global prevalence of norovirus in cases of gastroenteritis: a systematic review and meta-analysis. *Lancet Infect Dis* **14**, 725-30 (2014).
11. Kocher, J. & Yuan, L. Norovirus vaccines and potential antinorovirus drugs: recent advances and future perspectives. *Future Virol* **10**, 899-913 (2015).
12. Yang, X. & Yuan, L. Neonatal Gnotobiotic Pig Models for Studying Viral Pathogenesis, Immune Responses, and for Vaccine Evaluation. *British Journal of Virology* **1**, 87-91 (2014).
13. Bui, T. et al. Median infectious dose of human norovirus GII.4 in gnotobiotic pigs is decreased by simvastatin treatment and increased by age. *J Gen Virol* **94**, 2005-16 (2013).
14. Kocher, J. et al. Intranasal P particle vaccine provided partial cross-variant protection against human GII.4 norovirus diarrhea in gnotobiotic pigs. *J Virol* **88**, 9728-43 (2014).
15. Cheetham, S. et al. Pathogenesis of a genogroup II human norovirus in gnotobiotic pigs. *J Virol* **80**, 10372-81 (2006).
16. Licciardi, P.V. & Tang, M.L. Vaccine adjuvant properties of probiotic bacteria. *Discov Med* **12**, 525-33 (2011).
17. Schnadower, D., Finkelstein, Y. & Freedman, S.B. Ondansetron and probiotics in the management of pediatric acute gastroenteritis in developed countries. *Curr Opin Gastroenterol* **31**, 1-6 (2015).
18. Ng, S.C., Hart, A.L., Kamm, M.A., Stagg, A.J. & Knight, S.C. Mechanisms of action of probiotics: recent advances. *Inflamm Bowel Dis* **15**, 300-10 (2009).
19. Maragkoudakis, P.A., Chingwaru, W., Gradisnik, L., Tsakalidou, E. & Cencic, A. Lactic acid bacteria efficiently protect human and animal intestinal epithelial and immune cells from enteric virus infection. *Int J Food Microbiol* **141 Suppl 1**, S91-7 (2010).
20. Botic, T., Klingberg, T.D., Weingartl, H. & Cencic, A. A novel eukaryotic cell culture model to study antiviral activity of potential probiotic bacteria. *Int J Food Microbiol* **115**, 227-34 (2007).
21. Zhang, W. et al. Probiotic Lactobacillus acidophilus enhances the immunogenicity of an oral rotavirus vaccine in gnotobiotic pigs. *Vaccine* **26**, 3655-61 (2008).

22. Wen, K. et al. Lactobacillus rhamnosus GG Dosage Affects the Adjuvanticity and Protection Against Rotavirus Diarrhea in Gnotobiotic Pigs. *J Pediatr Gastroenterol Nutr* **60**, 834-43 (2015).
23. Wen, K. et al. Probiotic Lactobacillus rhamnosus GG enhanced Th1 cellular immunity but did not affect antibody responses in a human gut microbiota transplanted neonatal gnotobiotic pig model. *PLoS One* **9**, e94504 (2014).
24. Guandalini, S. et al. Lactobacillus GG administered in oral rehydration solution to children with acute diarrhea: a multicenter European trial. *J Pediatr Gastroenterol Nutr* **30**, 54-60 (2000).
25. Sindhu, K.N. et al. Immune response and intestinal permeability in children with acute gastroenteritis treated with Lactobacillus rhamnosus GG: a randomized, double-blind, placebo-controlled trial. *Clin Infect Dis* **58**, 1107-15 (2014).
26. Szajewska, H., Urbanska, M., Chmielewska, A., Weizman, Z. & Shamir, R. Meta-analysis: Lactobacillus reuteri strain DSM 17938 (and the original strain ATCC 55730) for treating acute gastroenteritis in children. *Benef Microbes* **5**, 285-93 (2014).
27. Henker, J. et al. The probiotic Escherichia coli strain Nissle 1917 (EcN) stops acute diarrhoea in infants and toddlers. *Eur J Pediatr* **166**, 311-8 (2007).
28. Henker, J. et al. Probiotic Escherichia coli Nissle 1917 versus placebo for treating diarrhea of greater than 4 days duration in infants and toddlers. *Pediatr Infect Dis J* **27**, 494-9 (2008).
29. von Buenau, R. et al. Escherichia coli strain Nissle 1917: significant reduction of neonatal calf diarrhea. *J Dairy Sci* **88**, 317-23 (2005).
30. Schroeder, B. et al. Preventive effects of the probiotic Escherichia coli strain Nissle 1917 on acute secretory diarrhea in a pig model of intestinal infection. *Dig Dis Sci* **51**, 724-31 (2006).
31. Hering, N.A. et al. TcpC protein from E. coli Nissle improves epithelial barrier function involving PKCzeta and ERK1/2 signaling in HT-29/B6 cells. *Mucosal Immunol* **7**, 369-78 (2014).
32. Splichalova, A. et al. Interference of Bifidobacterium choerinum or Escherichia coli Nissle 1917 with Salmonella Typhimurium in gnotobiotic piglets correlates with cytokine patterns in blood and intestine. *Clin Exp Immunol* **163**, 242-9 (2011).
33. Kandasamy, S. et al. Differential Effects of Escherichia coli Nissle and Lactobacillus rhamnosus Strain GG on Human Rotavirus Binding, Infection, and B Cell Immunity. *J Immunol* **196**, 1780-9 (2016).
34. Rubio-del-Campo, A. et al. Noroviral p-particles as an in vitro model to assess the interactions of noroviruses with probiotics. *PLoS One* **9**, e89586 (2014).
35. Miura, T. et al. Histo-blood group antigen-like substances of human enteric bacteria as specific adsorbents for human noroviruses. *J Virol* **87**, 9441-51 (2013).
36. Lei, S. et al. Enterobacter cloacae inhibits human norovirus infectivity in gnotobiotic pigs. *Sci Rep* **6**, 25017 (2016).
37. Sheflin, A.M. et al. Pilot dietary intervention with heat-stabilized rice bran modulates stool microbiota and metabolites in healthy adults. *Nutrients* **7**, 1282-300 (2015).
38. Henderson, A.J., Kumar, A., Barnett, B., Dow, S.W. & Ryan, E.P. Consumption of rice bran increases mucosal immunoglobulin A concentrations and numbers of intestinal Lactobacillus spp. *J Med Food* **15**, 469-75 (2012).
39. Park, H.Y. et al. Immunomodulatory Effects of Nontoxic Glycoprotein Fraction Isolated from Rice Bran. *Planta Med* **82**, 606-11 (2016).
40. Ray, B. et al. Chemically Engineered Sulfated Glucans from Rice Bran Exert Strong Antiviral Activity at the Stage of Viral Entry. *Journal of Natural Products* **76**, 2180-2188 (2013).
41. Kamiya, T. et al. Therapeutic effects of biobran, modified arabinoxylan rice bran, in improving symptoms of diarrhea predominant or mixed type irritable bowel syndrome: a pilot, randomized controlled study. *Evid Based Complement Alternat Med* **2014**, 828137 (2014).

42. Yang, X. et al. Dietary rice bran protects against rotavirus diarrhea and promotes Th1-type immune responses to human rotavirus vaccine in gnotobiotic pigs. *Clin Vaccine Immunol* **21**, 1396-403 (2014).
43. Yang, X. et al. High protective efficacy of rice bran against human rotavirus diarrhea via enhancing probiotic growth, gut barrier function, and innate immunity. *Sci Rep* **5**, 15004 (2015).
44. Guix, S. et al. Norwalk virus RNA is infectious in mammalian cells. *J Virol* **81**, 12238-48 (2007).
45. Tan, M. & Jiang, X. The p domain of norovirus capsid protein forms a subviral particle that binds to histo-blood group antigen receptors. *J Virol* **79**, 14017-30 (2005).
46. Kageyama, T. et al. Broadly reactive and highly sensitive assay for Norwalk-like viruses based on real-time quantitative reverse transcription-PCR. *J Clin Microbiol* **41**, 1548-57 (2003).
47. Lei, S. et al. Increased and prolonged human norovirus infection in RAG2/IL2RG deficient gnotobiotic pigs with severe combined immunodeficiency. *Sci Rep* **6**, 25222 (2016).
48. Meyer, R.C., Bohl, E.H. & Kohler, E.M. Procurement and Maintenance of Germ-Free Seine for Microbiological Investigations. *Appl Microbiol* **12**, 295-300 (1964).
49. Yuan, L. et al. Virus-specific intestinal IFN-gamma producing T cell responses induced by human rotavirus infection and vaccines are correlated with protection against rotavirus diarrhea in gnotobiotic pigs. *Vaccine* **26**, 3322-31 (2008).
50. Van Trang, N. et al. Association between norovirus and rotavirus infection and histo-blood group antigen types in Vietnamese children. *J Clin Microbiol* **52**, 1366-74 (2014).
51. Liu, P. et al. Genetic susceptibility to norovirus GII.3 and GII.4 infections in Chinese pediatric diarrheal disease. *Pediatr Infect Dis J* **33**, e305-9 (2014).
52. Ayouni, S. et al. Relationship between GII.3 norovirus infections and blood group antigens in young children in Tunisia. *Clin Microbiol Infect* **21**, 874 e1-8 (2015).
53. Cadwell, K. et al. Virus-plus-susceptibility gene interaction determines Crohn's disease gene Atg16L1 phenotypes in intestine. *Cell* **141**, 1135-45 (2010).
54. Chand, N. & Mihas, A.A. Celiac disease: current concepts in diagnosis and treatment. *J Clin Gastroenterol* **40**, 3-14 (2006).
55. Hodges, K. & Gill, R. Infectious diarrhea: Cellular and molecular mechanisms. *Gut Microbes* **1**, 4-21 (2010).
56. Tan, M. et al. Noroviral P particle: structure, function and applications in virus-host interaction. *Virology* **382**, 115-23 (2008).
57. Baldridge, M.T. et al. Commensal microbes and interferon-lambda determine persistence of enteric murine norovirus infection. *Science* **347**, 266-9 (2015).
58. Jones, M.K. et al. Enteric bacteria promote human and mouse norovirus infection of B cells. *Science* **346**, 755-9 (2014).
59. Lee, H. & Ko, G. Antiviral effect of vitamin A on norovirus infection via modulation of the gut microbiome. *Sci Rep* **6**, 25835 (2016).
60. Atmar, R.L. et al. Norovirus vaccine against experimental human Norwalk Virus illness. *N Engl J Med* **365**, 2178-87 (2011).
61. Debbink, K., Lindesmith, L.C. & Baric, R.S. The state of norovirus vaccines. *Clin Infect Dis* **58**, 1746-52 (2014).

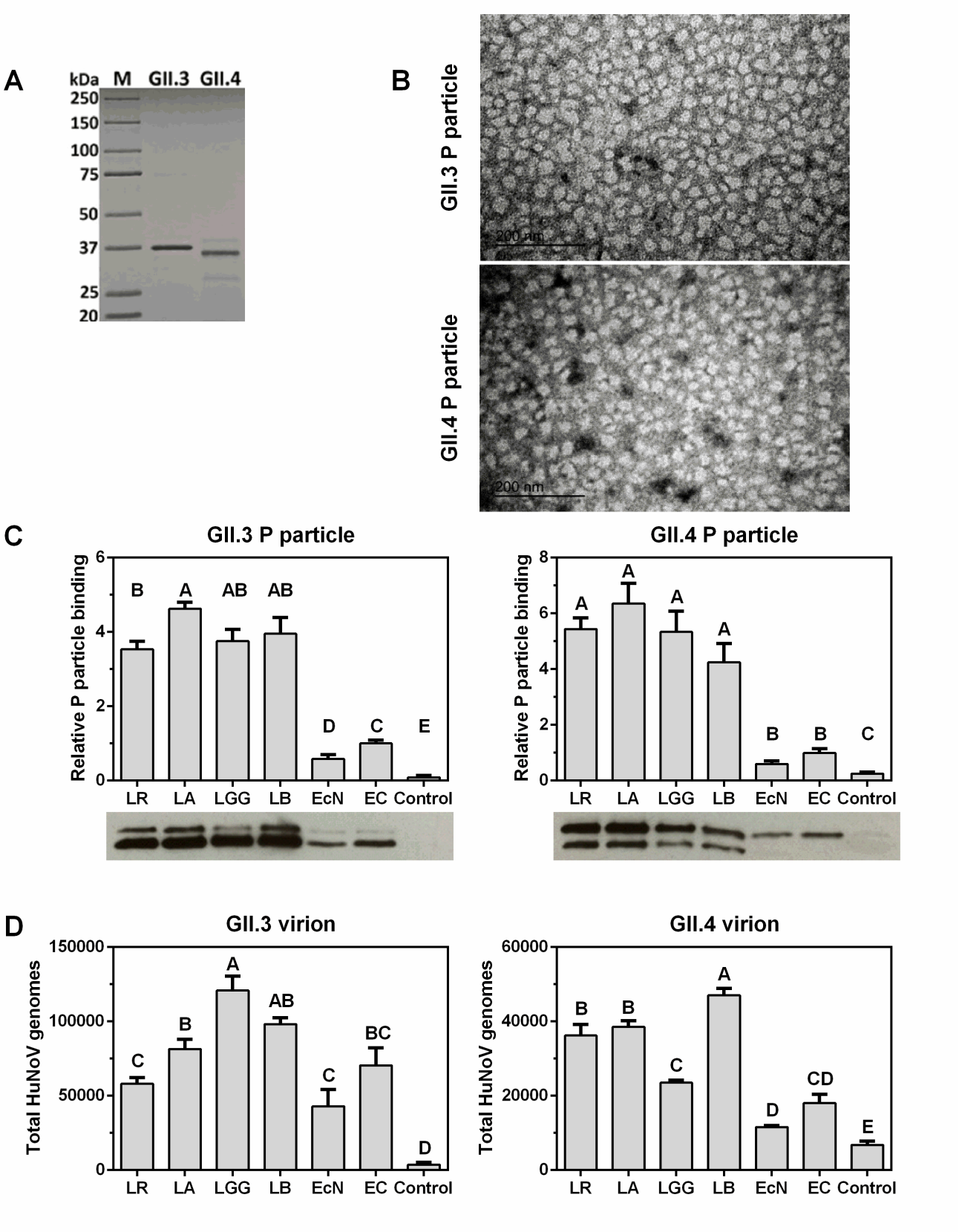
A
kDa
M
GII.3
GII.4
250
150
100
75
50
37
25
20
B
GII.3 P particle
GII.4 P particle
200 nm
200 nm
C
GII.3 P particle
GII.4 P particle
Relative P particle binding
B
A
AB
AB
D
C
E
A
A
A
A
B
B
C
LR
LA
LGG
LB
EcN
EC
Control
D
GII.3 virion
GII.4 virion
Total HuNoV genomes
C
B
A
AB
C
BC
D
B
B
C
A
D
CD
E

**Figure 1. Probiotic bacteria bind to HuNoV P particles and virions.** (**A**) SDS-PAGE analysis of the 6×His tagged P proteins expressed and purified from the prokaryotic system. Lane 1, protein standard marker. Lane 2 and 3, GII.3 and GII.4 P proteins. (**B**) Transmission electron micrographs of P particles. Scale bar, 200 nm. (**C**) Probiotic bacteria bind to P particles. Bottom panels, representative Western Blot using anti-His-Tag antibody showing the P particles bound to bacteria. Top panels, four independent experiments were analyzed by Image J. The relative bindings are referred to that of EC. (**D**) Probiotic bacteria bind to virions. The virions bound to bacteria were quantified by qRT-PCR for viral genomes. The experiments were repeated three times independently. Controls were heat-killed and A&H antigen antibodies-blocked EC. Data are presented as means ± SEM. Statistics was determined by one-way analysis of variance (ANOVA). Different letters indicate significant differences among groups ($P$<0.05), while shared letters indicate no significant difference.

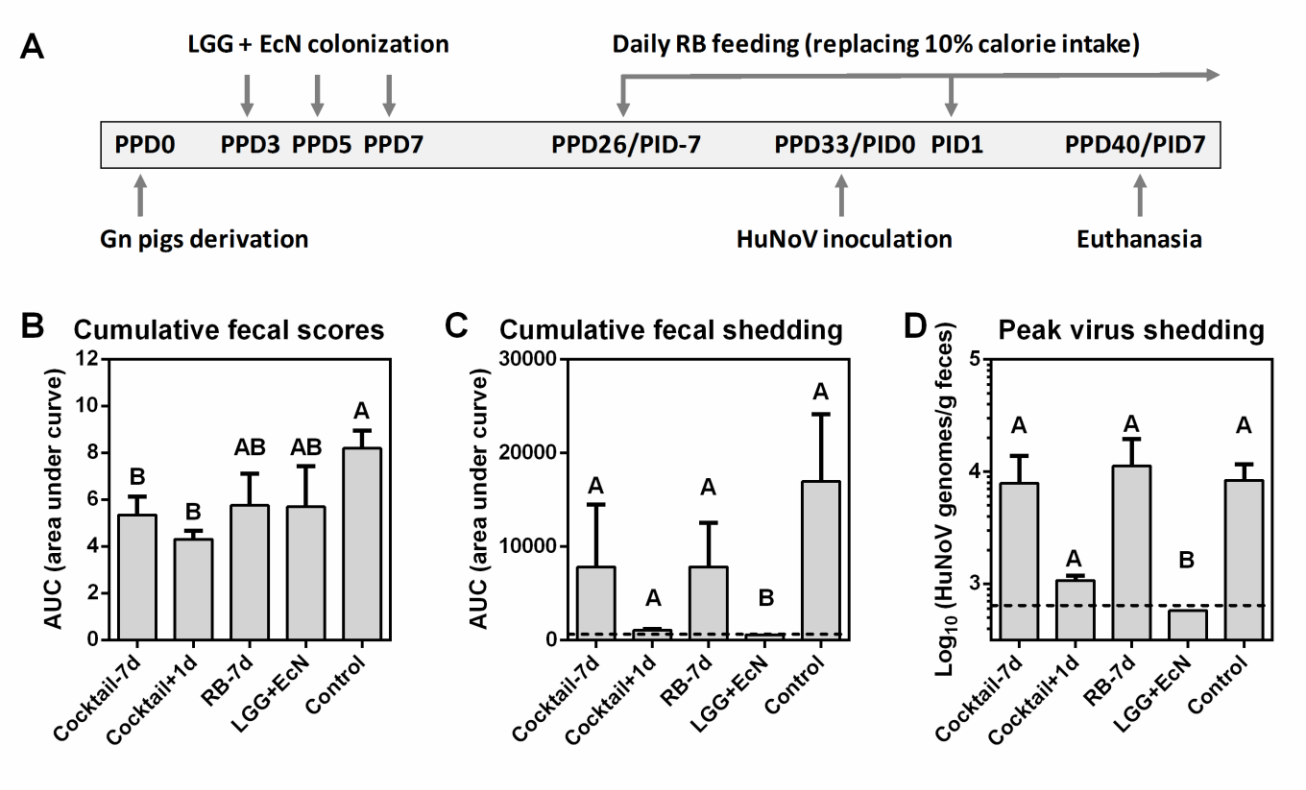


**Figure 2. Design and summary of Gn pig study.** (**A**) Experimental timeline. PPD, post-partum day. PID, post inoculation day. Cumulative fecal scores (**B**) and shedding (**C**) are shown as area under curve from daily measurements of individual pigs (Supplementary Figure 1). (**D**) Mean peak virus shedding titers from PID1 to PID7 in individual pigs. Sample sizes are shown in Table 1. Data are presented as means ± SEM. Dashed lines indicate limit of detection. Statistics were determined by Kruskal-Wallis test. Different letters indicate significant differences among groups ($P$<0.05), while shared letters indicate no significant difference.

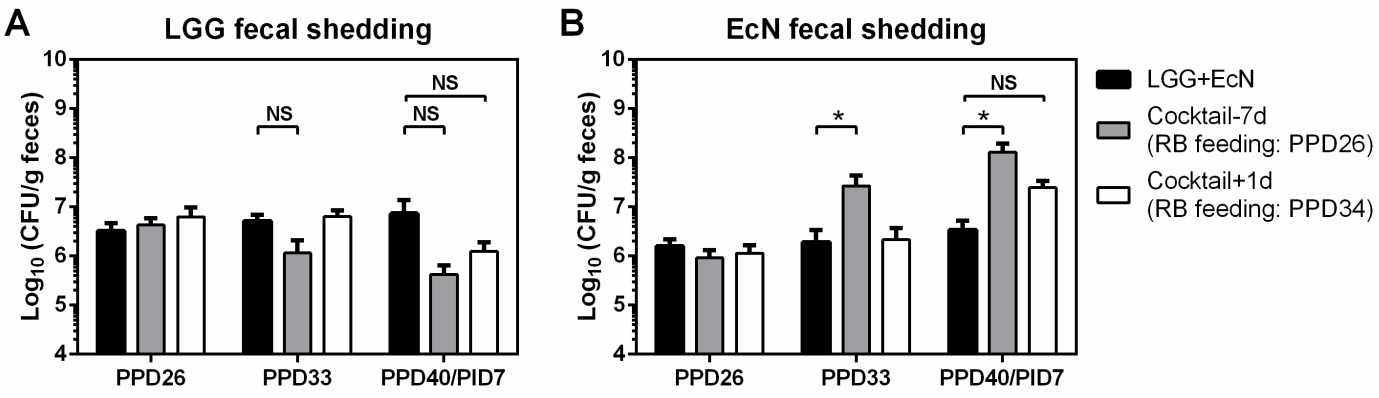


**Figure 3. LGG and EcN fecal shedding.** Pig feces were collected by rectal swab and suspended in PBS. The concentrations of LGG and EcN were determined in serial dilution of fecal samples and enumeration of colony forming unit (CFU) grown on MRS or LB media agar plates. Sample sizes are shown in Table 1. Data are presented as means ± SEM. Statistics were determined by Kruskal-Wallis test. NS, not significant, *$P$<0.05.

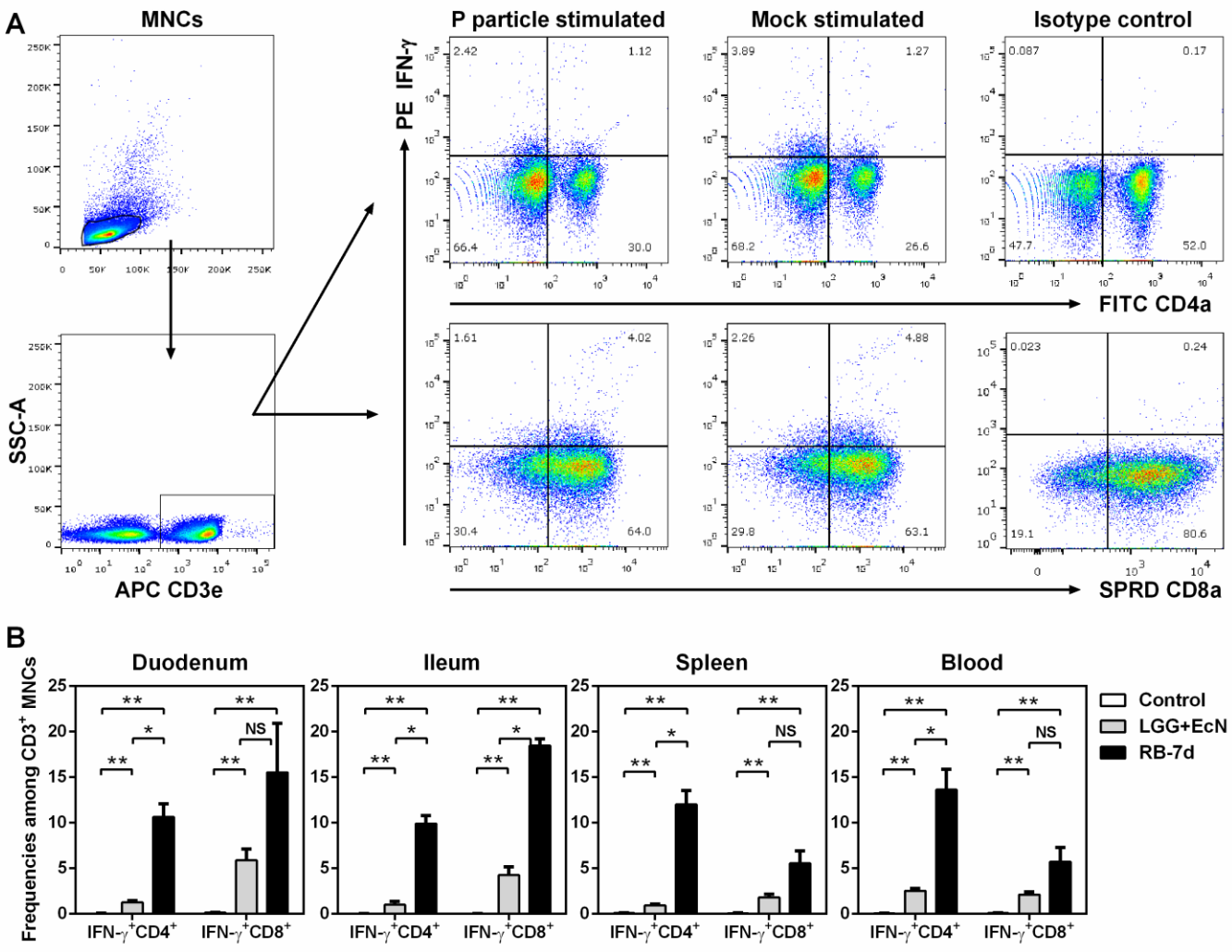


**Figure 4. LGG+EcN and RB stimulated IFN-γ⁺ T cell responses.** (**A**) Gating strategies for IFN-γ⁺ $CD3^+CD4^+$ (Th) cells and $CD3^+CD8^+$ (CTL) cells. Representative dot plots showing frequencies of HuNoV-specific (P particle stimulated) and non-specific (mock stimulated) IFN-γ⁺ T cells in ileum isolated from LGG+EcN colonized Gn pigs. SSC-A, side scatter area; APC, allophycocyanin; FITC, fluorescein isothiocyanate; SPRD, spectral red; PE, phycoerythrin. (**B**) Non-specific IFN-γ⁺ T cells in intestinal (duodenum, ileum) and systemic (spleen, blood) tissues on PID7. Sample sizes are shown in Table 1. Data are presented as means ± SEM. Statistics were determined by Kruskal-Wallis test. NS, not significant, **P*<0.05, ***P*<0.01.

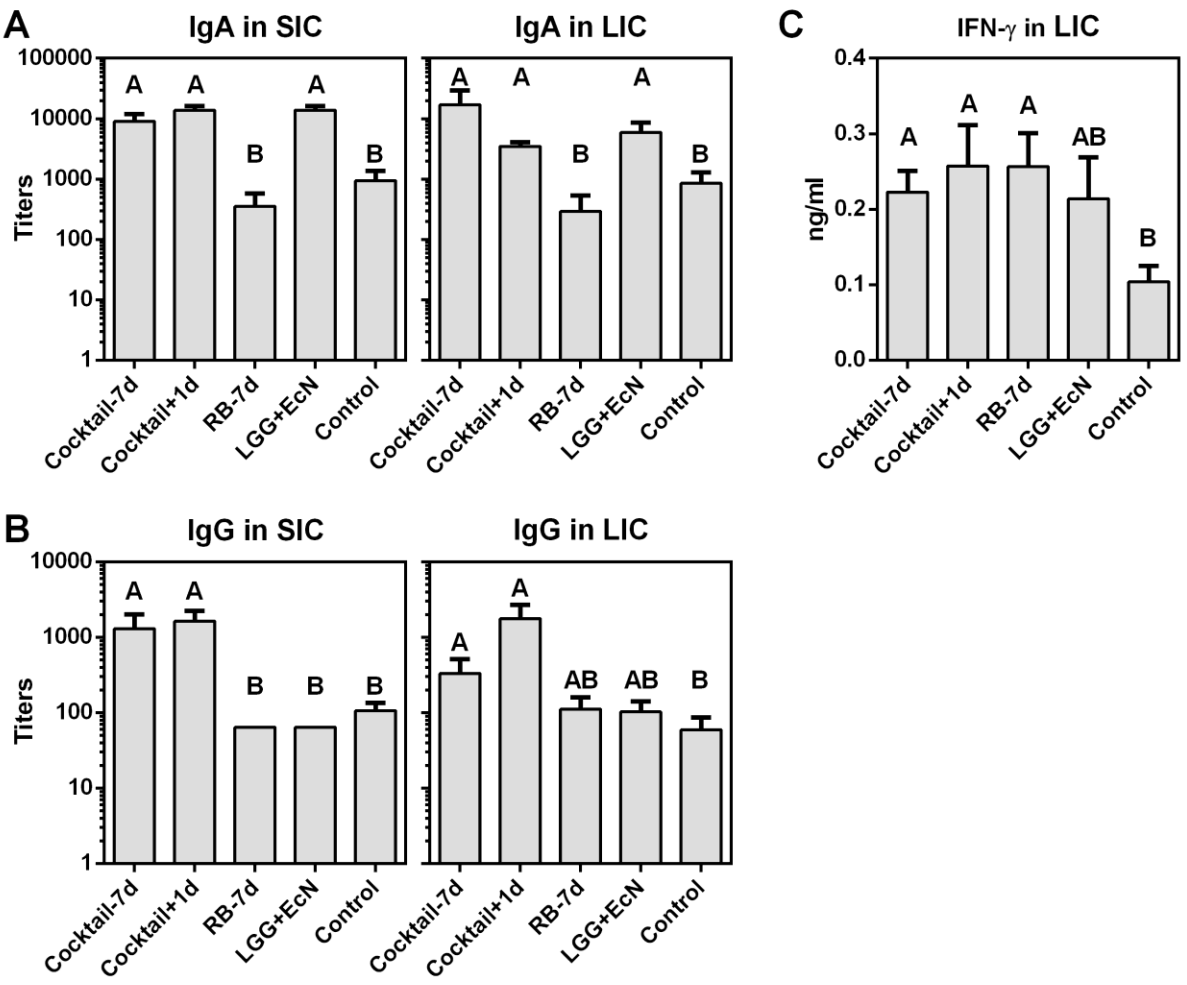


**Figure 5. IgA, IgG, and IFN-γ levels in intestinal contents after HuNoV infection.** Total IgA (**A**) and IgG (**B)** titers in small and large intestinal contents (SIC and LIC) were measured by ELISA. (**C**) IFN-**γ** concentration in LIC was measured by ELISA. Sample sizes are shown in Table 1. Data are presented as means ± SEM. Statistics were determined by Kruskal-Wallis test. Different letters indicate significant differences among groups ($P$<0.05), while shared letters indicate no significant difference.

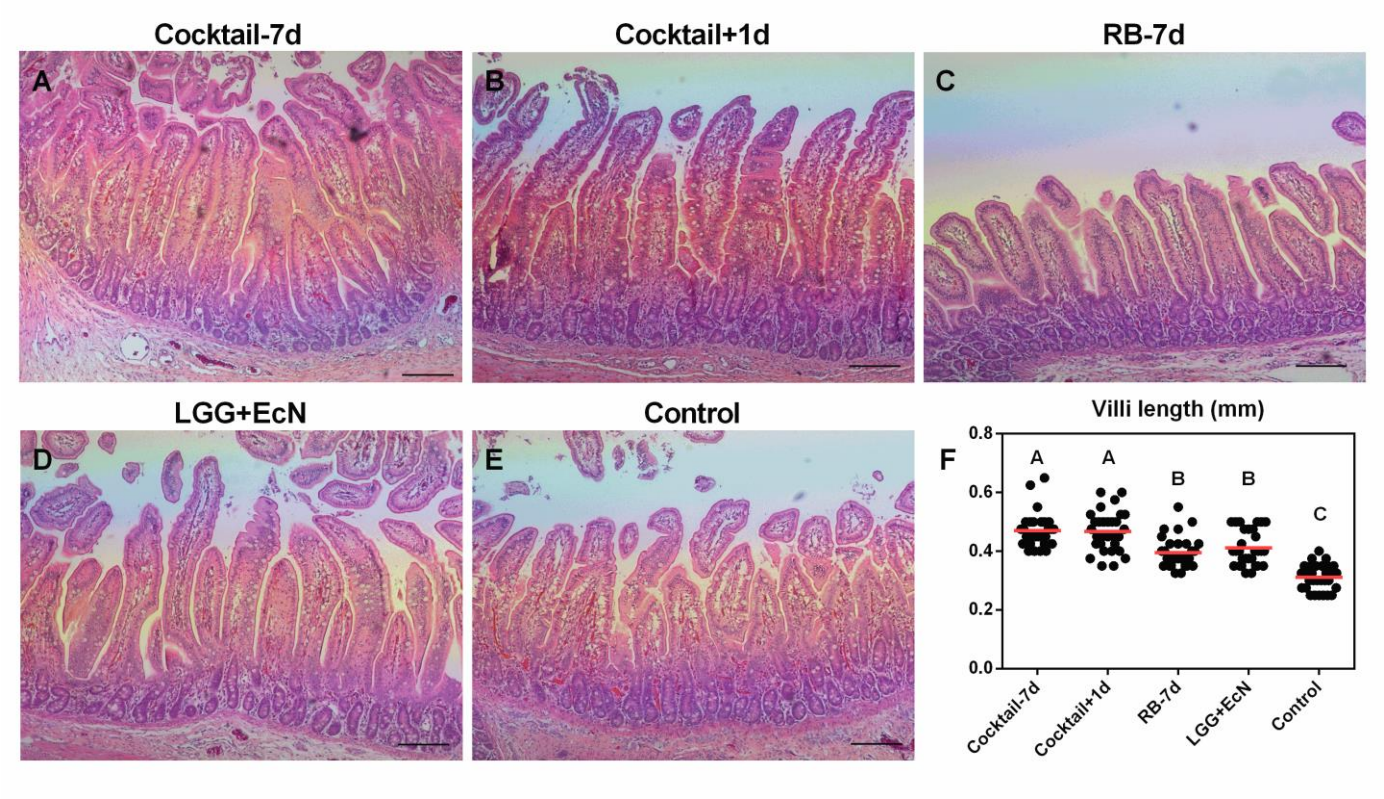


**Figure 6. LGG+EcN and RB are associated with longer villi.** (**A**-**E**) Representative images of H&E stained jejunum showing the villi length in the five groups. Scale bar, 0.25 mm. (**F**) 30 random villi including all pigs in each group were measured to quantify the villi length. Data are presented as means with individual points. Statistics were determined by Kruskal-Wallis test. Different letters indicate significant differences among groups ($P$<0.05), while shared letters indicate no significant difference.

**Table 1. Incidence of diarrhea and fecal virus shedding in Gn pigs after HuNoV GII.4 challenge[a]**

| Group | *n* | Diarrhea[b] | | | Virus shedding[b] | | |
|---|---|---|---|---|---|---|---|
| | | Pigs with diarrhea (%)* | Mean days to onset (SEM)** | Mean duration days (SEM)** | Pigs shedding virus (%)* | Mean days to onset (SEM)** | Mean duration days (SEM)** |
| Cocktail-7d | 5 | 1 (20%)$^{A}$ | 7.0 (1.0)$^{A}$ | 0.2 (0.2)$^{A}$ | 4 (80%)$^{A}$ | 4.0 (1.2)$^{AB}$ | 1.0 (0.3)$^{AB}$ |
| Cocktail+1d | 5 | 1 (20%)$^{A}$ | 7.2 (0.8)$^{A}$ | 0.2 (0.2)$^{A}$ | 5 (100%)$^{A}$ | 4.8 (0.2)$^{AB}$ | 1.0 (0)$^{A}$ |
| RB-7d | 4 | 3 (75%)$^{AB}$ | 3.3 (1.6)$^{AB}$ | 1.3 (0.5)$^{AB}$ | 3 (75%)$^{A}$ | 6.3 (0.8)$^{A}$ | 1.5 (0.6)$^{AB}$ |
| LGG+EcN | 5 | 3 (60%)$^{AB}$ | 4.0 (1.6)$^{AB}$ | 1.8 (1.1)$^{AB}$ | 0$^{B}$ | 8.0 (0)$^{C}$ | 0$^{C}$ |
| Control | 9 | 8 (89%)$^{B}$ | 3.9 (0.7)$^{B}$ | 2.2 (0.4)$^{B}$ | 8 (89%)$^{A}$ | 2.8 (0.8)$^{B}$ | 3.2 (0.9)$^{B}$ |

[a]Gn pigs were inoculated with a HuNoV GII.4 2006b variant 092895 at 33 days of age. Diarrhea and virus shedding were monitored by daily rectal swab sampling and RT-qPCR after inoculation. Calculation included all pigs in each group from PID1 to PID7.

[b]If diarrhea or virus shedding was not observed, the days to onset was recorded as 8 and the duration days was recorded as 0 for statistical purposes.

*Fisher's exact test or **Kruskal-Wallis test was used for comparisons. Different letters indicate significant differences among treatment groups ($P$<0.05), while shared letters indicate no significant difference.

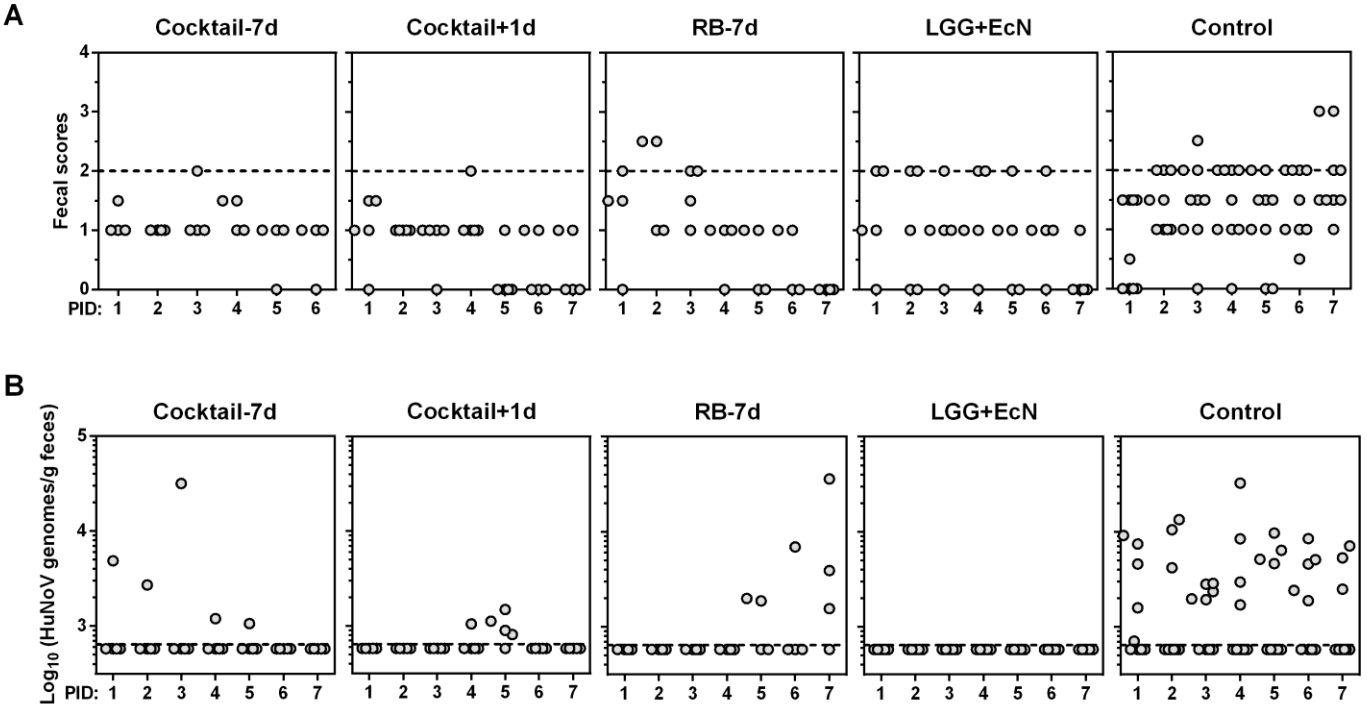


**Supplementary Figure 1. Fecal consistency scores and HuNoV shedding.** (**A**) Fecal consistency scores. Pig feces were collected by rectal swabs and scored as follows: 0, solid; 1, pasty; 2, semiliquid; and 3, liquid. Fecal scores of ≥2 as indicated by dashed lines were considered diarrheic. (**B**) Fecal HuNoV shedding. Viral titers in pig feces were measured by qRT-PCR, dashed lines indicate limit of detection. Data are presented as individual animal data points.

# Chapter 5

## General discussion and future directions

Shaohua Lei

Department of Biomedical Sciences and Pathobiology,

Virginia-Maryland College of Veterinary Medicine,

Virginia Tech, Blacksburg, VA 24061, USA.

## General discussion and future directions

Impacts of interactions between HuNoV-bacterium and HuNoV-host on the viral infectivity are the focus of this desseration study. Histo-blood group antigens (HBGAs) are complex carbohydrates present on mucosal epithelium or as free antigens in biological fluids[1], norovirus and rotavirus are found to recognize HGBAs for attachment in strain-specific patterns[2, 3]. In 2014, HBGA-bearing bacteria were screened out of a stool sample from a healthy adult, and *E. cloacae* SENG-6 was shown to have HuNoV binding capability[4]. Subsequently, B cells supplemented with free HBGA or *E. cloacae* was established as a novel HuNoV infection system[5], which redefined the range of HuNoV cell tropism and viral infection factors. Although many laboratories failed to grow HuNoV in B cells[6], the binding between bacteria and HuNoV is widely believed to mediate bacterial effects on viral infectivity. **In the first phase of this study**, we showed that the administration of *E. cloacae* in Gn pigs inhibited HuNoV infection[7], but the design of the treatment groups was questioned for the lack of non-binding bacterial strain as a control group[8]. *E. cloacae* was shown with specificity to bind HuNoV, but the screening procedure did not indicate that HuNoV bond to *E. cloacae* exclusively[4]. Consistent with the binding of all tested bacteria and all tested HuNoVs[9], we tried multiple bacterial strains, including Gram-positive and Gram-negative, but failed to obtain a single strain without HuNoV-binding property (data not shown), rising new debates on the role and importance of enteric bacteria on HuNoV infection. Nevertheless, in our ongoing project evaluating the effect of human gut microbiota on HuNoV infectivity in Gn pigs, increased virus genomes in fecal shedding and in intestinal tissues suggest the enhanced HuNoV infection in the presence of human gut microbiota, which serves as a control and validates the inhibitory role of *E. cloacae* on HuNoV infection *in vivo*. Given the lower

HuNoV replication in Gn pigs in the presence of *E. cloacae* than that of human gut microbiota, different bacterial strains may have divergent effects on HuNoV infection. There should be certain bacterial strains that enhance HuNoV infection and some others inhibit. The outcome is the average effects of human gut microbiota. Overall, further investigations are required to differentiate the effects of different bacterial strains on enteric virus infection, and the mechanisms underlying the altered viral infectivity could be elucidated by systematic analysis, including transcriptome analysis of intestinal tissues, metabolome profiling of intestinal contents and pathway analysis, and microbiome dynamics.

With the advances in genetic engineering technology, genetically modified animals have been emerging models in biomedical research, and the use of certain animal species has increasingly relied on the feasibility of utilizing genetic engineering. While genetically modified mice show genetic disorders that resemble human conditions and serve as models for a variety of diseases[10], the rising CRISPR/Cas9 system has significantly saved time and cost for the generation of genetically modified pigs as no cloning or breeding were needed[11], which further expanded the application of pig model in the exploration of virus-host interactions[12, 13]. **In the second phase of this study**, increased and prolonged HuNoV infection was observed in our RAG2/IL2RG deficient Gn pigs, but the increase was moderate with peak around $10^4$ viral genomes per gram of feces and the prolongation was limited within 27 days[7], presumably resulting from the host innate immune barrier of HuNoV infection. Similarly, RAG/IL2RG deficiency enabled subclinical HuNoV infection in Balb/c mice for less than 3 days[14], altogether indicating that the importance of host lymphocytes in HuNoV clearance is very limited. However, significantly increased and robust MNV infection was observed in mice with immunodeficiency

in STAT1[15], a key component in the interferon (IFN) signaling pathway in innate antiviral responses, and a recent study showed that systemic and intestinal persistence of MNV are controlled by IFN-αβ and IFN-λ, respectively[16]. Thus, it is likely that the innate immunity plays a pivotal role in host anti-HuNoV activity, and successful disruption of innate immunity, such as knockout of STAT1 or certain IFNs and Toll-like receptors, might remarkably promote HuNoV infection in Gn pigs. There is no doubt that HuNoV biology will be largely explored using human intestinal enteroids and probably other newly developed cell culture systems in the future, and genome-wide screening technologies such as RNA interference and CRISPR/Cas9 system would enable the discovery of key host component(s) against HuNoV infection, which paves the way for the generation of novel animal models supporting robust HuNoV infection.

Studies have suggested that probiotics reduce the severity of diarrhea through stimulating the expression of the $Cl^-/HCO_3^-$ exchanger DRA (down-regulated in adenoma) in intestinal epithelial cells to improve $Cl^-$ absorption[17, 18]. Probiotics can also increase the expression of the $Na^+/H^+$ exchanger NHE3 which contributes to the upregulation of intestinal electrolyte absorption[19]. However, LGG+EcN without rice bran did not confer significant protection **in the third phase of this study**, although HuNoV fecal shedding was below the limit of detection[20]. For future studies, other probiotic strains such as *Bifidobacterium bifidum* and *Lactobacillus acidophilus NCFM* can be considered to use alone or together with rice bran to obtain higher efficiency against HuNoV-induced diarrhea. Alternatively, genetic engineering has generated recombinant LGG and EcN with enhanced immunomodulatory activity[21, 22], and modified probiotics expressing HuNoV VLP or P particle should provide extra protection by stimulating viral specific immune response[23, 24].

It is important to note, the prominent characteristic of rice bran is that it is a natural complex with more than 450 distinct phytochemicals, which are balanced nutrients such as fibers, oils, proteins, and vitamins[25]. While component dissection and further functional investigation for each ingredient are in great demand to better understand the bioactive profile of rice bran, it merits our attention that the phytochemical components are likely working synergistically for the broad positive health benefits, including antioxidant, antimicrobial, antiviral, microbiota-regulating and/or immunomodulatory properties. The function of dietary rice bran usage to fight gastrointestinal diseases, diarrhea in particular, warrants further study and medical food application. All in all, the combination of probiotics and prebiotics represent a highly efficacious measure for the prevention and treatment of gastroenteritis induced by HuNoV, HRV, and potentially other enteric pathogens[20, 26].

Germ-free animal models provide an indispensable tool for the investigation of viral impacts on host intestinal physiology and immunity, as well as the evaluation of vaccine and therapeutics against enteric virus infection and gastroenteritis[27-29]. The Gn pig model with its distinct advantages has greatly contributed to studies of the effects and mechanisms of gut microbiota and probiotics on enteric virus infections and vaccines[30]. However, the drawbacks of applying Gn pigs in modeling human diseases are the fairly high cost and relative lack of species-specific molecular reagents compared with mouse models, which hinder in-depth mechanistic studies. Additionally, the Gn pig system has been using cross-breed piglets, leading to relatively high experimental variablity between individuals compared with mouse models, and such disadvantage could be overcome by developing inbred pig model in the future. Further optimization of the pig models, including genetic modification using CRISPR/Cas9 technology,

humanization of the immune system through stem cell transfer in immunodeficient pigs, and transplantation with human gut microbiota from donors representing different health, disease, and immune statuses will further improve the usefulness and reliability of the pig models for mimicking enteric virus infection and disease in humans. Unravelling the role of microbiome, specific probiotics, and prebiotics in the infectivity, pathogenesis, and immunity of enteric viruses will facilitate the development of strategies against those infections and diseases.

## Reference


1. Marionneau, S. et al. ABH and Lewis histo-blood group antigens, a model for the meaning of oligosaccharide diversity in the face of a changing world. *Biochimie* **83**, 565-73 (2001).
2. Bohm, R. et al. Revisiting the role of histo-blood group antigens in rotavirus host-cell invasion. *Nat Commun* **6**, 5907 (2015).
3. Huang, P. et al. Noroviruses bind to human ABO, Lewis, and secretor histo-blood group antigens: identification of 4 distinct strain-specific patterns. *J Infect Dis* **188**, 19-31 (2003).
4. Miura, T. et al. Histo-blood group antigen-like substances of human enteric bacteria as specific adsorbents for human noroviruses. *J Virol* **87**, 9441-51 (2013).
5. Jones, M.K. et al. Enteric bacteria promote human and mouse norovirus infection of B cells. *Science* **346**, 755-9 (2014).
6. Jones, M.K. et al. Human norovirus culture in B cells. *Nat Protoc* **10**, 1939-47 (2015).
7. Lei, S. et al. Enterobacter cloacae inhibits human norovirus infectivity in gnotobiotic pigs. *Sci Rep* **6**, 25017 (2016).
8. Bartnicki, E., Cunha, J.B., Kolawole, A.O. & Wobus, C.E. Recent advances in understanding noroviruses. *F1000Res* **6**, 79 (2017).
9. Almand, E.A., Moore, M.D., Outlaw, J. & Jaykus, L.A. Human norovirus binding to select bacteria representative of the human gut microbiota. *PLoS One* **12**, e0173124 (2017).
10. Chaible, L.M., Kinoshitay, D., Corat, M.A.F. & Dagli, M.L.Z. in Animal Models for the Study of Human Disease (ed. Conn, P.M.) 811-831 (Elsevier Inc, USA, 2013).
11. Ryu, J. & Lee, K. CRISPR/Cas9-Mediated Gene Targeting during Embryogenesis in Swine. *Methods Mol Biol* **1605**, 231-244 (2017).
12. Lei, S. et al. Increased and prolonged human norovirus infection in RAG2/IL2RG deficient gnotobiotic pigs with severe combined immunodeficiency. *Sci Rep* **6**, 25222 (2016).
13. Yang, H. et al. CD163 knockout pigs are fully resistant to highly pathogenic porcine reproductive and respiratory syndrome virus. *Antiviral Res* (2018).
14. Taube, S. et al. A mouse model for human norovirus. *MBio* **4**, e00450-13 (2013).
15. Karst, S.M., Wobus, C.E., Lay, M., Davidson, J. & Virgin, H.W.t. STAT1-dependent innate immunity to a Norwalk-like virus. *Science* **299**, 1575-8 (2003).
16. Nice, T.J. et al. Interferon-lambda cures persistent murine norovirus infection in the absence of adaptive immunity. *Science* **347**, 269-73 (2015).
17. Raheja, G. et al. Lactobacillus acidophilus stimulates the expression of SLC26A3 via a transcriptional mechanism. *Am J Physiol Gastrointest Liver Physiol* **298**, G395-401 (2010).
18. Borthakur, A. et al. The probiotic Lactobacillus acidophilus stimulates chloride/hydroxyl exchange activity in human intestinal epithelial cells. *J Nutr* **138**, 1355-9 (2008).
19. Singh, V. et al. Lactobacillus acidophilus upregulates intestinal NHE3 expression and function. *Am J Physiol Gastrointest Liver Physiol* **303**, G1393-401 (2012).
20. Lei, S. et al. High Protective Efficacy of Probiotics and Rice Bran against Human Norovirus Infection and Diarrhea in Gnotobiotic Pigs. *Frontiers in Microbiology* **7** (2016).
21. von Ossowski, I. et al. Using recombinant Lactococci as an approach to dissect the immunomodulating capacity of surface piliation in probiotic Lactobacillus rhamnosus GG. *PLoS One* **8**, e64416 (2013).
22. Ou, B. et al. Genetic engineering of probiotic Escherichia coli Nissle 1917 for clinical application. *Appl Microbiol Biotechnol* **100**, 8693-9 (2016).
23. Xu, Q. et al. A Bacterial Surface Display System Expressing Cleavable Capsid Proteins of Human Norovirus: A Novel System to Discover Candidate Receptors. *Front Microbiol* **8**, 2405 (2017).

24. Liu, L. et al. Recombinant Lactococcus lactis co-expressing OmpH of an M cell-targeting ligand and IBDV-VP2 protein provide immunological protection in chickens. *Vaccine* **36**, 729-735 (2018).
25. Zarei, I., Brown, D.G., Nealon, N.J. & Ryan, E.P. Rice Bran Metabolome Contains Amino Acids, Vitamins & Cofactors, and Phytochemicals with Medicinal and Nutritional Properties. *Rice (N Y)* **10**, 24 (2017).
26. Gonzalez-Ochoa, G., Flores-Mendoza, L.K., Icedo-Garcia, R., Gomez-Flores, R. & Tamez-Guerra, P. Modulation of rotavirus severe gastroenteritis by the combination of probiotics and prebiotics. *Arch Microbiol* **199**, 953-961 (2017).
27. Kernbauer, E., Ding, Y. & Cadwell, K. An enteric virus can replace the beneficial function of commensal bacteria. *Nature* **516**, 94-U223 (2014).
28. Yuan, L.J. & Saif, L.J. Induction of mucosal immune responses and protection against enteric viruses: rotavirus infection of gnotobiotic pigs as a model. *Veterinary Immunology and Immunopathology* **87**, 147-160 (2002).
29. Bhattarai, Y. & Kashyap, P.C. Germ-Free Mice Model for Studying Host-Microbial Interactions. *Mouse Models for Drug Discovery: Methods and Protocols, 2nd Edition* **1438**, 123-135 (2016).
30. Yuan, L., Jobst, P.M. & Weiss, M. in Gnotobiotics (eds. Schoeb, T.R. & Eaton, K.A.) (2017).